The Use of Atomic Force Microscopy to Evaluate Warm Mix Asphalt

Munir D. Nazzal, Ph.D., P.E.
Lana Abu Qtaish
Department of Civil Engineering
Ohio University
Athens, OH 45701

for the
Ohio Department of Transportation
Office of Statewide Planning and Research

and the
U. S. Department of Transportation
Federal Highway Administration

State Job Number 134626

January 2013

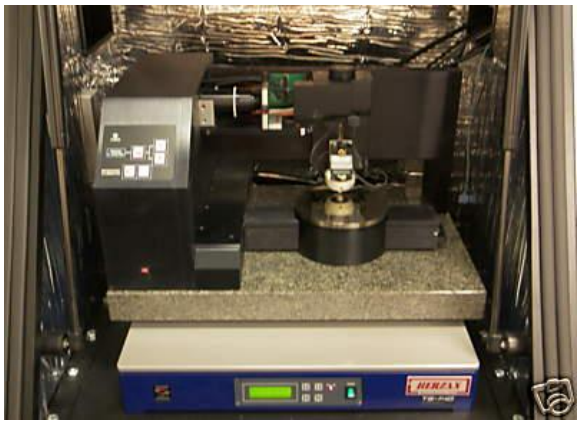

1. Report No. **FHWA/OH-2012/19**	2. Government Accession No.	3. Recipient's Catalog No.
4. Title and subtitle **The Use of Atomic Force Microscopy to Evaluate Warm Mix Asphalt**		5. Report Date **January 2013**
		6. Performing Organization Code
7. Author(s) **Munir D. Nazzal, Lana Abu Qtaish**		8. Performing Organization Report No.
		10. Work Unit No. (TRAIS)
9. Performing Organization Name and Address **Ohio University** **141 Stocker Center** **Athens, OH 45701-2979**		11. Contract or Grant No. **State Job No. 134626**
		13. Type of Report and Period Covered **Final Report**
12. Sponsoring Agency Name and Address **Ohio Department of Transportation** **1980 West Broad Street** **Columbus, OH 43223**		14. Sponsoring Agency Code

15. Supplementary Notes

16. Abstract: The main objective of this study was to use the Atomic Force Microscopy (AFM) to examine the moisture susceptibility and healing characteristics of Warm Mix Asphalt (WMA) and compare it with those of conventional Hot Mix Asphalt (HMA). To this end, different AFM techniques such as the tapping mode imaging and force spectroscopy experiments were conducted on two types of asphalt binders produced using various WMA technologies as well as a conventional HMA. The considered WMA technologies included: Advera, Evotherm M1, Sasobit, and foamed WMA. Dynamic Shear Rheometer (DSR) tests were conducted on the evaluated binders, and AASHTO T283 test was performed on mixtures prepared using those binders. The results of the AFM imaging showed that while the Sasobit additive has reduced the dimensions of the so called 'bee-like' structures within the neat and polymer modified asphalt binders, the other WMA technologies did not have any significant effect on these structures. In addition, the Sasobit resulted in increasing the relative stiffness of dispersed domains containing the 'bee-like' structure in comparison with the flat asphalt matrix for both types of binders, which explained the higher shear modulus values obtained in the DSR test for binders with this WMA additive. The results of the AFM force spectroscopy experiments indicated that all WMA technologies resulted in increasing the nano-scale adhesive forces for both types of asphalt binders prior to moisture conditioning. Advera and foamed WMA had the highest improvement to these forces, while the Sasobit had the least. This might be the cause for the lower indirect tensile strength value that was obtained for the Sasobit mixtures in comparison to other WMA mixtures. The AFM results also showed that the adhesive forces were significantly reduced due to moisture conditioning of the control and WMA 64-22 binders. However, the control and Evotherm WMA binders exhibited the least reduction, while the Advera WMA binder had the highest decrease, which may have contributed to reducing the tensile strength ratio values of the Advera 64-22 mixture. The Sasobit and Advera was also found to reduce the nano-scale cohesive forces within the considered asphalt binders upon moisture conditioning, indicating that it might adversely affect the cohesive bonds within the asphalt binder. The results of the AFM force spectroscopy experiments also suggested that the AASHTO T283 test results primarily depend on the adhesive forces between the aggregate and the binder. The AFM healing experiments indicated that all WMA technologies except the Sasobit resulted in improving the micro-crack closure rate in both types of asphalt binders considered in this study. In addition, only the Sasobit resulted in significant decrease in the cohesive bonding energy; indicating that it might adversely affect the intrinsic healing of the considered asphalt binders. On the contrary, the other WMA technologies improved the –OH cohesive bonding energy and did not significantly influence the –COOH cohesive bonding energy for both asphalt binders. Finally, the results of this study indicated that the AFM is a viable device to study the moisture damage and healing phenomena in asphalt materials.

17. Key Words	18. Distribution Statement
Warm mix asphalt, moisture induced damage, healing AFM, nanotechnology	No restrictions. This document is available to the public through the National Technical Information Service, Springfield, Virginia 22161

19. Security Classif. (of this report)	20. Security Classif. (of this page)	21. No. of Pages	22. Price
Unclassified	Unclassified	108	

Form DOT F 1700.7 (8-72) **Reproduction of completed pages authorized**

Final Report

State Job No. 134626

The Use of Atomic Force Microscopy to Evaluate Warm Mix Asphalt

Prepared by:

Munir D. Nazzal, Ph.D., P.E.
Department of Civil Engineering
Ohio University
Athens, OH 45701
nazzal@ohio.edu

&
Lana Abu-Qtaish
Department of Civil Engineering
Ohio University
Athens, OH 45701

Prepared in Cooperation with
The Ohio Department of Transportation
&
The U. S. Department of Transportation
Federal Highway Administration

January 2013

DISCLAIMER

The contents of this report reflect the views of the authors who are responsible for the facts and accuracy of the data presented herein. The contents do not necessarily reflect the official views or policies of the Ohio Department of Transportation (ODOT) or the Federal Highway Administration (FHWA). This report does not constitute a standard, specification or regulation.

ACKNOWLEDGEMENTS

The researchers would like to thank the Ohio Department of Transportation (ODOT) and the Federal Highway Administration (FHWA) for sponsoring this study. The researchers would like to extend their thanks to ODOT technical liaison, Mr. David Powers, for his valuable contributions to this report. Without his assistance, this work would not have been possible. The researchers would like also to thank Dr. Savas Kaya of School of Electrical Engineering and Computer Science at Ohio University and Dr. Ala Abbas of the Department of Civil Engineering at the University of Akron for allowing us to use equipment needed for the completion of this research work and for all of their helpful comments and suggestions. Finally, the researchers would like to thank Mr. Ed Morrison and Shelly and Sands, Inc. and Mar-Zane, Inc. for donating the asphalt binders and aggregates used in this study

TABLE OF CONTENTS

LIST OF TABLES

LIST OF FIGURES

THE USE OF ATOMIC FORCE MICROSCOPY TO EVALUATE WARM MIX ASPHALT

ABSTRACT

The main objective of this study was to use the Atomic Force Microscopy (AFM) to examine the moisture susceptibility and healing characteristics of Warm Mix Asphalt (WMA) and compare it with those of conventional Hot Mix Asphalt (HMA). To this end, different AFM techniques such as the tapping mode imaging and force spectroscopy experiments were conducted on two types of asphalt binders produced using various WMA technologies as well as a conventional HMA. The considered WMA technologies included: Advera, Evotherm M1, Sasobit, and foamed WMA. Dynamic Shear Rheometer (DSR) test was conducted on the evaluated binders, and AASHTO T283 test was performed on mixtures prepared using those binders. The results of the AFM imaging showed that while the Sasobit additive has reduced the dimensions of the so called 'bee-like' structures within the neat and polymer modified asphalt binders, the other WMA technologies did not have any significant effect on these structures. In addition, the Sasobit resulted in increasing the relative stiffness of dispersed domains containing the 'bee-like' structure in comparison with the flat asphalt matrix for both types of binders, which explained the higher shear modulus values obtained in the DSR test for binders with this WMA additive. The results of the AFM force spectroscopy experiments indicated that all WMA technologies resulted in increasing the nano-scale adhesive forces for both types of asphalt binders prior to moisture conditioning. Advera and foamed WMA had the highest improvement to these forces, while the Sasobit had the least. This might be the cause for the lower indirect tensile strength value that was obtained for the Sasobit mixtures in comparison to other WMA mixtures. The AFM results also showed that the adhesive forces were significantly reduced due to moisture conditioning of the control and WMA 64-22 binders. However, the control and Evotherm WMA binders exhibited the least reduction, while the Advera WMA binder had the highest decrease, which may have contributed to reducing the tensile strength ratio values of the Advera 64-22 mixture. The Sasobit and Advera was also found to reduce the nano-scale cohesive forces within the considered asphalt binders upon moisture conditioning, indicating that it might adversely affect the cohesive bonds within the asphalt binder. The results of the AFM

force spectroscopy experiments also suggested that the AASHTO T283 test results primarily depend on the adhesive forces between the aggregate and the binder. The AFM healing experiments indicated that all WMA technologies except the Sasobit resulted in improving the micro-crack closure rate in both types of asphalt binders considered in this study. In addition, only the Sasobit resulted in significant decrease in the cohesive bonding energy; indicating that it might adversely affect the intrinsic healing of the considered asphalt binders. On the contrary, the other WMA technologies improved the –OH cohesive bonding energy and did not significantly influence the –COOH cohesive bonding energy for both asphalt binders. Finally, the results of this study indicated that the AFM is a viable device to study the moisture damage and healing phenomena in asphalt materials.

Chapter 1 INTRODUCTION

1.1 Problem Statement

Warm Mix Asphalt (WMA) has received considerable attention in past few years due to its benefits in reducing energy consumption and pollutant emissions during production and placement of asphalt mixtures, and as a compaction aid during the construction process. However, many concerns and questions are still unanswered regarding the performance and durability of WMA. One key issue is the moisture susceptibility of WMA. Although the results of standard laboratory tests indicated that WMA may be more susceptible to moisture damage than Hot Mix Asphalt (HMA), data obtained from the field does not support those results. Some data also suggests that the resistance of WMA to moisture damage improves with time and may ultimately be equivalent to that of HMA. In addition, the healing characteristics of WMA have not yet been studied nor evaluated in a methodical, scientific manner. Therefore, research is needed to determine if the degree of healing in WMA is sufficient to increase their resistance to damage, and hence enhance their long term durability.

The fundamental understanding and evaluation of the moisture damage and healing characteristics of WMA requires careful consideration of the micro-mechanisms that influence the adhesive bonds between the asphalt binder and the aggregate, and the cohesive bonds within the asphalt binder. However, all standard laboratory tests that have been used to evaluate the WMA examine their integral, macro-scale behavior only. Therefore, those tests are limited in their ability to validate the moisture damage and healing mechanisms in an asphalt system, as they cannot examine and determine factors contributing to its response at the micro-scale.

This research aims at investigating a paradigm shift in the characterization of WMA such that the recent progress in nano-mechanics and material science can be utilized to study the moisture damage resistance and healing characteristics of WMA, and compare them to those of conventional HMA. The novelty of the pursued approach is to examine the nano-scale behavior for WMA using the Atomic Force Microscopy (AFM) and to identify nano-scale parameters that can be used to interpret the macro-scale field performance. The practical outcome of this project is an improved nano-to-macro understanding of WMA that can facilitate the successful

implementation of WMA in Ohio, and lead to the development of sustainable pavement structures.

1.2 Objectives of the Study

The main objective of this research project is to study the micro-scale behavior of WMA using the Atomic Force Microscopy (AFM). The specific objectives of this study include:

- Develop sample preparation procedure and testing protocols for nano-scale AFM testing on asphalt materials.
- Identify the AFM testing parameters that can be utilized in the evaluation of moisture susceptibility and healing characteristics of asphalt materials.
- Quantify the nano-scale level adhesive and cohesive forces in a WMA system under dry and wet conditions using AFM and compare it to that in a control HMA.
- Evaluate the influence of WMA technologies on the healing characteristics of asphalt binders.

1.3 Report Organization

This report is organized into six chapters. Chapter 2 presents a literature review of subjects pertinent to this study. It provides an overview of the results of studies that evaluated the moisture induced damage and healing of WMA and HMA mixtures. Chapter 3 presents the aggregate and asphalt materials as well as the different WMA technologies investigated this study, followed by a discussion of the mix design verification procedure. Chapter 4 provides a detailed description of the experimental testing program conducted in this study. Chapter 5 presents the results of the experiments as well as the outcome of the statistical analysis. Finally, Chapter 6 presents the main conclusions and recommendations for future study.

Chapter 2 LITERATURE REVIEW

This chapter summarizes the main findings of previous studies that have been performed to evaluate the moisture sensitivity and healing characteristics of WMA mixtures at the macro and micro-scale levels. In addition, a background on atomic force microscopy and its application to asphalt materials is also provided.

2.1 Warm Mix Asphalt

WMA is a generic term used to describe asphalt mixtures that are produced and compacted at temperatures lower than those used for the traditional HMA mixes. It was developed in Europe with the aim of reducing greenhouse gases produced by manufacturing industries (Moulthrop, 2007). While heat is used to reduce asphalt viscosity and to dry aggregate during mixing of conventional asphalt mixtures, WMA reduces asphalt viscosity by including special organic or chemical additives or introducing cool water into the heated molten asphalt under controlled temperature and pressure conditions, resulting in so-called foamed asphalt binder. The reduction in viscosity still allows the asphalt binder to adequately coat the aggregates during mixing.

Various WMA technologies have been proposed and used during the past decade. Those technologies can be classified into two main types. The first type uses some form of organic or chemical additives to produce WMA. Examples on this type include: Sasobit, Evotherm DAT, Evotherm 3G, Rediset WMX, and Cecabase RT. The second type of WMA technologies is produced by foaming the asphalt binder, which is achieved by adding a small amount of water to the binder, either via a foaming nozzle or a hydrophilic material such as Aspha-min. Examples on foaming systems used in the asphalt plants include: Terex, Ultrafoam GX, and Astec Double Barrel Green systems.

Several studies have been conducted in the last decade to evaluate the performance of WMA mixtures and characterize its properties (e.g. Bonaquist, 2011, Nazzal et al. 2011, Abbas et al. 2012, Kvasnak et al. 2010, Kanitpong et al., 2007, Kristjansdottir et al., 2007, Hurley and Prowell, 2006, Hurley and Prowell, 2005). These studies revealed several benefits for using

WMA technology, which included: significant reduction in the green gas emission due to the lower temperatures, reduction in the fuel cost, longer paving season, longer haul distances, and less oxidative hardening of the asphalt mixture resulting in a reduction of block and thermal cracking in the pavements.

Despite the advantages of using WMA, there are still concerns about its long-term performance and durability. Specifically, one of the major concerns with WMA is its ability to resist moisture induced damage. The WMA resistance to moisture damage was evaluated in several studies. The proceeding sections introduce the moisture induced damage phenomenon in asphalt materials and summarizes the findings of studies performed to evaluate the moisture susceptibility of different types of WMA.

2.2 Moisture-Induced Damage of Asphalt Mixtures Pavements

Moisture-induced damage is one of the most significant problems in asphalt mixtures. It is considered one of the main causes of distress and premature failure in asphalt pavement, which result in significant maintenance and rehabilitation costs (Copeland, 2005). Moisture damage is caused by the failure in the adhesive bonds between the binder and aggregates or by the failure in the cohesive bonds within the binder itself due to the presence of moisture in the mixture (Tarefder & Zaman, 2010). Figure 2.1 shows the moisture damage mechanisms in an asphalt mixture. Several factors have been recognized as causes of moisture damage, these include: aggregate type and chemical composition, chemical and physical properties of the asphalt binder, asphalt content, asphalt mixtures properties, the nature of water the mix is being exposed to, and the climate and traffic conditions (Abu Al-Rub et al., 2010).

Over the past decade, several studies were conducted to evaluate moisture induced damage resistance of WMA and compare it to that of HMA asphalt mixtures. Most of these studies used macro-scale tests such as: modified Lottman (AASHTO T283), dynamic modulus, and Hamburg wheel tracking tests. Some studies have also used micro-mechanical approaches such as the surface energy methods and the dynamic mechanical analyzer to examine the moisture susceptibility of WMA (e.g., Estakhri et al., 2010; Wasiuddin et al., 2008; Bhasin et al., 2006). A summary of the results of the different studies that have been performed to assess moisture susceptibility of WMA is provided in the proceeding sections.

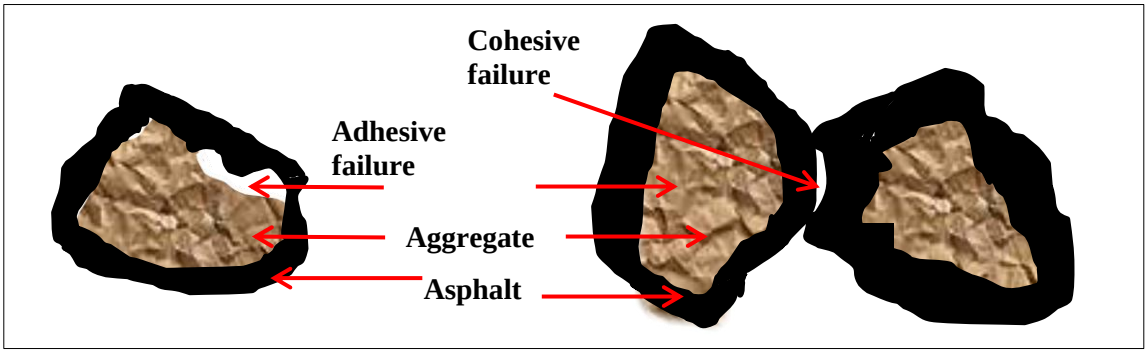

Figure 2.1: Moisture damage mechanisms in asphalt mixtures.

2.2.1 Macro-Scale Evaluation of Moisture Damage in WMA

The performance of WMA has been investigated widely in the past few years, mostly using conventional macro-scale laboratory and field tests. Numerous laboratory and field studies were performed to evaluate the moisture sensitivity of various types of WMA mixtures. Hurley & Prowell (2006) evaluated the moisture damage resistance of WMA mixtures prepared using three different processes: Aspha-min zeolite, Sasobit, and Evotherm. ASTM D4867 (very similar procedure to AASHTO T283) and Hamburg wheel tracking tests were employed in this study. The results from both tests confirmed that the presence of Aspha-min reduced the tensile strength ratio (TSR) value and made the mixture more sensitive to moisture damage; this was attributed to moisture residue left from the foaming process of Aspha-min or the moisture left in aggregate due to an incomplete drying process. The TSR values for the Sasobit and Evotherm WMA mixtures were either higher or lower than the corresponding TSR values for HMA mixtures depending on the type of aggregates used. On the other hand, Hamburg wheel tracking test results showed good moisture damage resistance for asphalt mixtures containing Sasobit. The indirect tensile strengths for Sasobit mixtures were lower compared to control HMA mixes; this was attributed to the anti-aging properties of Sasobit. The result showed that moisture sensitivity of WMA depends on several factors such as aggregate type and WMA process.

Kvasnak el al. (2009) evaluated the moisture susceptibility of WMA mixtures prepared using Evotherm and HMA mixtures, both mixes were produced in the laboratory and plant for comparison between laboratory and plant mixtures. Indirect tensile strength tests and Hamburg wheel tracking tests were used to evaluate moisture damage. The results of this study indicated that the HMA mixtures were less prone to moisture damage than WMA. In addition laboratory

produced WMA mixtures were more susceptible to moisture damage compared to plant mixtures.

Bonaquist (2011) has completed a study for National Cooperative Highway Research Program (NCHRP 9-43) to develop a mix design procedure for the current WMA technologies in the different states and to evaluate their performance as compared to conventional HMA mixes. The moisture sensitivity for the WMA mixtures was examined in this study using the AASHTO T283 test. The study concluded that the TSR values of WMA mixtures containing anti-strip remained the same as HMA or improved in 67% of the evaluated mixtures. Nevertheless, TSR values did not improve and decreased in 79% of the WMA mixtures that did not contain any anti-strip additives. The results of the project mainly showed that the moisture susceptibility of the WMA mixtures is mainly dependent on the type of the WMA technology used.

Aschenbrener et al. (2011) conducted a study to evaluate the laboratory and field performance of different types of WMA in comparison to control HMA mixes. The types of WMA used were: Advera, Evotherm, and Sasobit. Moisture Damage was evaluated using the AASHTO T283 test. The results of the laboratory test indicated that WMA mixtures may be more susceptible to moisture damage when compared to HMA mixtures. Dynamic modulus and flow number tests were done to evaluate stiffness of mixture; the results showed that HMA mixes were slightly stiffer than WMA. This indicated that WMA sections might be me more susceptible to rutting. However, field performance for WMA was excellent and comparable to HMA and the tensile strength for cores taken after two and three years showed no difference between HMA control sections and WMA sections. WMA sections performed as well as HMA control sections in terms of resistance to rutting, cracking and raveling.

Buss et al. (2011) reported the results of a study to evaluate the performance of mixtures produced using four types of WMA technologies and compare it with that of HMA mixes. The considered WMA technologies included: Evotherm 3G, Revix, Sasobit, and Double Barrel Green foaming. Field compacted and reheated field samples were produced and tested. The mix testing included the AASHTO T283, dynamic modulus, and flow number tests. The results of this study showed that the foamed WMA mixtures had the best performance in the dynamic modulus and flow number tests. In addition, the TSR values for all WMA mixtures except the foamed WMA

were less than these of the HMA for both field and laboratory compacted specimens. However, these values were greater than the passing criteria of 0.80. Buss et al. (2011) demonstrated that WMA technologies may impact the mixture response to moisture conditioning and recommended that the use of foaming technology should be further investigated under a higher degree of control.

Alavi et al. (2012) studied the effect of WMA additives and the production temperature on the moisture damage and adhesive properties of WMA materials. The adhesion properties were evaluated using a new experimental testing procedure called bitumen bond strength (BBS). In this test a pull stub adhered to an aggregate substrate is subjected to a normal force created by increasing pneumatic pressure, the bond strength is the maximum pull off pressure excreted by the machine. This test was used to measure the strength of bond at the aggregate/asphalt interface and evaluate the effect of WMA on this bond for dry/wet conditioned samples to determine the bond strength ratio (BSR). The moisture susceptibility of mixtures was evaluated using the dynamic modulus (|E*|) test after subjecting the asphalt samples to multiple freeze and thaw cycles. The dynamic modulus stiffness ratio (ESR) was determined by taking the ratio between the |E*| for moisture conditioned samples to and that of control unconditioned samples and was used as a parameter for evaluating moisture susceptibility. Different types of materials were used for the evaluated mixtures. These included two types of asphalt binders: namely, PG 64-22 and PG 76-22M, three types of WMA additives: Advera, Rediset and VR-1, and two aggregates types: granite and rhyolite. The results showed that the dry bond strength was significantly impacted by the aggregate type; however the wet bond strength was mainly affected by the presence of WMA additives. The |E*| data showed a potential moisture damage problem for Advera mixtures when used with granite; however, better results were obtained when it was used with rhyolite. An increase in moisture resistance was observed in some of the mixtures that used Rediset and VR-1. It was concluded from both the BBS and |E*| tests results that the right selection of WMA additive in the mix design process could potentially enhance the moisture damage resistance and mitigate the effect of lower production temperatures.

2.2.2 Micro-Scale Evaluation Of Moisture Damage In WMA

During the past decade, micro-scale approaches have also been employed to evaluate the moisture damage susceptibility of WMA (Cheng et al., 2002; Wasiuddin et al., 2008; Mogawer

et al., 2011). The used techniques include: surface free energy method, dynamic mechanical analyzer, and dynamic shear rheometer based techniques. Surface energy of the asphalt binder and aggregate has been empirically related to the moisture-susceptibility of asphalt mixtures (Wasiuddin et al., 2008). While the Wilhelmy plate method has been typically used to quantify the asphalt surface energy, aggregate surface energy has been measured using the universal sorption method. Wasiuddin et al. (2008) investigated the effect of using Aspha-Min and Sasobit on the adhesion and wettability of WMA mixtures using surface energy method. Adhesion and wettability properties were then used to explain moisture susceptibility in WMA mixtures using these two additives. Two types of asphalt binders were used in this study, namely, PG 64-22 and a SBS polymer modified PG 76-28M binders. In addition, two aggregate types were investigated: sandstone and limestone. It was found that the Sasobit increased the wettability between the binder and the aggregates significantly. Nevertheless, Sasobit decreased the adhesion between binders and aggregates. Moisture induced damage remained unaffected by the addition of Sasobit for neat PG 64-22 binder; however it increased for PG 76-28M. Aspha-Min did not significantly affect the wettability. However, for the PG 76-28M binder, Aspha-Min increased the adhesion and thus enhanced the moisture resistance.

The Sasobit influence on the performance of asphalt was also investigated by Wei et al. (2010) using the surface energy method. Surface energy for the binder was determined by measuring the contact angle between asphalt and the liquid. Sasobit increased the contact angle between the binder and water; therefore, it resulted in reducing the surface free energy of the asphalt binder. The reduction of the surface energy may improve the wettability of the asphalt binder on the aggregate, hence increasing the adhesion and improving the moisture resistance. However, this conclusion may be debated due to the lack of surface free energy measurements for the aggregates.

The dynamic mechanical analyzer (DMA) has also been employed to examine the moisture damage in WMA mixtures. This test involves applying cyclic torsional strain controlled load to cylindrical asphalt mixture prepared using fine aggregates and asphalt binder to examine their fatigue life of asphalt mixtures under dry and wet conditions and predict the moisture susceptibility of asphalt mixtures. Mogawer et al. (2011) investigated the fracture characteristics of WMA mixtures under dry and wet conditions using the DMA. The testing specimens had

different aging time and temperature to evaluate the effect of aging on moisture damage. The tested specimen included control, Advera, and SonneWarmix (Wax) mixtures. A crack growth index for each specimen was calculated using a fracture model for viscoelastic materials and the data obtained from the DMA test. The results showed that the crack growth index for conditioned sample was higher than that for dry samples indicating damage due to the presence of moisture. The WMA mixtures using Advera were more susceptible to moisture damage compared to control samples. However, the increase in aging time for the WMA mixture improved their moisture damage resistance as the results were more comparable to the control mix. Estakhri et al. (2010) also used the DMA to estimate the fatigue life for wet and dry HMA and WMA mixtures. The dry WMA mixtures had higher fatigue life compared to HMA mixtures. However the fatigue life for wet WMA specimens decreased drastically as it was much lower than the fatigue life for dry WMA specimens indicating that WMA mixtures are more prone to moisture damage than HMA mixtures.

In summary, there is no consensus on the effect of WMA on the moisture susceptibility of asphalt mixtures; while some studies showed that the HMA had better moisture damage resistance than the WMA; other studies found that the indirect tensile strength and tensile strength ratio values obtained in AASHTO T283 test were not significantly affected by the use of WMA technologies. Furthermore, the type of WMA technology was reported to be one of the factors affecting the moisture resistance in asphalt mixtures. Despite the number of studies conducted in the past on WMA, previous studies have failed to provide a good understanding of the moisture damage phenomenon in WMA mixtures since they did not examine it mechanisms. Macro and micro-scale tests such as AASHTO T283 test and DMA examine the overall behavior but do not differentiate between the cohesive or adhesive failures within the asphalt system. In addition, the surface free energy method fails to distinguish between the actions of the asphalt binder chemical groups under wet conditions. It also does not evaluate the interaction between the WMA additives and the asphalt constituents. Also, the Wilhelmy plate method used in measuring the surface free energy of asphalt binder does not capture the effect of amine anti-strip additives. Moreover, the universal sorption method involves vacuum degas preconditioning that does not represent the atmosphere in the asphalt plant. Finally, the previous studies did not investigate the changes that WMA brings to the asphalt binder micro-structure.

2.3 Healing In Asphalt Materials

Although the results of some laboratory studies suggested that the WMA may be more susceptible to moisture damage than HMA, field data did not show to date an inferior performance of WMA as compared to HMA (Aschenbrener et al., 2011). The healing characteristic of WMA is an important factor that has a significant impact on its performance, and might partially explain the differences observed between the laboratory and the field test results. Healing, in this context, can be briefly defined as the process by which the crack growth in asphalt binders or mixtures, which occurs due to repeated loading, is partially or completely reversed. The healing phenomenon in asphalt materials consists of two main mechanisms: wetting and intrinsic healing (Bhasin et al., 2011). Wetting is the mechanism in which cracked surfaces come into contact with each other. It depends on the mechanical properties (including viscoelastic properties) and work of cohesion for the asphalt binder. In addition, the intrinsic healing is the strength gained by a wetted crack interface. The intrinsic healing is dictated by the cohesive forces with asphalt binder.

During the past few years, several studies were conducted to investigate the healing characteristics of asphalt material (e.g. Bhasin el al., 2011; Estakhri et al., 2010; Bhasin et al., 2008; Qui et al., 2009; Shen et al., 2010). However, the healing characteristics of WMA have not been widely studied yet. Hence, in order to interpret the healing characteristics of WMA mixtures a thorough understanding of the healing properties of both WMA and HMA should be acquired.

Bhasin et al. (2008) introduced a framework to predict the effect of healing on the performance of asphalt by combining the mechanical and material properties of the asphalt. The study proposed a model that describes healing in asphalt materials. The model was based on previous work done on polymers healing by Wool and O'Connor (1981) and assumed that healing in asphalt occurs due to two main processes: wetting process, which occurs due to the wetting of the two surfaces of the micro crack, and intrinsic healing process that occurs due to the immediate gain in the strength caused by the interfacial cohesion between the crack phases, and a long term gain in the strength that occurs due to the dispersion of molecules from one face to the other. The wetting process was presented by the wetting function and it directly depends

on the mechanical properties of the material, Poisson's ratio, length of the healing process area, work of cohesion (surface energy) and the tensile strength that bond the two faces. The intrinsic healing process depends on the surface energy of the binder and self-diffusion of the asphalt molecules at the crack interface. DSR and surface energy methods were used to estimate the parameters for these two functions. This study provided a novel method to evaluate healing and the authors managed to provide a better interpretation for the healing process. However estimation for two of the wetting function parameters, the bonding tensile strength and the length of healing process zone, was not provided.

Shen et al. (2010) investigated the cohesive healing within the asphalt binder by employing the ratio of dissipated energy change (RDEC) approach. In this approach, the changes in the dissipated energy in the asphalt binder were investigated during the process of applying external loading. Two types of asphalt binders were tested; PG 64-22 and PG 70-28M. The Dynamic shear rheometer was used to conduct the healing testing on the binders. The binders were tested at two different temperatures (59°F (15°C) and 77°F (25°C)) and various stress and strain levels to evaluate the effect of the temperature, stress and strain on healing rates. In order to simulate loading conditions similar to that in the field, rest periods that ranged between 0-6 seconds were used every 10 load cycles. The results of this study showed that the neat asphalt binder had lower healing rate compared to the polymer modified binder, the lower temperature decreased the healing rate for the binders while the higher temperature improved the healing. The strain level was inversely related to the healing rate. Nevertheless, the stress level was not clearly related to the healing rate.

Although previous studies contributed significantly to advancing the knowledge of the moisture susceptibility and healing characteristics of WMA materials, they have used tests that cannot examine the moisture damage and healing mechanisms in an asphalt system. In addition, most of these tests cannot evaluate the asphalt material response at the micro-scale. Understanding the behavior at this scale is important as the typical asphalt binder thickness coating aggregates in an asphalt mixture is in the order of a few microns. The use of nano-mechanical techniques can help in solving this problem by providing an enhanced characterization and modeling tool for the interfacial properties between the aggregate and the binder as well as the mechanical properties of the asphalt binder itself.

2.4 Atomic Force Microscopy

One of the nanotechnology techniques that has received increasing attention for examining the behavior of different materials is the Atomic Force Microscopy (AFM) (Figure 2.2). AFM is a flexible high-resolution scanning probe microscopy technique, which uses a laser-tracked cantilever with a sharp underside tip (probe) to raster over while interacting with the sample. AFM is an ideal tool for measuring nano and micro-scale forces within a composite material (Beach et al. 2002; Nguyen et al., 2005). It has been widely used in high-tech materials, polymer, rubber, paint, biomaterials, and paper industries. The forces that can be measured in AFM include, but are not limited to, mechanical contact force, friction, van der Waals forces, capillary forces, chemical bonding, electrostatic and magnetic forces. The modern AFM systems can accurately map a particular force in various imaging modes with nano meter resolution or track the dependence of different components as a function of tip-surface distance with sub-nanometer resolution.

Force measurement using the AFM has been broadly used in previous studies. Many investigators applied AFM to measure adhesive forces between AFM tip and different materials (Abraham, Christendat, Karan, Xu, and Masliyah, 2002; Beach, Tormoen, & Drelich, 2002; Eastman & Zhu, 1996). Eastman & Zhu (1996) measured the adhesive forces between a mica surface and AFM tips coated with different materials. The force-distance curves were plotted using the AFM; the forces that were measured were the van der Waals for hydrophobic tips and capillary forces for hydrophilic tips. Another study that was performed by Beach et al. (2001) measured the pull-off feces between hexadecanethiol self-assembled monolayers tips and gold coated silicon wafer.

Bhushan & Qi (2003) studied the sources of phase contrast in AFM images and the effect of the free amplitude and set point on this contrast by testing nanocomposites and molecularly thick lubricant films. The authors wanted to develop a technique to map surface composition of polymer nanocomposites and lubricant film thickness. Tapping mode was used in imaging the samples. The results showed that the phase contrast becomes very poor at high free amplitude or set point. For given free amplitude, phase angle contrast decreases with decreasing set point. Hence, to study the adhesion properties low free amplitude and set-point should be used for best

results. However, high free amplitude and set-point are more suitable for studying viscoelastic properties of the samples.

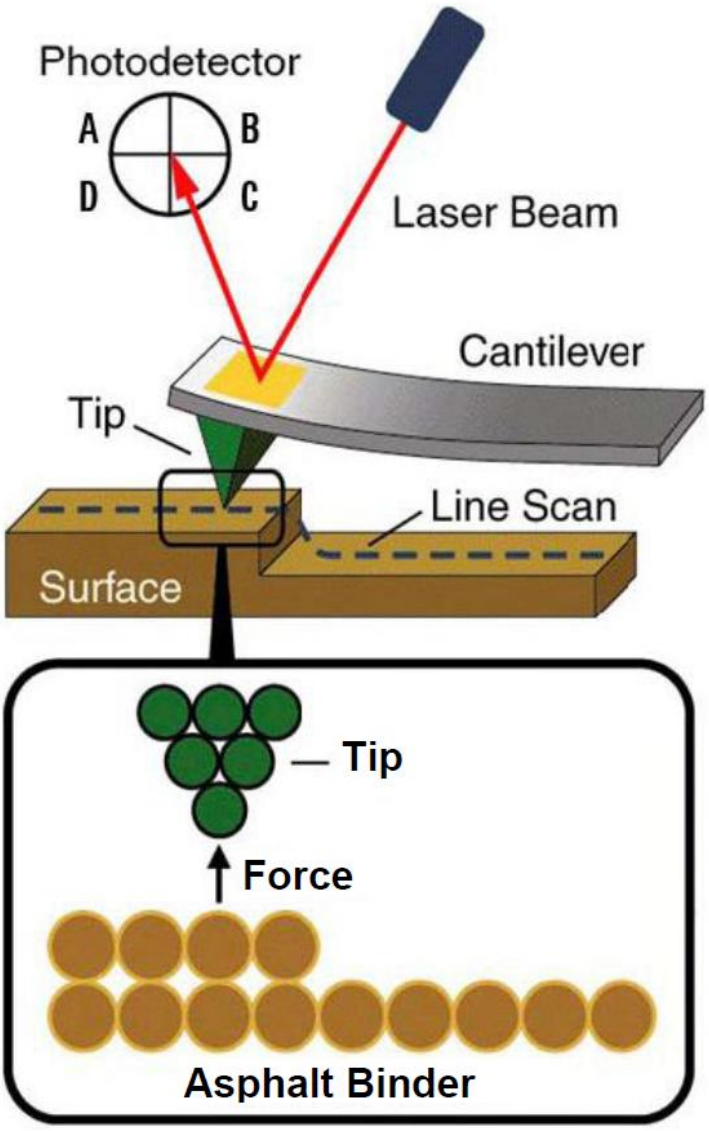

Figure 2.2: Schematic diagram of AFM, adapted from (Agilent Inc. 2006).

During the past few years some research studies have also used AFM to study the asphalt materials behavior (i.e. Nguyen et al., 2005; Huang et al 2005; Tarefder & Zaman, 2010). The Western Research Institute (WRI) had evaluated different techniques for measuring adhesive properties in eight different types of asphalt binders. AFM was used to measure the surface force of asphalt cast onto glass substrates. Glass bead tips were used in the AFM

experiments conducted in this study. The measured forces were used to determine the work of adhesion between asphalt binder and aggregates. There results showed that the moisture damage in the asphalt binder correlate with polyaromatic hydrocarbon concentration (Huang et al., 2005).

Jager et al. (2004) identified four material phases in bitumen using the AFM. The bitumen specimens were scanned using two modes, namely, non-contact mode and pulse-force mode to identify the surface topography and mechanical properties of bitumen. Five different types of bitumen were tested. Images using the non-contact mode showed "bee-like" structures that formed due to peaks and depressions in the topography of the bitumen, the "bee-shaped" structures were surrounded by relatively flat matrix. The matrix had two domains that could be differentiated by a slight difference in the topography. Thus, the authors have identified four phases in the tested bitumen; the lower and higher parts of the bee structures and two phases in the surrounding matrix. Pulse-force mode (PFM) measurements were conducted to assess if the identified four topographic phases poses different mechanical properties. PFM measurements provided an insight into the stiffness properties for the four different topographic domains through the data collected from the cantilever deflection. The peaks in the "bee-like" structure had the highest relative stiffness value while the depression in this structure had the lowest relative stiffness. The flat matrix also exhibited same behavior as the "bee-like" structure. The authors assumed that the "bee-like" structure contains asphaltene and resins since it had the highest stiffness values. On the other hand, the soft part of the matrix may contain saturates and aromatics. The study helped in relating topographic groups in asphalt to chemical groups. However, the research did not include phase image analysis which has been widely used to evaluate mechanical properties of materials.

Masson et al. (2006) investigated the morphology of 13 types of asphalt binders by studying the images obtained by AFM. However, this study did not include any mechanical characterization of the considered asphalt binders. The results of the AFM images obtained in this study showed that an asphalt binder could possibly have up to four phases of different rheology and composition. The asphalt binders were classified into three groups ruled by the variation in stiffness of the fused-aromatic rings in them. The first group included asphalt binders with fine domains about 0.1-0.7μm in size dispersed in the homogeneous asphalt matrix. In

addition, the asphalt binders in the second group had 1μm flake-like dispersions. Finally, the third group included asphalt binders with up to four different phases with different sizes.

Tarefder & Zaman (2010) recently studied the moisture damage in neat and polymer modified asphalt binders at a nano-scale level using the AFM. The adhesive and cohesive forces within the asphalt mix were measured by employing the AFM force spectroscopy experiments. In order to evaluate moisture damage, the forces were measured for dry and moisture conditioned asphalt binder samples. The results of this study demonstrated the ability of the AFM to measure the adhesive and cohesive forces within an asphalt material. The results of AFM experiments showed that the polymer modification for the asphalt binder enhanced its resistance to moisture-induced damage. Furthermore, three percent polymer content was found to yield the optimum performance for both SB and SBS polymers.

Recently, researchers have also used the AFM to study the influence of aging on the microstructure and morphology of various types of asphalt binders (Zhang et al., 2011; Zu et al., 2010; Scarpas et al., 2010). Zhang et al. (2011) used the AFM imaging technique to examine the morphology of unmodified and organo-montmorillonite modified (OMMT) asphalt binder before and aging. The results of their study indicated that after aging, the dimension and the amount of 'bee-like' structures were reduced, and the contrast between the flat asphalt matrix and the dispersed domains was decreased. Finally, recent studies have also developed computational models for studying the healing of asphalt binders that were based on images obtained using the AFM (Kringos et al., 2012).

Chapter 3 MATERIAL DESCRIPTION

In this chapter a description of all the materials that were used in this research is provided. These include the asphalt binders, WMA additives and the aggregate used in the mix design procedure.

3.1 Binders

Two types of asphalt binders that are typically used in the production of asphalt mixtures in Ohio were considered in this study. This included a styrene-butadiene-styrene (SBS) polymer modified asphalt binder meeting specifications for PG 70-22M and one neat asphalt binder meeting PG 64-22 specifications. Table 3.1 presents the binder properties for each of those binders.

Table 3.1: Properties of asphalt binders.

	PG 70-22M		PG 64-22	
Test Property	Spec	Sample Result	Spec	Sample Result
Original Binder				
Rotational Viscosity @135°C Pa.s	≤3.0	0.9375	≤3.0	0.4375
G*/ Sin δ, kPa	≥1.00 @70°C	1.440 @70°C	≥1.00 @64 °C	1.230 @64 °C
Tests on RTFO Residue				
G*/Sin δ, kPa	≥2.20 @70°C	4.030	≥2.20 @64 °C	3.070
Elastic Recovery, 25°C, 10 cm	≥ 60%	72.5%	N/A	N/A
Tests on PAV Residue				
G* Sin δ, kPa	≤5000 @28 °C	2270 @28 °C	≤5000 @25 °C	3740 @25 °C
Bending Beam Creep Stiffness, S_{max}, MPa, tested at -12 °C	≤300	150	≤300	190
Bending Beam Creep, m value tested at -12 °C	≥0.300	0.311	≥0.300	0.308

3.2 Aggregates

The aggregates used in the mix design were obtained from one of ODOT's approved aggregate suppliers, Stocker S & G – Gnadenhutten. The aggregate blend consisted of four types of aggregates: crushed gravel No. 9, crushed gravel No.8, Natural sand, and manufactured sand. Table 3.2 shows the gradation for each type of aggregate as provided by the supplier.

Table 3.2: Aggregates gradation.

	Crushed gravel No.8	Crushed gravel No. 9	Natural sand	Manufactured sand
Sieve	% Passing	% Passing	% Passing	% Passing
1/2" (12.5)	100.0	100.0	100.0	100.0
3/8" (9.5)	95.0	100.0	100.0	100.0
#4 (4.75)	20.0	100.0	98.0	100.0
#8 (2.36)	2.0	59.0	87.0	99.0
#16 (1.18)	2.0	10.0	73.0	92.0
#30 (0.6)	2.0	2.0	47.0	72.0
#50 (0.3)	2.0	2.0	14.0	57.0
#100 (0.15)	2.0	2.0	2.0	30.0
#200 (0.075)	2.0	2.2	2.6	10.5

The aggregates that were used in the Superpave mix design met the material requirement in terms of the course aggregate angularity (% fractured) and fine aggregate angularity (FAA). The bulk specific gravity for each type was obtained from ODOT. Table 3.3 shows the coarse and fine aggregate properties as provided by the supplier.

Table 3.3: Consensus properties of coarse and fine aggregates.

Coarse aggregates			
Aggregate type	% in blend	% fractured	ODOT G_{sb}
Crushed Gravel #9	53	92.2	2.561
Crushed Gravel #8	18	69	2.466

Fine aggregates			
Aggregate type	% in blend	% FAA	ODOT G_{sb}
Natural Sand	15	41	2.609
Manufactured Sand	14	50	2.588

3.3 WMA Technologies

Four types of WMA technologies were evaluated in this study, which included: Sasobit, Evotherm M1, Advera, and foamed WMA produced by the water injection method. Each type of the asphalt binders considered in this study was produced using the selected types of WMA technologies as well as a conventional HMA. A description of the evaluated WMA technologies is provided in below.

3.3.1 Advera

Advera is a WMA additive that is manufactured in the US by PQ Corporation, Malvern, PA. It is an aluminosilicate or hydrated zeolite powder that contains 18-20% of chemically and structurally bounded water in its porous crystalline structure. Advera has a form of free flowing powder with a white color as shown in Figure 3.1. During production the trapped water in Advera is released in the form of finely dispersed water vapor, which creates a volume expansion of the binder that results in the formation of asphalt foam. This increases the wettability and workability of the binder and enhances the aggregate coating at lower temperature allowing for the reduction in production and compaction of asphalt mixtures by up to 50-70 °F.

3.3.2 Evotherm M1

Evotherm M1 is one type of Evotherm 3G (third generation) that was developed by a partnership between MeadWestvaco Paragon Technical Services and Mathy Technology & Engineering. It is a water-free low viscosity liquid with a dark amber color (Figure 3.2) that is introduced at the asphalt plant or asphalt terminal and blends easily with asphalt binder. Evotherm M1 contains additives and agents that improve the workability, coating and compaction. It also includes surfactants that increase the adhesion between the asphalt and aggregates. When used in the production of WMA Evotherm M1 can reduce the mixing and compaction temperature by 63 to 90 °F compared to HMA. It can be used with different types of

asphalt including polymer modified asphalt without affecting its performance grade. The manufacturer recommended dosage rate for Evotherm M1 ranges from 0.25 percent to 0.75 percent by the weight of asphalt cement. The typical properties of Evotherm M1 are shown in Table 3.4.

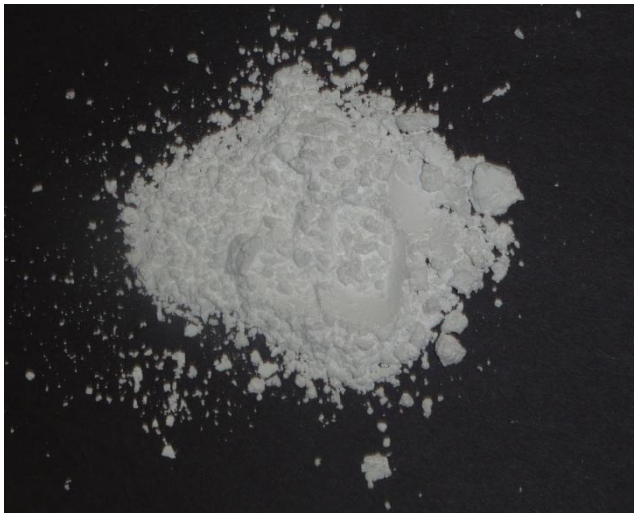

Figure 3.1: Advera powder

Figure 3.2: Evotherm M1

Table 3.4: Evotherm M1 properties.

Property	Typical value
Density at 77°F	0.97
Specific gravity at 77°F	2.2
Viscosity at 80 °F (centipoises)	280-560

3.3.3 Sasobit

Sasobit is a paraffin wax produced from coal gasification using the Fischer Tropsch (FT) process, Figure 3.3. It is a fine crystalline, hydrophobic, long-chained aliphatic hydrocarbon. Therefore, the addition of this wax to an asphalt binder causes the binder to become more hydrophobic (Sasol Wax Co., 2008). Sasobit dissolves in the asphalt at a temperature of 248°F or above; it has longer chains length compared to the natural occurring waxes in bitumen causing it to have lower melting point. Therefore, the addition of Sasobit results in a reduction in the binder's viscosity, allowing for lower production temperatures. Sasobite manufacturer, Sasol wax, recommends adding Sasobit into the binder using a rate between 0.8 and 3 percent by weight of binder.

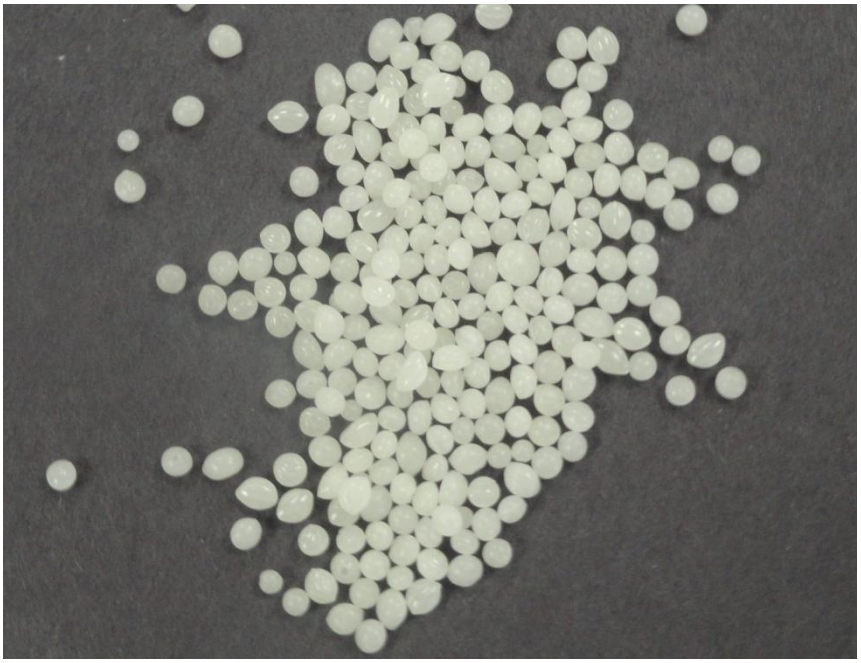

Figure 3.3: Sasobit WMA Additive

3.3.4 Foamed WMA

Foamed WMA is produced by injecting small amount of cold water into the heated asphalt via a foaming nozzle device. The added water turns to steam and expands upon contact with asphalt. This results in a reduction of viscosity due to the expansion of the liquid asphalt binder, which allows mixing and compaction of the asphalt at lower temperature. This technology allows the production of WMA through a one-time mechanical plant modification by attaching a foaming device such as Astec, Gencor, and Terex to the end of the asphalt binder line, which minimize the impact of increased material costs identified with other WMA technologies. Figure 3.4 shows a typical Astec foaming device commonly used with their Double Barrel Green system.

Figure 3.4: Multi-Nozzle foaming device (after Astec, Inc.).

Foamed WMA can also be produced using a laboratory scale asphalt binder foaming device such as the Wirtgen WLB10 (Figure 3.5), which was used in this study. This device utilizes a process similar to that used by the foaming devices used in the field. As shown in Figure 3.5, the WLB10 device consists of an asphalt binder tank, a water tank, an air tank, an asphalt pump, heating components, a foaming nozzle, air and water pressure regulators, and a control panel. The asphalt binder for the foamed WMA is heated to the standard mixing

temperature used for the HMA to ensure pumpability within the foaming device. The foaming rate was 1.8 percent of the total weight of the asphalt binder.

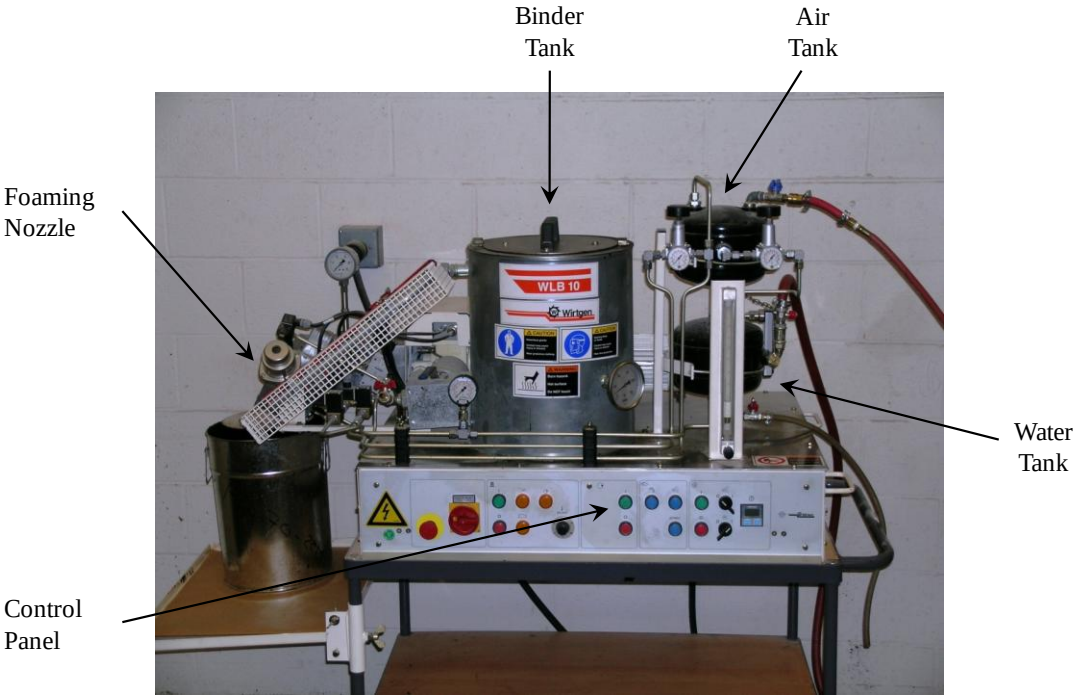

Figure 3.5: Wirtgen WLB10 asphalt foaming device (Abbas et al. 2011).

3.4 Mix Design Verfication

In this project, the moisture susceptibility of HMA and WMA mixtures was evaluated at a macro-scale level using AASHTO T283 test method. The considered asphalt mixtures had a ½ inch (12.5 mm) nominal maximum aggregate size (NMAS) and were designed to meet ODOT specification for Item 442 Type B for heavy traffic surface mixtures. The job mix formula for the asphalt mixtures was obtained from Shelly and Sands, Inc. and Mar-Zane, Inc. but was verified by the research team as described below.

3.4.1 Aggregate blend

The four aggregate types (i.e. crushed gravel#9, crushed gravel #8, natural sand, manufactured sand) were blended to produce the gradation that meets the ODOT requirement for Superpave mixtures. Figure 3.6 shows the 0.45-power chart for the selected aggregate gradations.

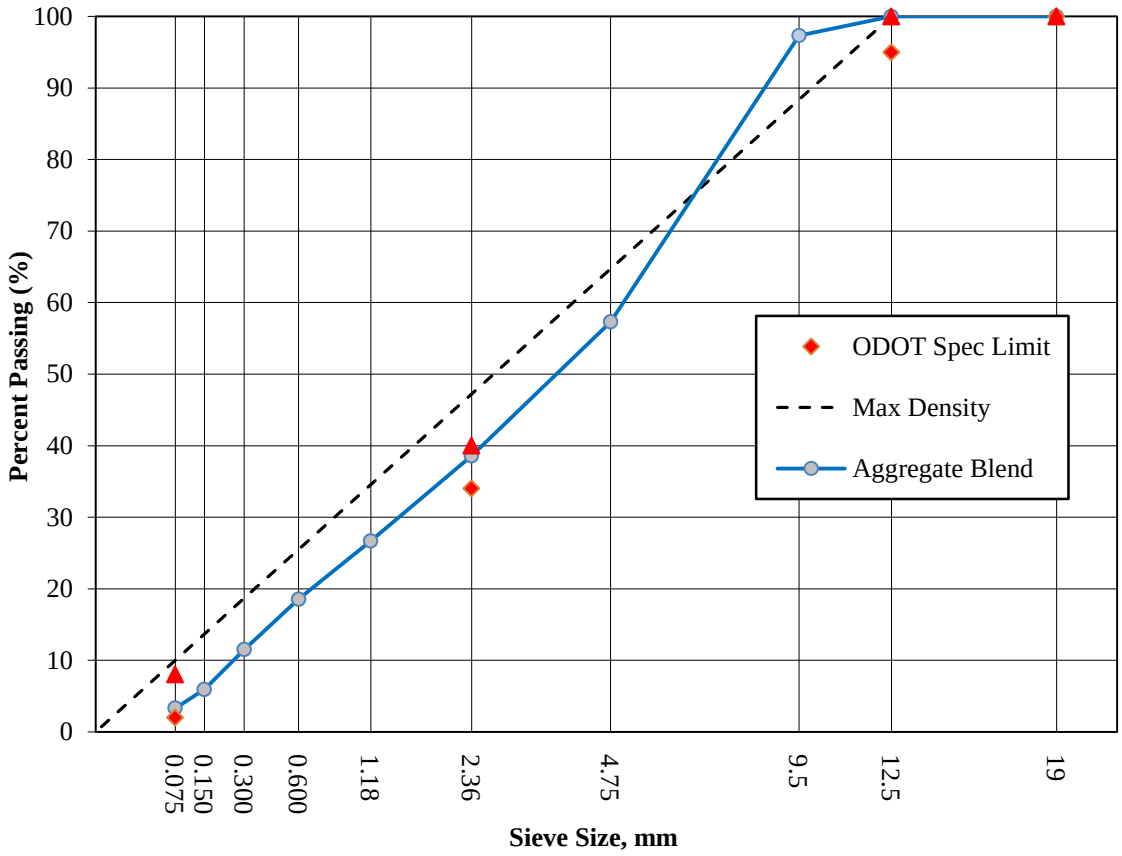

Figure 3.6: Aggregate blend gradation.

3.4.2 Optimum Asphalt Content

Superpave mix design was performed to verify the optimum asphalt content for the selected aggregate gradation provided by the asphalt contractor. The optimum asphalt content was found for the HMA only as some studies proved that there are no significant differences in the volumetric properties between HMA and WMA mixtures (Bonaquist, 2011). It is worth noting that the optimum asphalt content provided by Shelly and Sands, Inc. and Mar-Zane, Inc. was provided for the PG 70-22M binder only, and it was 5.8 percent. The verification process involved evaluating the volumetric properties of mixtures prepared at four different asphalt contents ranging between 5.3 to 6.3 percent. Two samples were prepared for each asphalt binder content. To prepare each sample, the binder and aggregate were first heated overnight at a temperature 15°C higher than the mixing temperature. In addition, the asphalt binder was heated for three hours at the specified mixing temperature for each type of binder. The asphalt binder and the aggregates were then mixed using the Humboldt mixing machine. The mixture was aged

in the oven for two hours at the compaction temperature. The aged mix was then compacted in a gyratory compactor. The design number of gyration used was 65 according to ODOT Specification for item 442. Some of the prepared mixture was left loose and was used to determine the mix maximum specific gravity.

The maximum specific gravity G_{mm}, mix bulk specific gravity G_{mb}, VTM, VMA, VFA, % G_{mm} @ N_{design}, and % G_{mm} @ $N_{initial}$ were computed for the prepared samples. The data were then analyzed to select the optimum asphalt binder content that corresponds to an air void of 4 percent. A summary of the mix design results for the 70-22M and 64-22 mixtures is presented in Table 3.5.

Table 3.5: Superpave mix design parameters for the evaluated mixtures.

Mix property	70-22M Mix	64-22 Mix	Specification
% binder	5.9	6.1	>5.7%
Air Void %	4	4	4
VMA	15.2	15.45	15
VFA	70	72	-
%Gmm @N_{ini}	89	88.8	-
%Gmm @N_{design}	95.8	95.7	96
Dust /binder ratio	0.67		0.6-1.6
Unit weight (pcf)	138.4	138.2	-

Chapter 4 TESTING PROGRAM

4.1 Introduction

Nano and macro-scale experiments were used to study the effect of various WMA technologies on the moisture susceptibility and healing characteristic of asphalt materials. The macro-scale experiments included conducting AASHTO T283 and the dynamic shear rheometer tests. In addition, different AFM based techniques were used to study the behavior of the WMA and HMA asphalt binders at the micro and nano-scale. The following sections provides a description of the employed testing experiments and approaches as well as the preparation procedures developed and used to prepare representative samples for these experiments.

4.2 Sample Preparation for AASHTO T283

The AASHTO T283 was the macro-scale test used in this study to evaluate the moisture susceptibility of the HMA and WMA mixtures. Cylindrical samples 4 inch (100 mm) in diameter and about 2.5 inch (63.4 mm) high were used in those tests. The samples were compacted using a Superpave gyratory compactor at target air void of 7.0 ± 0.5 percent. For preparing the Advera, Evotherm, and Sasobit WMA samples, the asphalt binder was first heated to the mixing temperature for three hours. WMA additives where then added slowly to the heated binder while it was stirred using a laboratory mixer. The loading rates used in this study for the Advera, Evotherm M1, and the Sasobit were 4.5 percent, 0.5 percent, and 2 percent of the asphalt binder weight, respectively. This was selected based on the recommendation by the manufacturers of these WMA additives. To prepare the foamed WMA samples, the Wirtgen WLB10 laboratory scale foaming device was used to produce the foamed asphalt binder. The amount of water used to foam the asphalt binder was 1.8 percent of the total weight of the asphalt binder. This quantity represents the maximum water content permitted by ODOT in the production of foamed WMA mixtures. To produce foamed WMA mixtures, the foaming device was first calibrated; the foamed asphalt binder was then discharged from the foaming nozzle into a mixing bowl that contains the aggregates, which has been preheated to the prescribed mixing temperature. Finally, the mixing bowl was then transferred to a mechanical mixer for mixing.

All WMA mixtures were mixed at a temperature 30°F lower than that of the HMA to ensure consistent comparison between the different types of WMA mixtures. In accordance with ODOT test protocol, the HMA and WMA mixtures were aged for four hours in the oven at a temperature of 275°F (135°C). After aging, the WMA and HMA mixtures were heated for 15 minutes at the required compaction temperature. Table 4.1 presents the mixing and compaction temperatures used for the WMA and HMA mixtures.

Table 4.1: Production temperatures for WMA mixtures.

Binder type	WMA technology	Mixing temperature		Compaction temperature	
		(°F)	(°C)	(°F)	(°C)
70-22M	Control	325.4	163.0	309.2	154.0
	Advera	294.8	146.0	278.6	137.0
	Evotherm	294.8	146.0	278.6	137.0
	Sasobit	296.6	147.0	280.4	138.0
	Foamed	294.8	146.0	278.6	137.0
64-22	Control	309.2	154.0	291.2	144.0
	Advera	278.6	137.0	260.6	127.0
	Evotherm	278.6	137.0	260.6	127.0
	Sasobit	278.6	137.0	260.6	127.0
	Foamed	278.6	137.0	260.6	127.0

4.3 AFM Sample Preparation

Prior to mixing the asphalt binder with the aggregate for each HMA and WMA mixture, samples of the asphalt binder were obtained and used for preparation of the AFM slides. Two different preparation methods were evaluated. The proceeding section provides a description of those methods.

4.3.1 Method I

The first method evaluated was similar to that presented by Tarefder & Zaman in (2010). The following steps were used to prepare the AFM samples in this method:

1. Two strips of tape were placed in parallel one inch apart on the top surface of a pre-cleaned glass slide.
2. A syringe was used to place about 0.5 ml of hot asphalt binder that was obtained during preparation of asphalt mixtures between the two strips of tape.

3. The slide was then placed in the oven for 15 minutes to allow for the asphalt to spread out.
4. The prepared samples were then placed in an airtight container and left to cool down.
5. After cooling down to the room temperature, the airtight container was placed in a Ziploc vacuum bag.

Figure 4.1 presents pictures taken during the preparation of AFM samples using method I. This method was found to be the optimum one to form uniform and consistent surfaces required for all AFM characterization techniques.

Figure 4.1: Preparation of AFM samples using method I.

4.3.2 Method II

The second method evaluated was a modified version of the Asphalt Research Consortium (ARC) method. The following steps were used to prepare the AFM samples in this method:

1. A very small amount of asphalt binder is placed on a pre-cleaned glass slide.
2. The micro slide is then covered by another slide and topped by 0.22 lb. (100 g.) weight.

3. The whole stack is then placed in the oven at a temperature of 248°F (120°C) for 20 minutes to ensure an equal distribution of the asphalt binder.
4. The two slides are then separated by sliding them.
5. Each of the two slides was finally placed in the oven for 15 minutes to allow for the asphalt to spread out.

Figure 4.2 illustrates the preparation of AFM samples using method II. This method creates a thin film of asphalt and is used to get good images for the asphalt surface. However, the thickness of the asphalt films might not be consistent through the sample, which might influence the results of the AFM force spectroscopy experiments due to boundary effects.

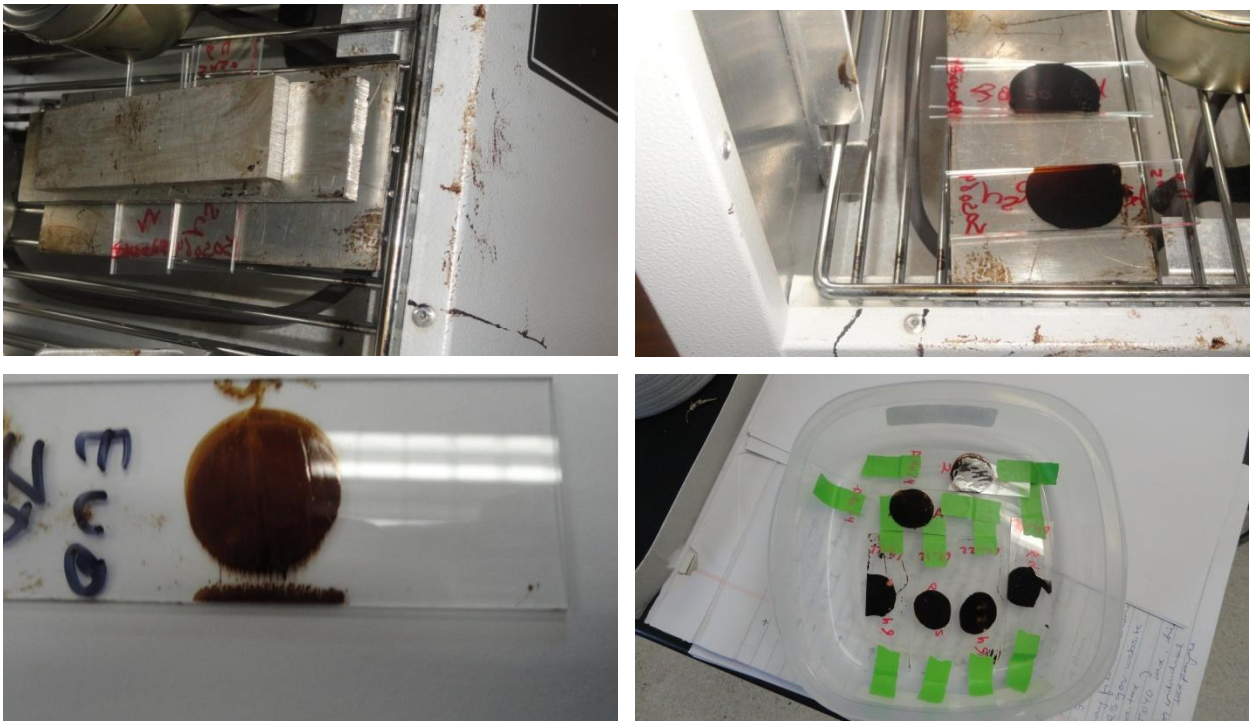

Figure 4.2: Preparation of AFM samples using method II.

4.4 Macro-Scale Charecterization of Asphalt Mixtures

4.4.1 AASHTO T283 Test

The moisture susceptibility of HMA and WMA samples was evaluated using the AASHTO T283 test procedure modified according to the standard practices implemented in the State of Ohio. At least six samples were prepared for each WMA and HMA mixture. The samples were then divided into two groups. The first group, control samples, was wrapped with

Saran-Wrap and stored at room temperature for testing in the dry condition. In addition, the second group was conditioned. The conditioning procedure involved partially saturating the samples to a level between 70 to 80 percent in a water bath under a 2.9 psi (20 kPa) vacuum pressure for approximately two to three minutes. The partially saturated samples were then wrapped and placed in a plastic bag, and 10 ml of water was added to the bag. The samples were then subjected to a freezing cycle by placing them for 16 hours in an environmental chamber set at a temperature of 0°F (–18°C). After the freezing cycle, the samples are thawed in a water bath at 140°F (60°C) for about 24 hours. Finally, the samples were conditioned for 2 hours in a water bath at a temperature of 77°F (25°C) before testing.

The indirect tensile strength test was conducted on the dry and conditioned wet samples. In this test, the cylindrical sample is loaded to failure at a deformation rate of 2 inch /min (50.8 mm/min) using a MTS 810 machine. The maximum peak load required to break he sample is recorded and used to compute the indirect tensile strength using the following equation:

$$ITS = \frac{2P}{\pi DT} \tag{4.1}$$

where,

P = the peak load, lb.

D = specimen diameter, inch

T = specimen thickness, inch

The tensile strength ratio (TSR) was then computed as the ratio between the average indirect tensile strength of the wet conditioned specimens to average indirect tensile strength of the dry unconditioned specimens. The TSR ratio is a measure of the resistance of the asphalt mixture to moisture damage. The higher the TSR ratio is, the better the resistance of the asphalt mixture to moisture-induced damage.

4.4.2 Dynamic Shear Rheometer (DSR)

Dynamic shear rheometer (DSR) test was conducted on all considered WMA and HMA binders to evaluate their viscoelastic behavior at the intermediate and high service temperatures. The binder samples for this test were obtained during the preparation of mixtures for AASHTO

T283 test. Temperature and frequency sweeps were conducted using a research grade DSR device from Rheometric Scientific. The frequency range used was between 0.1 to 100 Hz, while the temperatures ranged from 40 ^{o}F to 130^{o}F (5^{o}C to 54.4^{o}C). The dynamic shear modulus, |G*|, and phase angle, δ, were computed at different each loading frequency and testing temperatures. The rheological properties of the binders were examined by constructing a master curve for different binders. The master curve provides a relationship between binder stiffness (G*) and the reduced frequency over a range of temperatures and frequencies. Accordingly, the master curve makes it possible to estimate the viscoelastic properties over a wide frequency and temperature ranges, beyond those actually measured in the DSR test.

4.5 Micro & Nano-Scale Characterization

Various AFM based techniques were conducted on the prepared thin films of WMA and HMA asphalt binders to study their nano/micro-structure and evaluate their moisture susceptibility and healing characteristics. The following sections provide a detailed description of the used AFM equipment as well as the experiments conducted in this study.

4.5.1 AFM Equipment

The Agilent 5500LS AFM (Figure 4.3) was used to perform all the AFM experiments in this study. This device has a large, motorized stage that enables fast, accurate probe positioning for imaging and mapping large samples at nanometer-scale resolution. This stage is ideal for imaging large samples in air and fluids providing a versatile tool for characterization of different material. Samples up to six inch in diameter are easily scanned without rotation or repositioning. Agilent 5500 LS AFM can be operated with many different contact and non-contact imaging modes allowing elastic (contact), viscoelastic (FMM), magnetic (MFM), electrostatic (EFM), lateral-force (LFM) and friction (FFM) forces to be mapped. All aspects of this AFM including alignment, imaging, and calibration are controlled by PicoView software package. This software can be also used for post processing of the obtained AFM images and data. In this study PicoView software version 1.8.2 was used. Figure 4.4 presents a screenshot of this software.

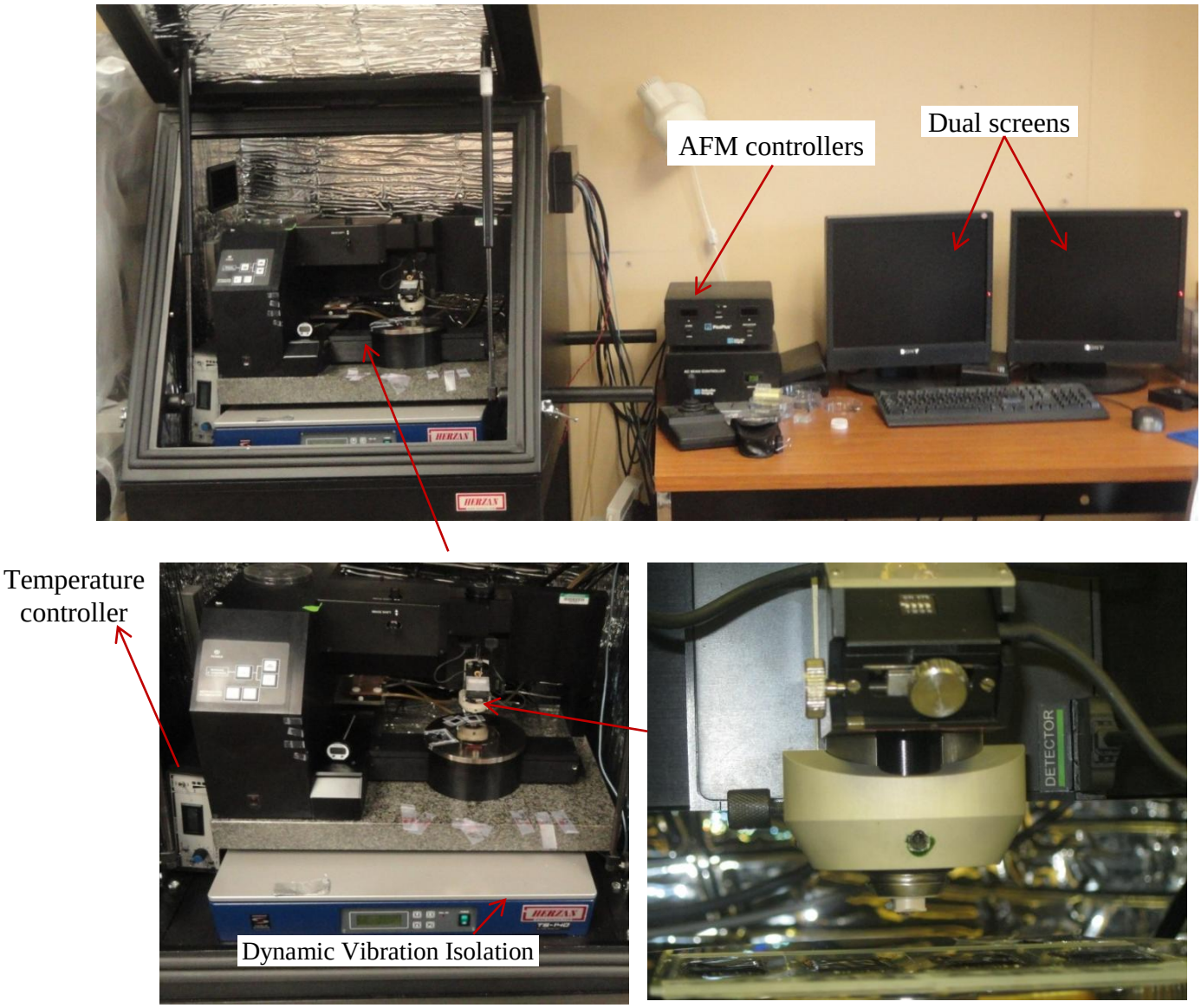

Agilent 5500LS AFM **AFM Scanner**

Figure 4.3: AFM testing setup.

4.5.2 AFM Imaging Technique

AFM imaging was performed on the prepared HMA and WMA samples using tapping mode to characterize their nano/micro-structure. The AFM tapping mode imaging technique is a versatile and powerful tool for scanning the surfaces of soft materials because it was developed to minimize sample deformation and avoid the surface and/or tip damage found in contact mode AFM. In this technique, the AFM cantilever/tip system is oscillated at its resonant frequency and

the piezo-driver is adjusted using feedback control to maintain a constant tip-to-sample distance (setpoint) (Bhushan and Qi, 2003). The amplitude of the resultant oscillations changes as the tip scans over the features on the surface. Thus, topographical characteristics of the sample can be obtained. However, in addition to the amplitude changes, the cantilever will also exhibit a phase lag in comparison with the piezo signal that drives the cantilever/tip assembly. This phase-shift is analogous to that obtained during rheological measurements where tan(ϕ)= loss modulus/storage modulus (Ferry, 1999).

One generally accepted theory is that phase contrast arises from differences in the energy dissipation between the tip and the sample (Cleveland et al., 1998; Tamayo and Garcia, 1998). According to this theory, the relation between the phase angle (ϕ) and the energy dissipated by the tip–sample interactions (Edis) per period can be described using Equation 4.2.

$$\sin\phi = \frac{\omega}{\omega_0}\frac{A_t(\omega)}{A_0} + \frac{QE_{dis}}{\pi k A_0 A_t(\omega)} \tag{4.2}$$

where

k: is the cantilever spring constant,

ω_0: is the natural resonance frequency,

Q: is the quality factor driven at a frequency ω,

A_0: is the free amplitude, and

A_t: is the tapping amplitude defined as the setpoint times the free amplitude.

Equation 4.3 only provides the dependence of phase angle on the total energy dissipation of the tip–sample interaction. However, energy dissipation occurs as a result of viscoelastic properties and interfacial adhesion (Garcia et al., 1999). Bhushan and Qi (2003) showed that when using high free amplitude or setpoint values the viscoelastic properties are the main source of the phase angle contrast. On the contrary, the effect of adhesion on phase angle contrast becomes more pronounced at low free amplitudes or setpoints. In this study, a relatively high set-point of 88% and free amplitude of 240 nm were selected to detect the discrepancies in the viscoelastic properties within the asphalt binder and map out domains with different viscoelastic properties.

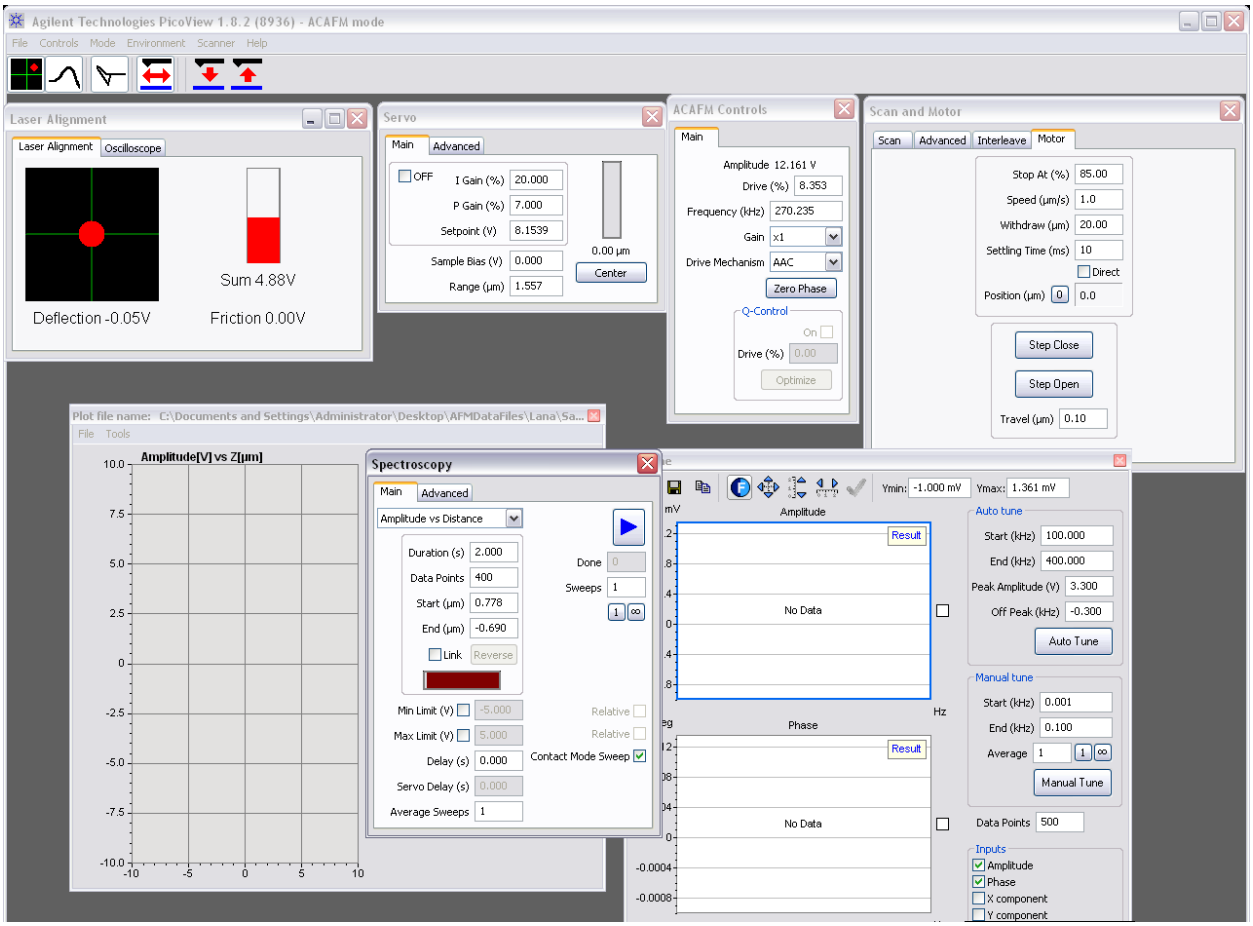

Figure 4.4: Screenshot of PicoView software.

4.5.3 Force Spectroscopy Experiments

Force spectroscopy experiments were conducted at a temperature of 77°F (25°C) on the prepared asphalt samples to measure the cohesive forces within an asphalt system. These experiments involved measuring the contact forces between the AFM tip and the sample as the tip approaches, probes, and withdraws from sample surface. The penetration depth was selected deep enough to minimize the surface effect, but was less than 10% of the film thickness so that measurements are not be affected by the glass substrate below the asphalt film. The same indentation depth and speed (350 nm/s) was used for all the experiments.

In this study, the force spectroscopy experiments were conducted with silicon nitride tips to examine adhesive forces between the asphalt and gravel aggregate. Furthermore, the interaction between asphalt molecules (i.e. cohesive forces) was examined by using tips that are chemically functionalized by two of the main chemical groups found in asphalt binders, namely

Hydroxyl (-OH) and carboxyl (-COOH) group. The tip functionalization was performed at Novascan Technologies in Ames, Iowa. The cantilevers used in this study had the same properties: 125μm long with a drive frequency ranging between 120 kHz and 160 kHz and spring constant of 4 N/m.

Force spectroscopy experiments were conducted on unconditioned and moisture-conditioned samples. Samples were conditioned by placing them in a bath of tap water at a temperature of 77°F (25°C) for 24 hours. The samples were then removed and were left to dry out for 24 hours in a dry chamber. Nitrogen gas was then used to ensure complete dryness of the surface. Unconditioned samples were also kept inside a dry chamber at the same temperature to maintain equal testing conditions.

4.5.4 AFM Experiments for Healing

An AFM-based approach that was developed in a previous work by the principle investigator (Nazzal et al. 2012) was employed in this study to examine the healing characteristics of HMA and WMA binder. The healing phenomena in asphalt materials can be described as a combination of two mechanisms: the wetting and intrinsic healing. The employed approach evaluates the wetting mechanism of the healing process, by probing (indenting) the asphalt sample using the AFM tip at a fixed location and indentation depth, to create a nano-crack in the sample. AFM images are then continually taken to record the asphalt crack recovery with time. The AFM imaging is done using tapping (intermittent-contact) mode. The topographical images are post-processed and analyzed to measure the closure of the initiated crack with time, which can be used to evaluate the wetting rate for the tested asphalt materials. The employed approach also evaluates the intrinsic healing, which is the mechanism in which the strength is gained by the wetted crack interface. This is done by determining the energy required to overcome the cohesion bonds within the asphalt material, referred to as the cohesive bonding energy, by utilizing the results of the force spectroscopy experiments performed using tips functionalized with –OH and –COOH.

Chapter 5 TEST RESULTS AND DATA ANALYSIS

5.1 Introduction

This chapter presents the results of the macro-scale tests and the different AFM experiments that were conducted on the WMA and HMA materials to evaluate their micro-structure, moisture susceptibility, and healing characteristics. A comparison between the results obtained in macro-scale tests and AFM experiments is also provided. The chapter is divided into several sections. The layout of each section includes first the presentation and discussion of the test results. This is followed by summarizing the outcome of the statistical analyses that were conducted on the experimental data.

5.2 AASHTO T283 Test Results

AASHTO T283 was the macro-scale test employed in this study to evaluate the moisture susceptibility of WMA and HMA mixtures. The test was conducted on dry and wet conditioned samples, and the indirect tensile strength was determined for those samples. The tensile strength ratio (TSR) was also computed by dividing the average ITS value of the wet conditioned samples by that of the dry samples. The proceeding section provides the results for WMA and HMA mixtures considered in this study.

5.2.1 *Results of 70-22M Mixtures*

Figure 5.1 presents the average and standard deviation of the ITS values for the dry WMA and HMA mixtures prepared using the PG 70-22M binder. It is noted that all WMA mixtures except the foamed WMA mixture had lower ITS value. The Sasobit had the least value among all other WMA mixtures. Previous researchers attributed the lower ITS values in WMA mixtures to the reduction in mixing and compaction temperature, which may result in less aging of those mixtures as compared to the HMA. In addition, the influence of WMA technologies on the asphalt binder properties have been used to explain the decrease in the ITS value. This influence was evaluated in this study using the AFM experiments as discussed in the proceeding sections.

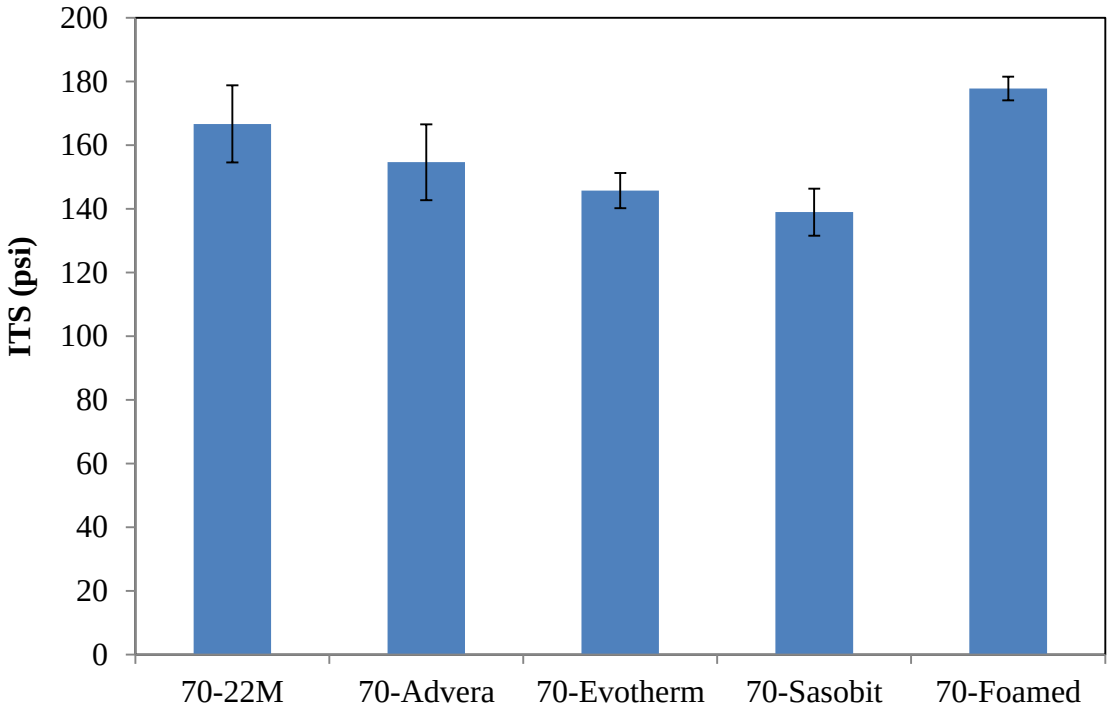

Figure 5.1: ITS of dry HMA and WMA 70-22M samples.

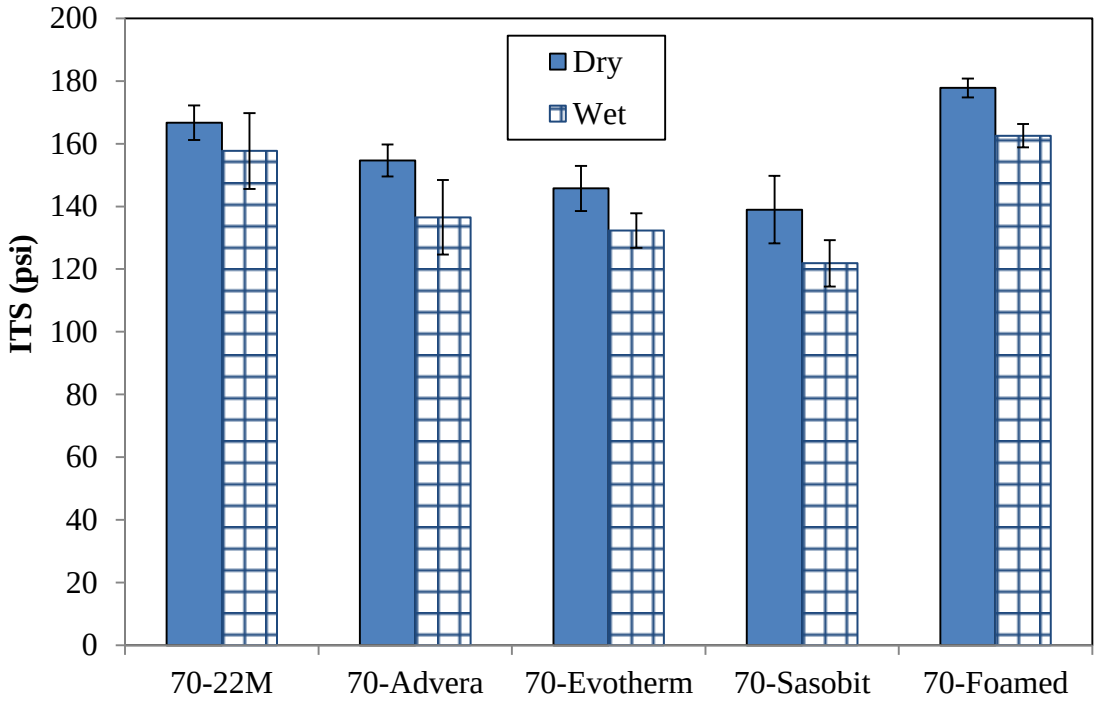

Figure 5.2: ITS of conditioned HMA and WMA 70-22M samples.

Figure 5.2 compares the average ITS values for wet and dry WMA and HMA samples prepared using PG 70-22M binder. The conditioning of the HMA and WMA mixtures has resulted in reducing their average ITS values. The conditioned WMA mixtures exhibited lower ITS values as compared to the conditioned HMA, but the mixtures still had the same rankings as that observed for the dry ones. The Sasobit and Advera had slightly higher reduction in the ITS values upon conditioning as compared to the other types of WMA mixtures as well as the HMA mixture. This can be also noticed in Figure 5.3, which presents the TSR values for the different WMA and HMA mixture containing PG 70-22M binder. It is worth noting that all mixtures had TSR values higher then 0.8, which is the minimum TSR value specified in ODOT C&MS for heavy traffic Superpave surface mixtures.

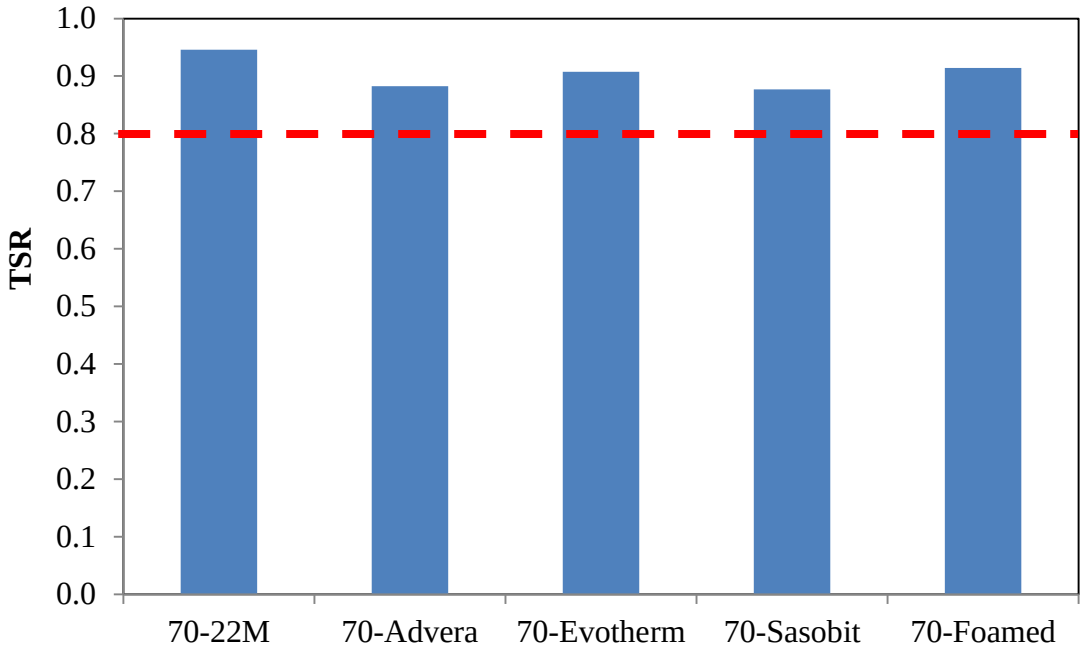

Figure 5.3: TSR values for HMA and WMA 70-22M mixtures.

Single factor Analysis of Variance (ANOVA) and post ANOVA Least Square Mean (LSM) analyses were conducted using Statistical Analysis Software (SAS) (SAS Institute Inc., 2004) to statistically evaluate the results in Figures 5.1 and 5.2. Table 5.1 presents the results of the ANOVA analysis. At 95% confidence level (p-value<0.05), the effect of WMA technology was significant on the ITS of the dry and conditioned samples. Table 5.2 presents the results of the grouping of the different asphalt mixtures that was determined using the post ANOVA LSM

analysis. In this table, the groups are listed in descending order with the letter "A" assigned to the highest mean followed by the other letters in appropriate order. In addition, groups with same letter next to them are not significantly different. It is noted that the for dry mixtures, 70-Sasobit mixture had statistically lower ITS values than the control HMA mix, while others were statistically indistinguishable from it. In addition, for the conditioned mixtures, the ITS values of all WMA mixes were statistically similar except for the foamed one that had higher value, which was statistically similar to that of the control HMA mix.

Table 5.1: Results of ANOVA analysis on ITS of 70-22M mixtures.

Effect	F Value	p-value
WMA Technology - Dry Samples	17.26	<.0001
WMA Technology - Conditioned Samples	13.78	<.0001

Table 5.2: Results of Post ANOVA LSM analyses on ITS of 70-22M mixtures.

Grouping Of Dry 70-22M Mixtures		
WMA Technology	ITS (psi)	Letter Group
70-Foamed	177.29	A
70-22M (Control)	166.60	AB
70-Advera	154.67	BC
70-Evotherm	145.76	C
70-Sasobit	138.96	D
Grouping Of Conditioned 70-22M Mixtures		
Mixture Type	ITS (psi)	Letter Group
70-Foamed	167.61	A
70-22M (Control)	157.68	A
70-Advera	136.51	B
70-Evotherm	132.31	B
70-Sasobit	121.86	B

5.2.2 *Results of 64-22 Mixtures*

Figure 5.4 presents the average ITS values for the dry WMA and HMA mixtures containing the PG 64-22 binder, respectively. The ITS values of those mixtures shows the same trend and rankings observed for the mixtures containing PG 70-22M binder, such that the foamed WMA mixture had the highest average ITS value that was similar to that of the HMA, while the Sasobit WMA had the lowest value. Figure 5.5 shows the average ITS values for conditioned and dry WMA and HMA samples prepared using PG 64-22 binder. The average ITS values of conditioned HMA and WMA samples were lower than those of the dry ones. In addition, the conditioned WMA mixtures showed lower ITS values as compared to the conditioned control HMA. The Advera and Sasobit had much more pronounced reduction in the ITS values upon conditioning as compared to the other WMA and HMA. Figure 5.6, shows the TSR values for different WMA and HMA mixtures. It is noted that the TSR values of the WMA and HMA mixtures prepared with the PG 64-22 binder are lower than those prepared with the PG 70-22M binder. Furthermore, the Advera had the lowest TSR value among all WMA and HMA mixtures, while the Evotherm had highest value. This high TSR value of the Evotherm might be attributed to the anti-strip liquid that this type of WMA technology contains.

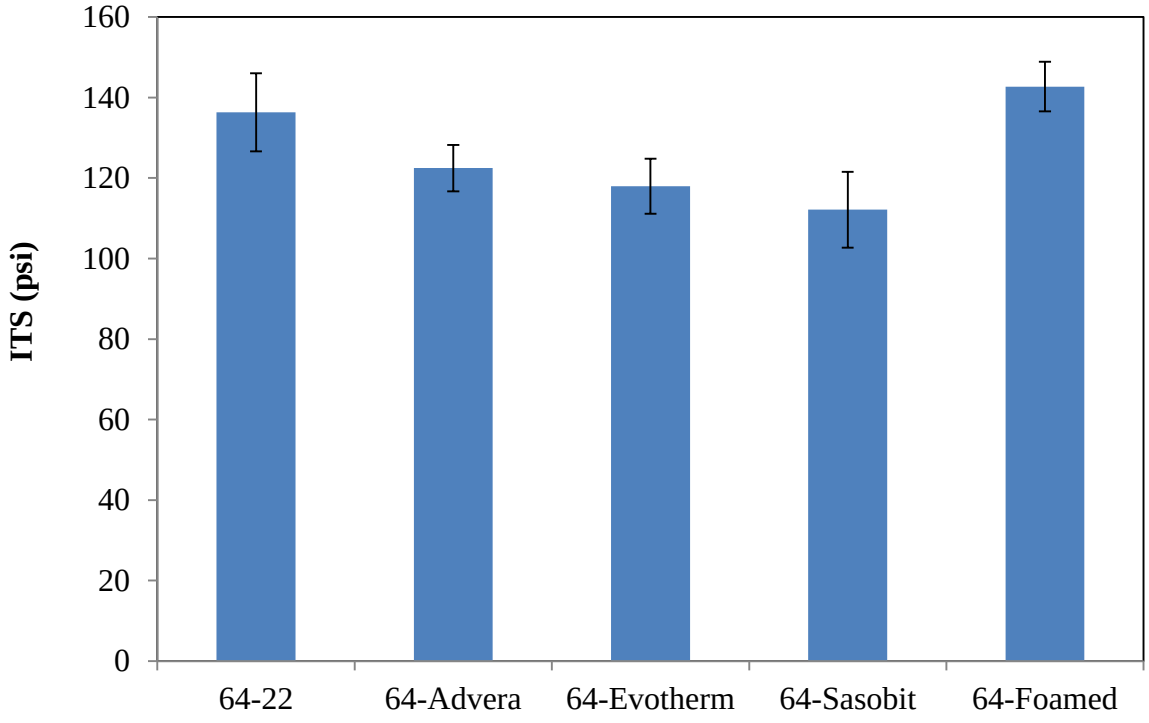

Figure 5.4: ITS of dry HMA and WMA 64-22 samples.

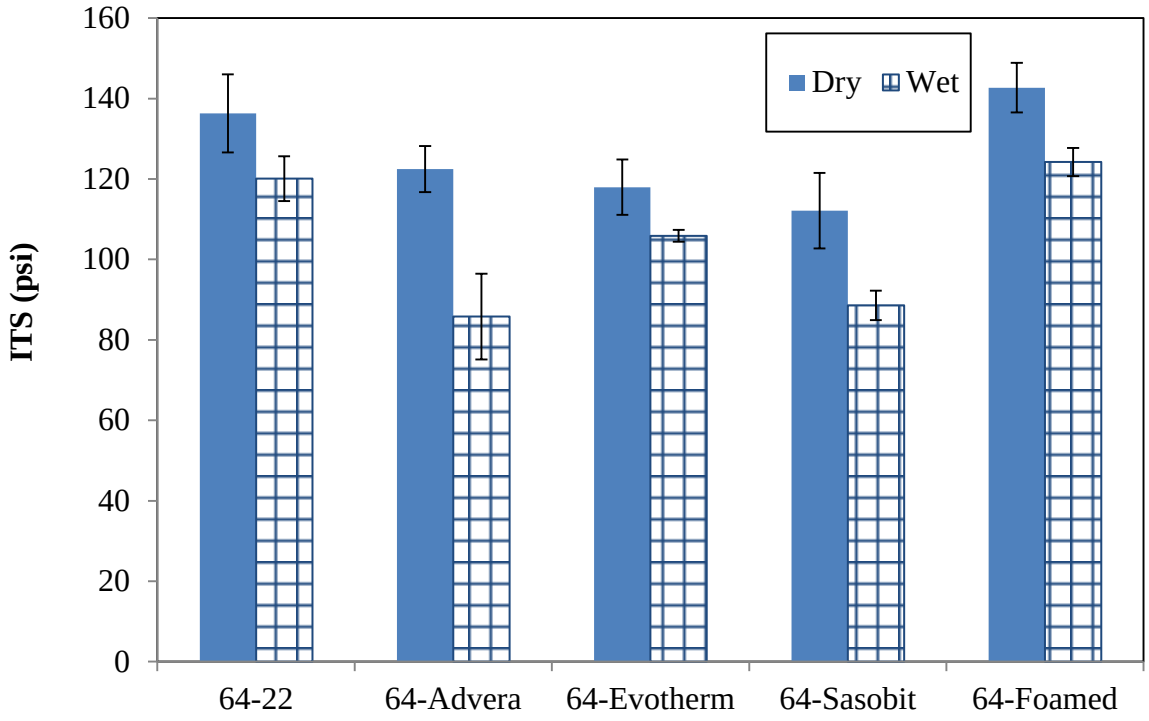

Figure 5.5: ITS of conditioned HMA and WMA 64-22 samples.

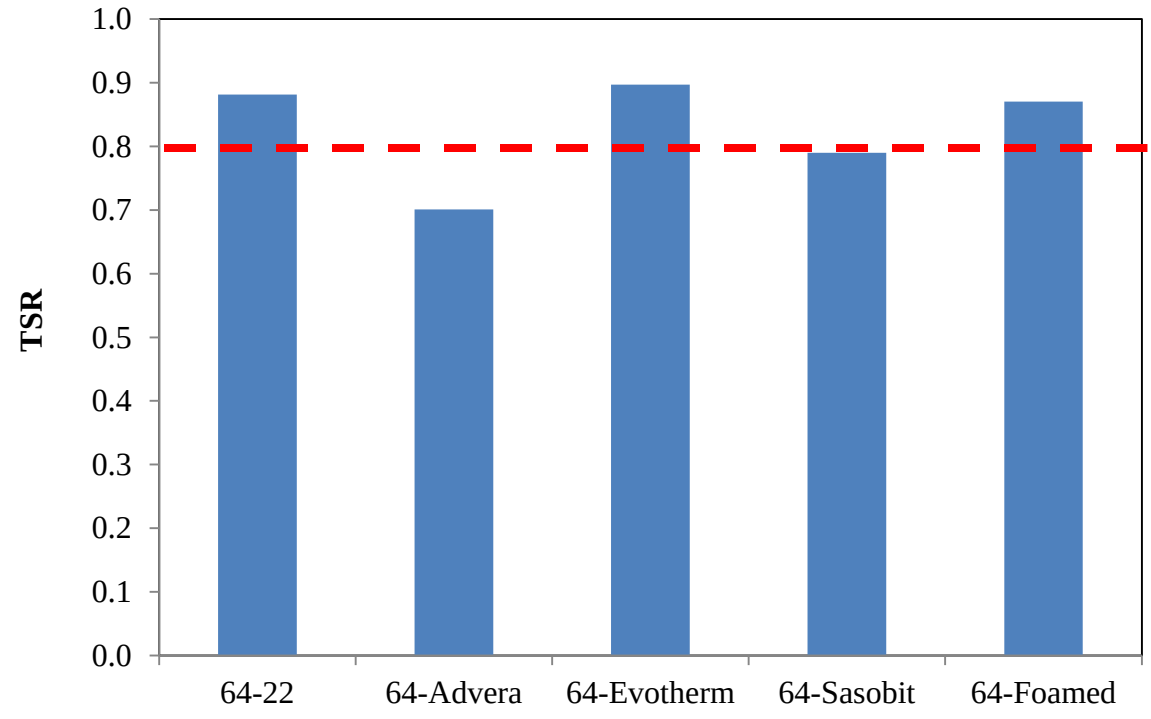

Figure 5.6: TSR values for HMA and WMA 64-22 mixtures.

A single factor ANOVA analyses were conducted to statistically evaluate the effects of the mixture type on the ITS values of dry and conditioned samples. Table 5.3 presents the results of the ANOVA analyses. The effect of WMA technology on the ITS values of dry and conditioned samples was significant at 95% confidence level (p-value<0.05). However, the WMA technology had more pronounced effect on the conditioned samples, as indicated by the F-value. This suggests that the use of some WMA technologies may significantly affect the moisture sensitivity of asphalt mixtures. Table 5.4 provides the ranking of the different asphalt mixtures that was determined using the post ANOVA LSM analyses. It is noted that the for dry unconditioned mixtures, only the 64-Sasobit mixture had statistically lower ITS value than the control HMA mix, while the other WMA mixtures had statistically similar ITS values. On the other hand, for conditioned mixtures, the ITS values of the Advera and Sasobit WMA mixture exhibited statistically lower ITS values than that of the HMA control mixture. The Evotherm and foamed WMA had statistically indistinguishable ITS values from that of the control HMA mix.

Table 5.3: Results of ANOVA analysis on the ITS of 64-22 mixtures.

Effect	F-value	p-value
WMA Technology - Dry Samples	5.44	0.0137
WMA Technology - Conditioned Samples	16.31	0.0002

5.2.3 Influence of Different Factors on ITS

Multi-factor ANOVA analysis was conducted on AASHTO T283 test results for all mixtures prepared with the different binders to examine effect of binder type, WMA technology, conditioning and their interactions on the ITS value. A linear Completely Random Design (CRD) model presented Equation 5.1 was used in this analysis. The dependent variable used in the analysis was the ITS.

$$ITS = \mu + \tau_{1i} + \tau_{2j} + \tau_{3k} + \tau_1\tau_{2ij} + \tau_1\tau_{3ik} + \tau_2\tau_{3jk} + \tau_1\tau_2\tau_{3ijk} + \varepsilon_{ijkl} \quad 5.1$$

where

μ: is the overall mean

τ_{1i} : is the effect of binder type

τ_{2j} : is the effect of WMA technology

τ_{3k} : is the effect of conditioning

$\tau_1\tau_{2ij}$: is effect of the interaction between the binder type and WMA technology

$\tau_1\tau_{3ik}$:is effect of the interaction between the binder type and conditioning

$\tau_2\tau_{3ik}$: is effect of the interaction between the WMA technology and conditioning

$\tau_1\tau_2\tau_{3ijk}$: is effect of the interaction between the binder type, WMA technology and conditioning

ϵ_{ijkl} : is the random sampling variation.

Table 5.4: Results of Post ANOVA analyses on the ITS of 64-22 mixtures.

Grouping Of Dry 64-22 Mixtures		
WMA Technology	ITS (psi)	Letter Group
64-Foamed	142.71	A
64-22	136.31	AB
64-Advera	122.46	ABC
64-Evotherm	117.97	BC
64-Sasobit	112.12	C
Grouping Of Conditioned 64-22 Mixtures		
WMA Technology	ITS (psi)	Letter Group
64-Foamed	126.24	A
64-22	111.26	AB
64-Evotherm	100.51	BC
64-Sasobit	88.56	C
64-Advera	85.82	C

Table 5.5 presents the results of the multi-factor ANOVA analysis. It is noted that, at a 95% confidence level, the binder type, WMA technology and conditioning had significant effect on the ITS value. The binder type was the most significant factor affecting the ITS values, as indicated by the F-value. The binder type and conditioning interaction ($\tau_1\tau_{2ij}$) effect was significant at 95% confidence level. This suggests that the influence of moisture conditioning

varies between the two types of binders, which is expected as the use of polymer modified binder improves the moisture susceptibility of the asphalt mixture. Furthermore, the results in Table 5.5 indicates that the WMA technology -binder type interaction had significant effect at a confidence level of 91% only. This may suggest that the effect of WMA technology depends to a certain extent on the type of binder used.

Table 5.5: Results of multi-factor ANOVA analyses on ITS values.

Effect	F Value	p-value
Binder type	332.42	<.0001
WMA technology	45.43	<.0001
Binder* WMA technology	2.15	0.0895
Conditioning	95.01	<.0001
Binder*Conditioning	8.25	0.0061
WMA technology*Conditioning	1.77	0.1500
Binder*WMA technology*Conditioning	0.46	0.7671

5.3 Results of DSR

The shear modulus (G*) values obtained from the DSR test results were used to construct the master curves of all considered polymer modified and neat asphalt binders. The master curve provides the relationship of the G* as a function of the reduced frequency (ω_r). In this study, the Christensen-Anderson model (Equation 5.2) was used to develop the master curve at a reference temperature of 77°F (25°C), which is the temperature at which all other tests were conducted.

$$G^*(\omega) = G_g\left[1+\left(\frac{\omega_c}{\omega_r}\right)^{\frac{\log 2}{R}}\right]^{\frac{-R}{\log 2}} \quad (5.2)$$

where,

$G^*(\omega)$: is the complex shear modulus

G_g : is the glass modulus assumed equal to 1GPa

ω_r : is the reduced frequency at the defining temperature, rad/sec

ω_c : is the cross over frequency at the defining temperature, rad/sec

ω : is the frequency, rad/sec

R : is the rheological index

Figure 5.7 presents the master curves obtained for the control and WMA 70-22M binders. It is noted that the foamed WMA binder had lower G* values as compared to the control PG 70-22M binder. On the other hand, the Sasobit had higher G* values, particularly at lower reduced frequency values and hence at high temperature and low frequency values. Finally, the Advera and Evotherm did not show any significant effect on the stiffness of the PG 70-22M binder.

Figure 5.8 shows the master curves for the different PG 64-22 binders. It is clear that the Sasobit have stiffened the PG 64-22 asphalt binder and resulted in higher G* modulus values. Furthermore, the Evotherm had resulted in a slight increase in the G*. However, the Advera resulted in a decrease in the G* of the PG 64-22 binder. Finally, the foaming of the PG 64-22 binder did not have a significant effect on its G* values and hence its stiffness.

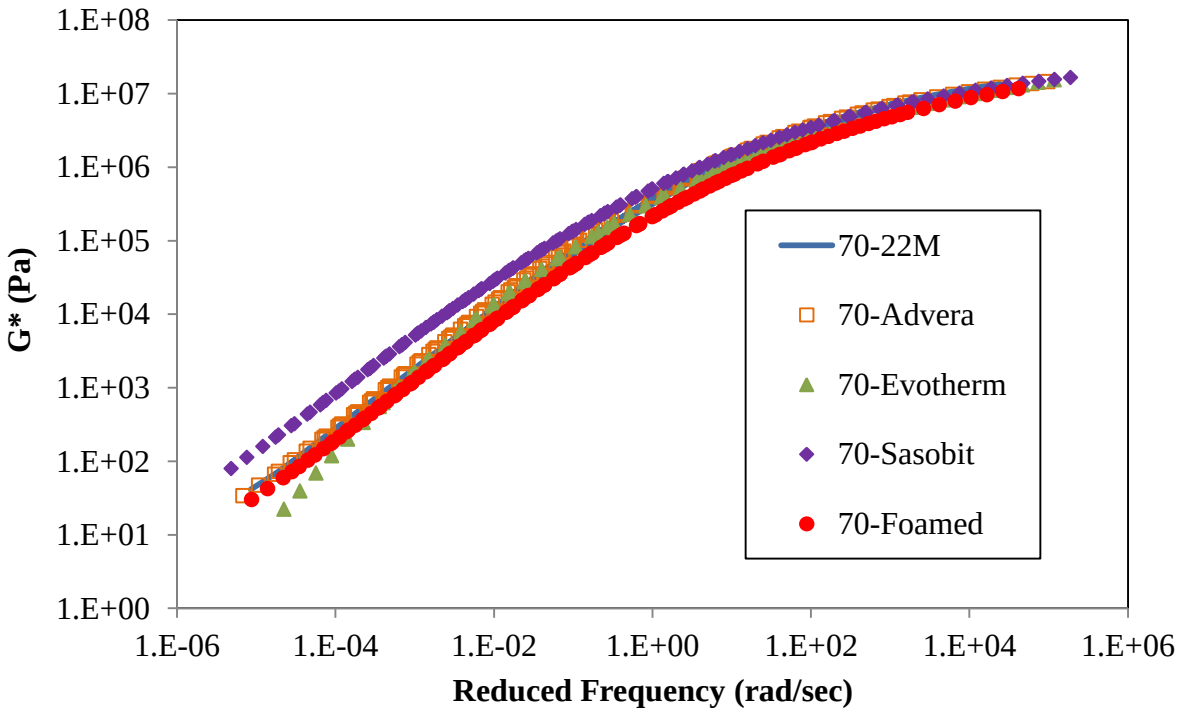

Figure 5.7: Master curve for 70-22M binders.

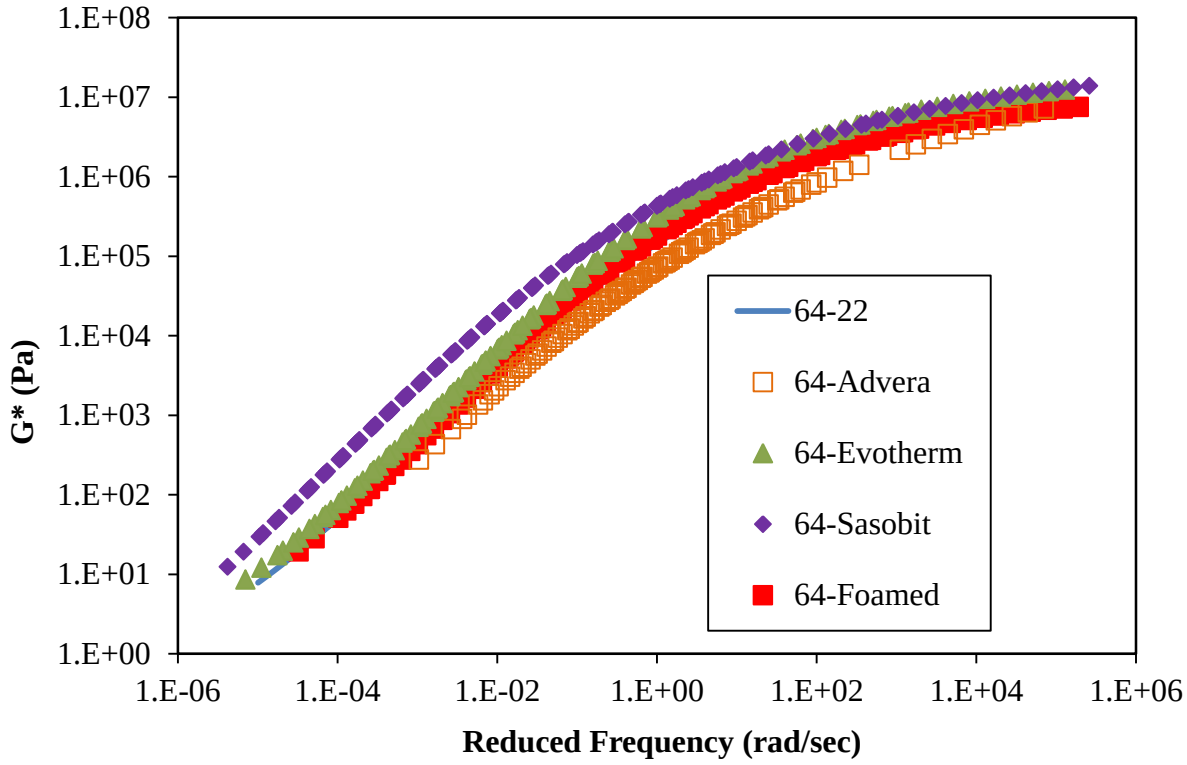

Figure 5.8: Master curve for 64-22 binders.

5.4 Results of AFM Imaging

5.4.1 Micro & Nano-Structure Characterization of 70-22M Binders

The images obtained using the tapping AFM mode was used to examine the effects of the WMA additives on the nano/micro-structure of the PG 70-22M asphalt binder. Figures 5.9 through 5.13 present the topographical and phase images of control 70-22M, Advera, Evotherm, Sasobit, and foamed asphalt binders, respectively. It is noted that those images are representative of many similar scans that were consistently observed across the prepared samples. Asphalt binder is a mixture of hydrocarbons but contain a variety of functional groups such as heteroatoms of carbon and hydrogen, and metals like vanadium and nickel. The phase images show that the investigated asphalt materials are not perfectly homogeneous and that not all the hydrocarbons are mutually soluble at room temperature. In these images there is a flat background in which another phase characterized by a darker color is dispersed. Included in this darker phase is an elongated structure identified by succession of pale and dark lines, which is often called ‘bee-like’ structure. Previous researchers have attributed the appearance of the ‘bee-like’ structure to the asphaltene content (Loeber et al., 1998). Asphaltene is the high-molecular

weight component of an asphalt binder that is insoluble in aliphatic solvents, but soluble in aromatic solvents (e.g. in toluene or benzene) and have the highly polar molecular structure (Petersen, 1984).

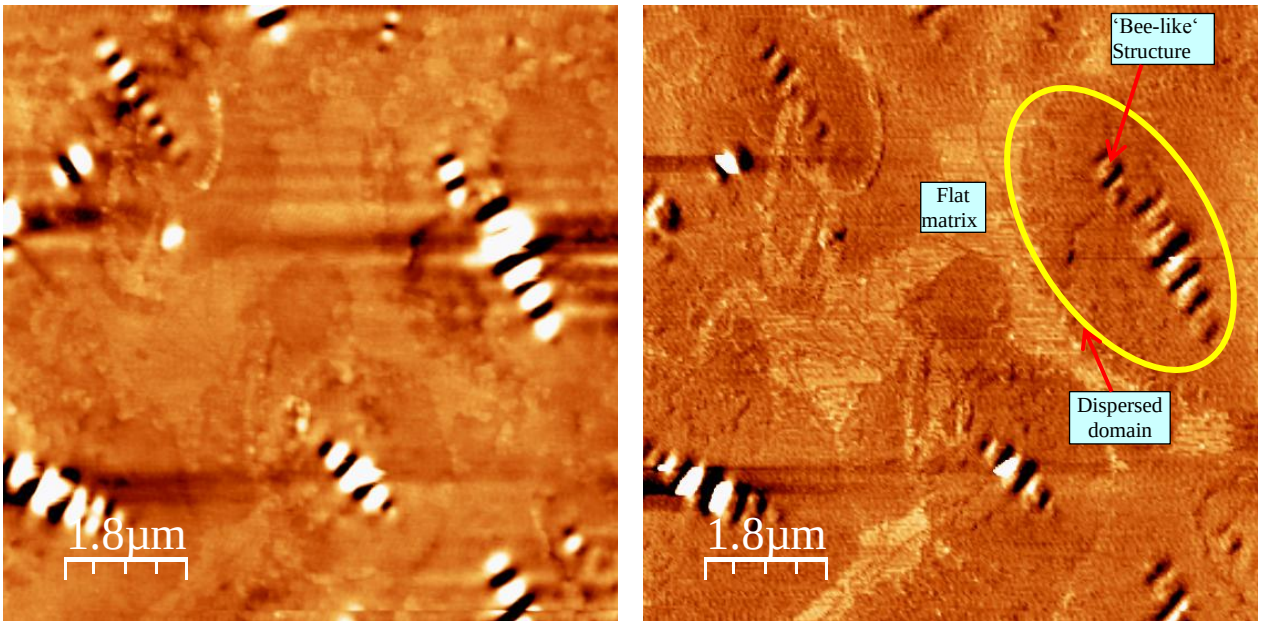

Figure 5.9: AFM images of control 70-22M binder: (a) Topographical images (b) Phase images.

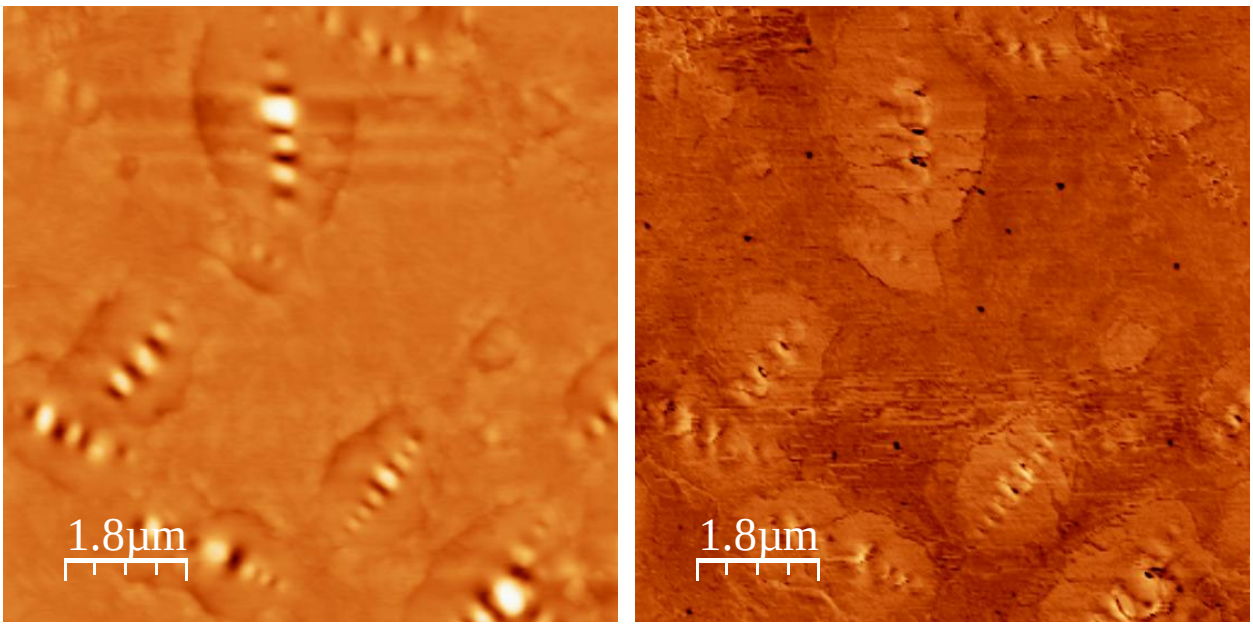

Figure 5.10: AFM images of 70-Advera binder: (a) Topographical images (b) Phase images.

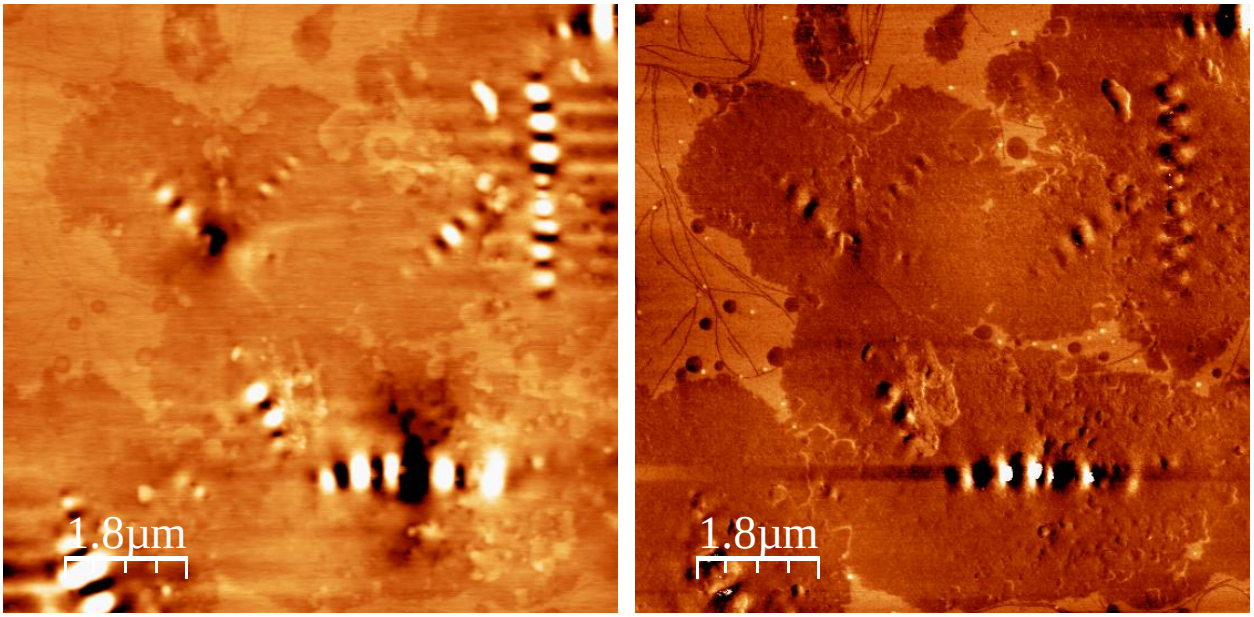

Figure 5.11: AFM images of 70-Evotherrm binder: (a) Topographical images (b) Phase images.

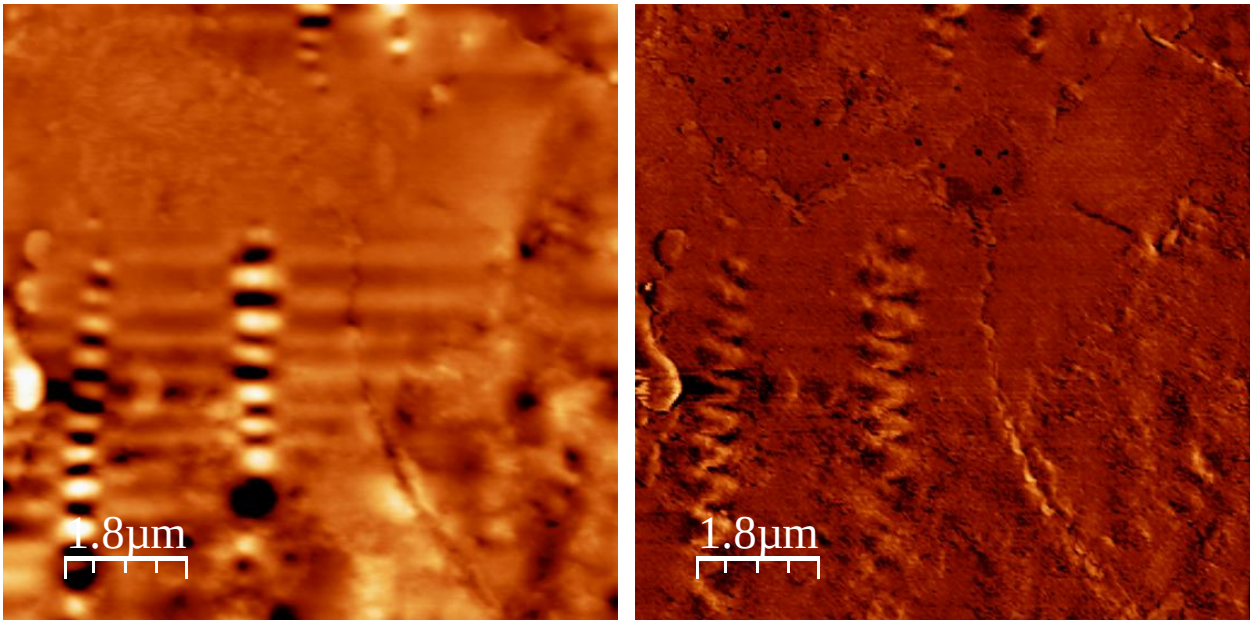

Figure 5.12: AFM images of 70-Sasobit binder: (a) Topographical images (b) Phase images.

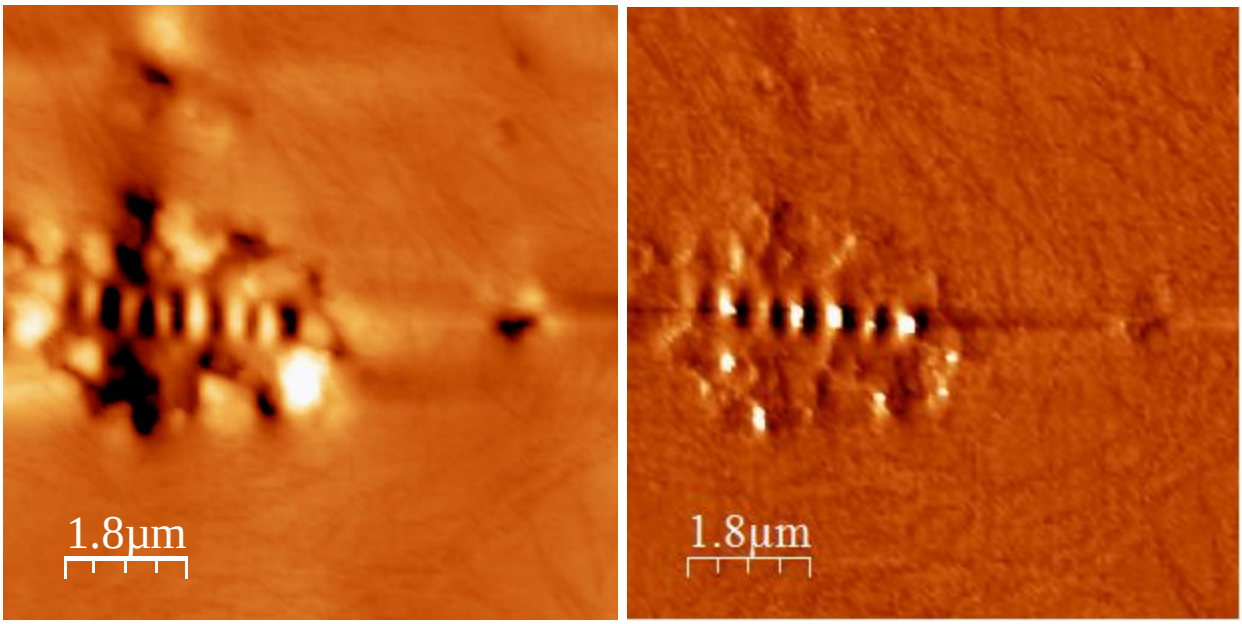

Figure 5.13: AFM images of 70-Foamed binder: (a) Topographical images (b) Phase images.

The ‘bee-like’ structures can be also attributed to the microcrystalline waxes and the highly aromatics and long alkyl chain asphaltenes (waxy molecules) contained in asphaltenes, which crystallize during cooling to the testing temperature (Lu et al., 2005). This results in highly insoluble organic composites in the asphalt that forms a phase-separated microstructure, which contributes to the formation of ‘bee-like’ structures. Masson et al. (2006) also suggested that the ‘bee-like’ structure is related to the vanadium and nickel content in the asphalt binder. It is worth noting that asphaltene polarity has known to be attributed to the heteroatoms in the asphalt (Petersen, 1984). Thus, the results by Masson et al. (2006) may indicate that the ‘bee-like’ structure is affected by the asphaltene polarity.

Figures 5.10, 5.11 and 5.13 show that the AFM images for the inclusion of Advera and Evotherm additives or the foaming of the PG 70-22M asphalt binder did not significantly affect the dimension of the ‘bee-like’ structures. On the other hand, the inclusion of the Sasobit additives (Figure 5.12) has affected the bee-like structures by reducing their size, such that the bee structures appeared in long chains with much smaller width than those in the control asphalt binder. This may be attributed to the waxy molecules of the Sasobit that obstructs the movement of asphalt molecule chains, and results in preventing the crystallization of microcrystalline waxes and waxy molecules.

By comparing phase images obtained for the control asphalt binder (Figure 5.9) with those WMA modified asphalt binder (Figures 5.10-5.13), it is noted that the phase contrast between the dispersed domains and the flat asphalt matrix is inverted upon the inclusion of the Advera additive. This result may indicate that the Advera resulted in reducing the stiffness of the dispersed domain, such that the relative difference between the stiffness of those domains and the flat asphalt matrix is reversed. Furthermore, the Evotherm did not have a significant influence on the phase contrast observed in the control binder. Finally, the phase contrast between the dispersed domains and the flat matrix is increased with the inclusion of the Sasobit. According to the phase contrast changes between the dispersed domains and the matrix, the dispersed domains will be stiffer after adding the Sasobit material. The stiffer domains may result in enhancing of the stiffness properties of the Sasobit modified asphalt as compared to the control asphalt binder. This is consistent with the DSR test results that were conducted on the different binders and showed that the 70-Sasobit binder had the highest G* values and hence stiffness. Finally, Figure 5.13 is showing that the phase contrast difference between the dispersed domain and flat matrix observed in the control 70-22M binder was reduced due to the foaming; indicating that relative stiffness of the dispersed domain was reduced. It is worth noting that the 70-foamed binder had lower G* values as compared to the other 70-22M binders, which may be explained by the changes in the micro-structure noticed in the AFM images.

5.4.2 Micro & Nano-Structure Characterization of 64-22 Binders

Figures 5.14 through 5.18 present the topographical and phase images for the control and WMA 64-22 binders. These figures are also indicating that these binders are not perfectly homogeneous such that not all the hydrocarbons are mutually soluble at testing temperature. Similar to the 70-22M binder, the 64-22 binder is characterized by a flat asphalt matrix with dispersed domains that contain the so called ‘bee-like’ structures. However, phase difference between the flat asphalt matrix and the dispersed domains is reduced when compared to the 70-22M binder. This is expected as the 70-22M binder is a stiffer, as indicated by the DSR test results. In general, all the WMA technologies except the Sasobit did not affect the dimensions of the ‘bee-like’ structures. Similar to the 70-22M binder, the Sasobit reduced the width of these structures in the 64-22 binder, which may be explained by its waxy molecules that restrains the movements of the asphalt molecules.

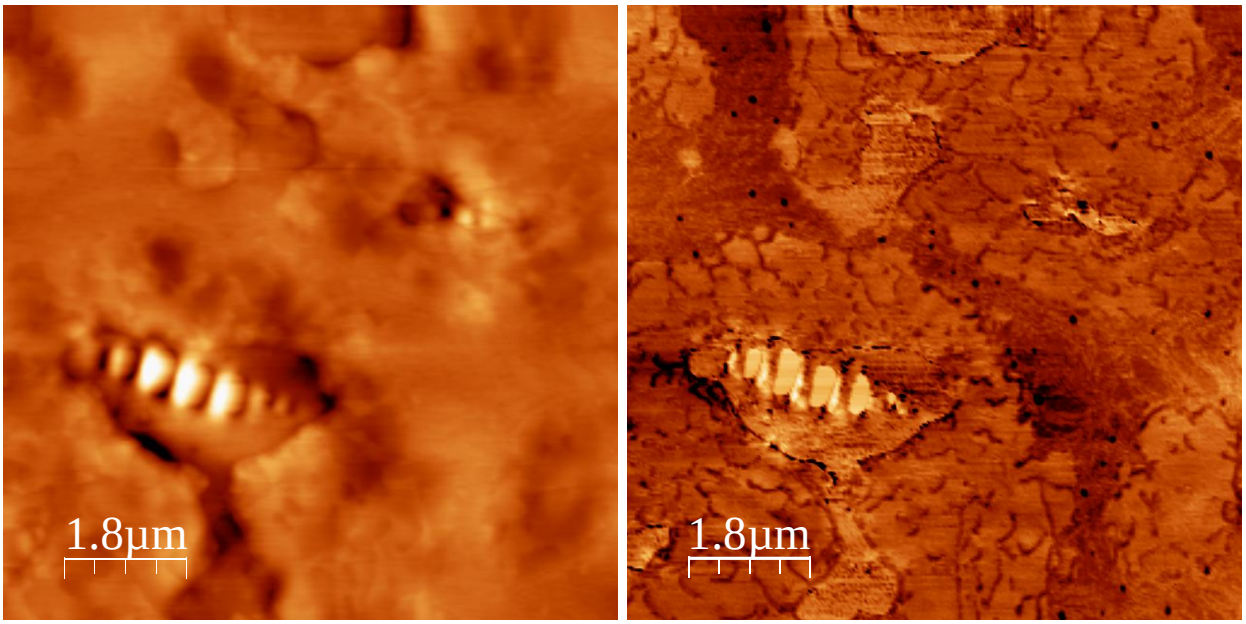

Figure 5.14: AFM images of control 64-22 asphalt binder: (a) Topographical images (b) Phase images.

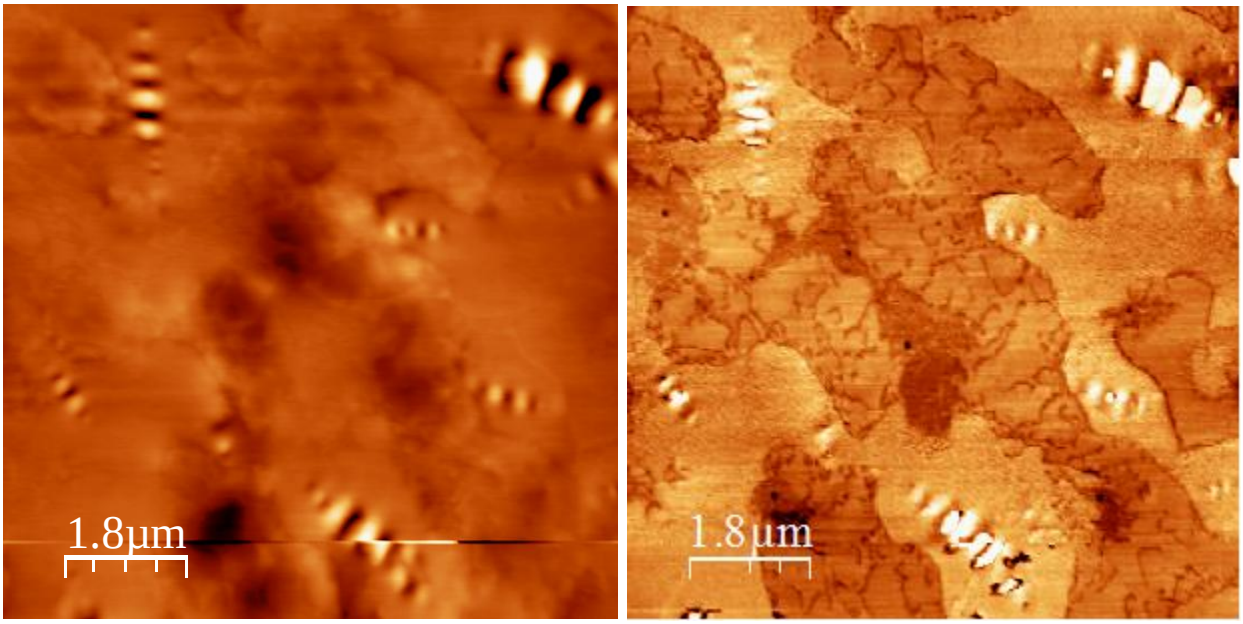

Figure 5.15: AFM images of 64-Advera binder: (a) Topographical images (b) Phase images.

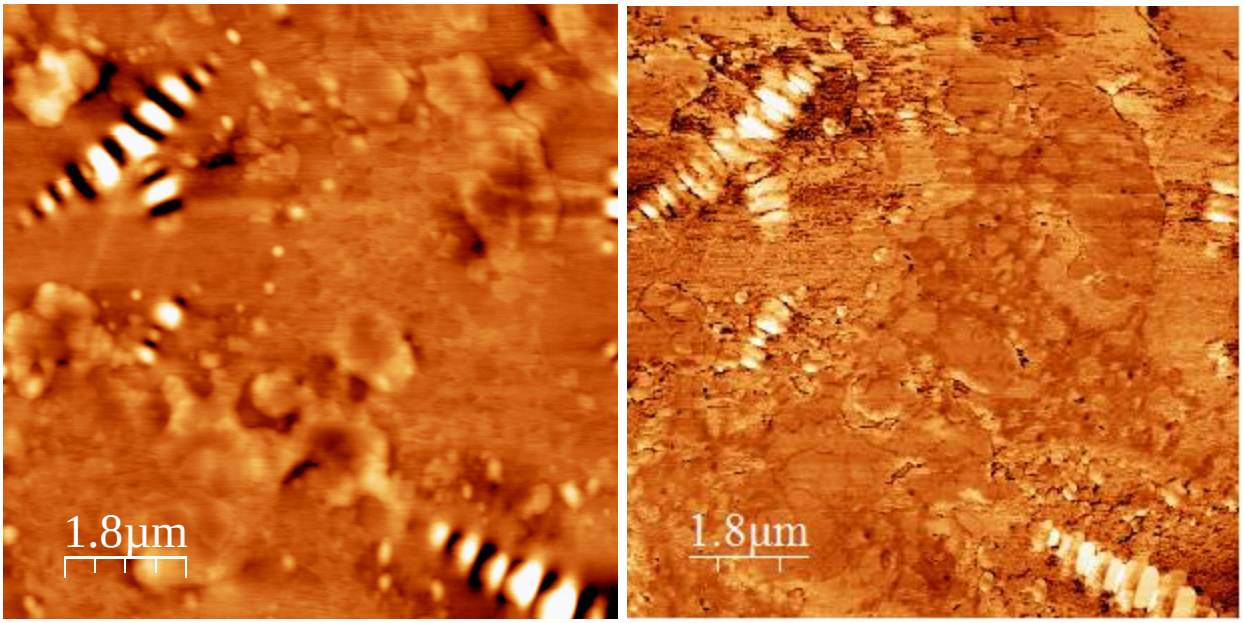

Figure 5.16: AFM images of 64-Evotherrm binder: (a) Topographical images (b) Phase images.

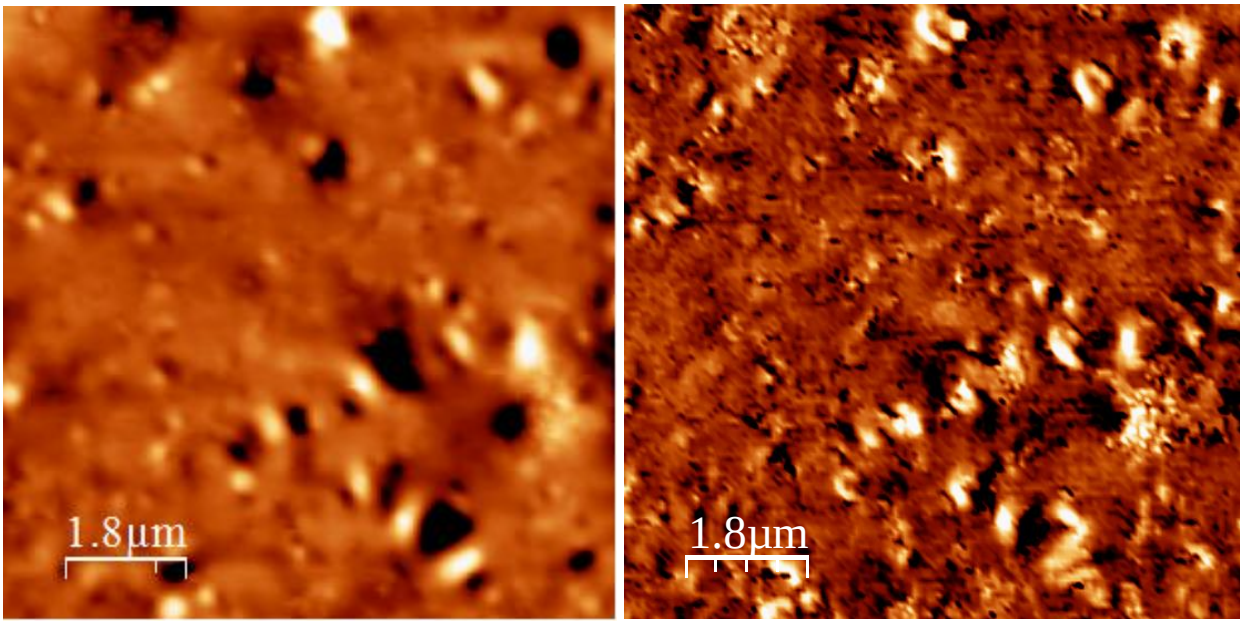

Figure 5.17: AFM images of 64-Sasobit binder: (a) Topographical images (b) Phase images.

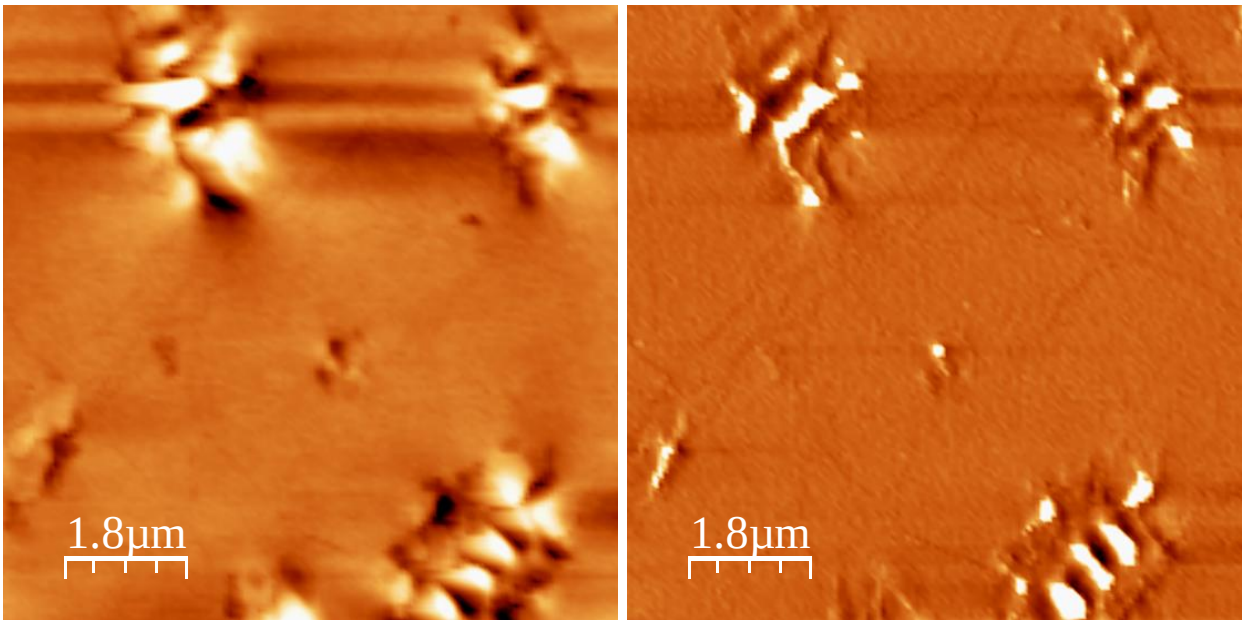

Figure 5.18: AFM images of 64-Foamed binder: (a) Topographical images (b) Phase images.

The phase images in Figure 5.15 are showing that the phase contrast between flat asphalt matrix and dispersed domain inverted due the inclusion of the Advera, which is similar to that observed in the PG 70-22M binder. Figure 5.16 indicates that the phase image was not significantly affected by the Evotherm. On the other hand, Figure 5.17, is clearly showing an increase in the phase contrast due to the Sasobit inclusion, which may suggest an increase in the binder stiffness. This is in agreement with the results obtained in the DSR test. Finally, the phase image in Figure 5.18 shows that the phase contrast between the flat matrix and the dispersed domains remained unchanged due to the foaming of the PG 64-22 asphalt binder.

5.4.3 AFM Samples Surface Roughness

The surface roughness of each of the scanned samples was evaluated by conducting roughness analysis using WSxM version 5.0 software (Horcas et al.,2007) on the obtained topographical images. In this analysis, the absolute mean of the difference between the average height and the height of each single point of the sample is computed and used to measure the average roughness. The average of values obtained from the analysis conducted on all samples for each of the control and WMA 70-22M binders is presented in Figure 5.19. It is noted that all values were less than 10 nm. In addition, it is clear that the Advera, Evotherm, and foamed WMA samples had lower average roughness value in comparison with those of the control 70-22M asphalt binder. On the contrary, the Sasobit samples had much higher the roughness.

Figure 5.20 presents the average roughness value for the control and WMA 64-22 samples. The control and WMA 64-22 samples had lower average roughness values as compared to its corresponding 70-22M samples. This indicates that the 64-22 samples had smoother surface. The surface roughness results are clearly indicating that the method used in preparing the AFM samples yields smooth asphalt films with consistent thickness. This is essential for the AFM force spectroscopy and healing experiments.

5.5 Results of Force Spectroscopy Experiments

Force distance curve is the main result obtained from force spectroscopy experiments. This curve presents a plot of the forces acting on the sample as a function of piezo-driver displacement. The forces are calculated based on the cantilever deflection using Hook's law:

$$F=-k_c\, d \tag{5.3}$$

where

F: is the acting force on the sample

d: is the deflection

k_c : is the cantilever spring constant

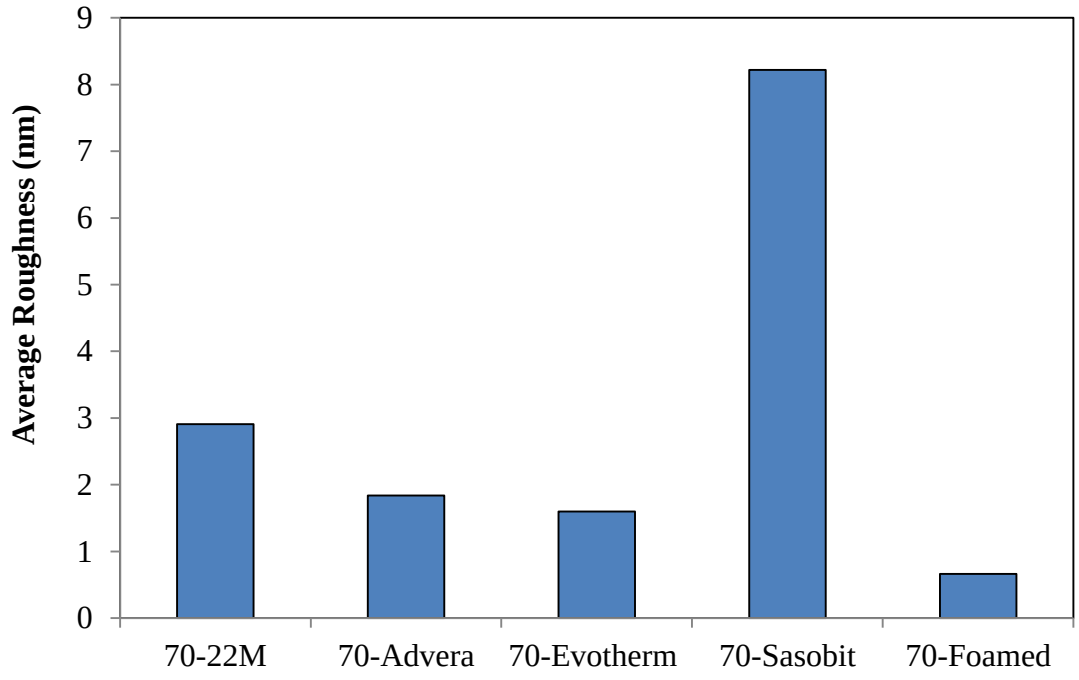

Figure 5.19: Average roughness of AFM images for 70-22M binders.

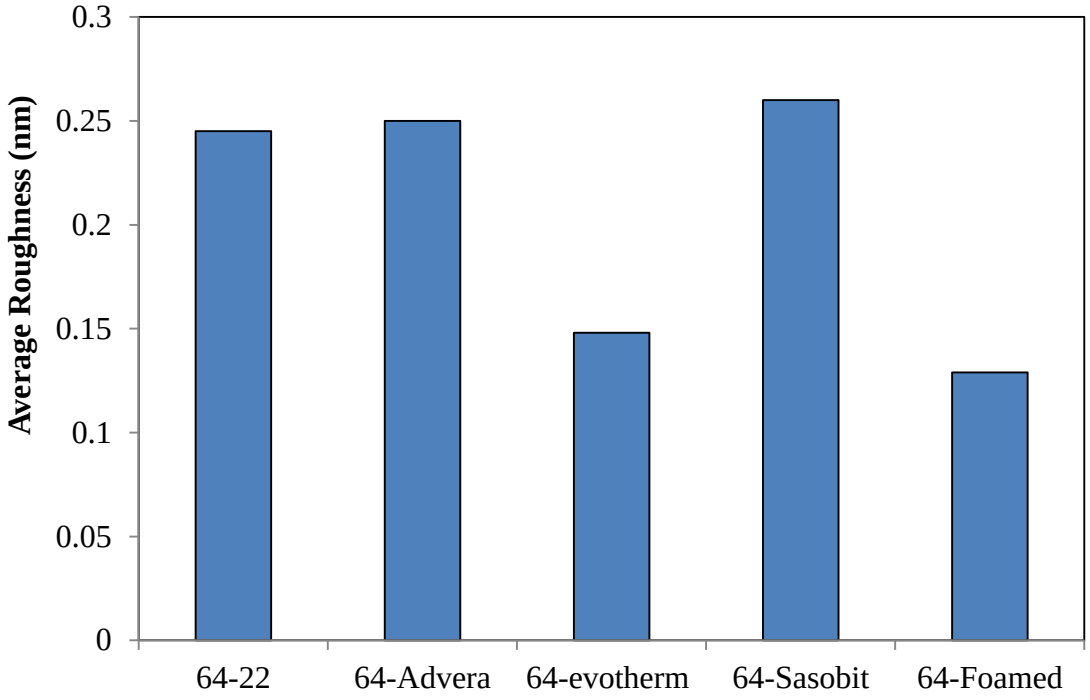

Figure 5.20: Average roughness of AFM images for 64-22 binders.

Figure 5.21 presents typical force distance curves for the investigated 70-22M asphalt materials. This curve can be divided into two regions the approaching region where the tip is brought close to the sample until a contact between the tip and sample occurs and the retracting region where the tip starts to pull away from the sample. In the former region, the tip starts to approach the sample surface by moving towards the sample. Initially, the tip will be far away from the sample and no deflection will happen until it is brought close enough to the surface where it start to deflect due to the repulsive force. The repulsive force increases until reaching to a specified depth of indentation. In the retracting region, initially the repulsive force, hence the deflection is reduced. However, as the retraction continues, the tip sticks to the sample surface due to the attractive forces for a certain time till it finally snaps off the surface and springs back to its original position. The maximum force needed to pull the tip away from the sample is called the pull-off force, which is also the adhesive force between the tip and the tested sample.

Force spectroscopy experiments were conducted on at least 20 points for each asphalt sample. The obtained force distance curves were post-processed to allow appropriate normalization of the raw data, and to obtain the maximum pull-off forces in each force

spectroscopy experiment. The following sections present the results of the force spectroscopy experiments conducted in this study.

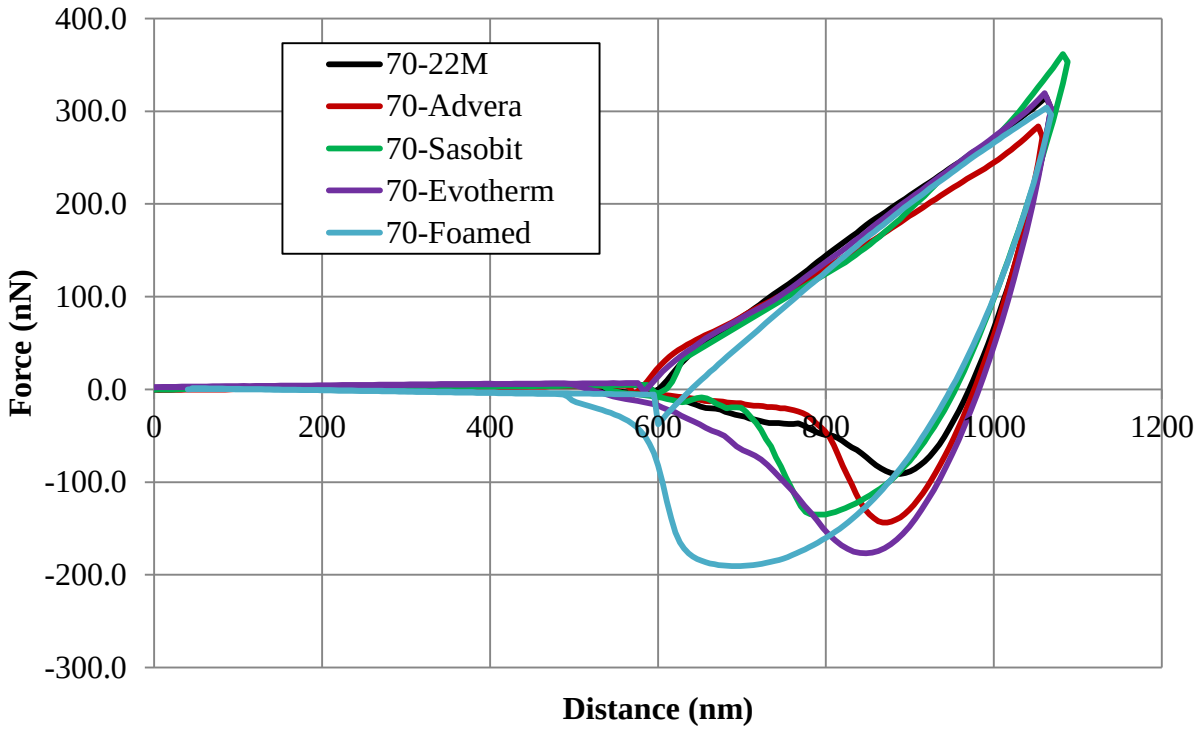

Figure 5.21: Typical force-distance curves obtained from force spectroscopy experiments.

5.5.1 Results of Unconditioned 70-22M samples

Figure 5.22 compares the average adhesive force values of the WMA binders with that of the control asphalt binder, which were obtained in experiments, conducted using silicon nitride tips. It is noted that the inclusion of the WMA additives enhanced the adhesive forces. This improvement will induce effects on the corresponding work of adhesion for the asphalt aggregate system. The Evotherm and foamed WMA resulted in the highest improvement; while the sasobit WMA had the least improvement.

The -OH and –COOH functionalized tips were used to evaluate the cohesive forces of the different binders. Figures 5.23 and 5.24 compare the maximum pull-off force for the WMA binders with that of the control one when using –OH and –COOH functionalized tips, respectively. It is noted that different trends were obtained for these tips. For the –OH tip, the Evotherm and Advera WMA additives had resulted in an increase in the interaction forces

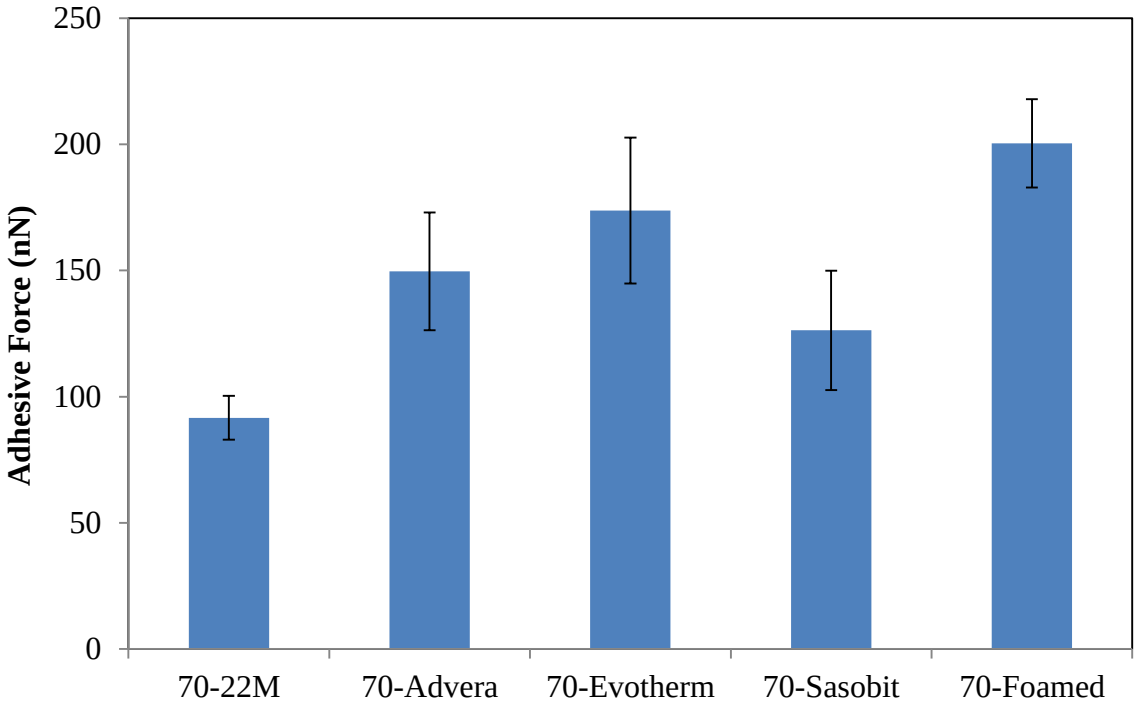

Figure 5.22:Adhesive force for unconditioned dry 70-22M samples.

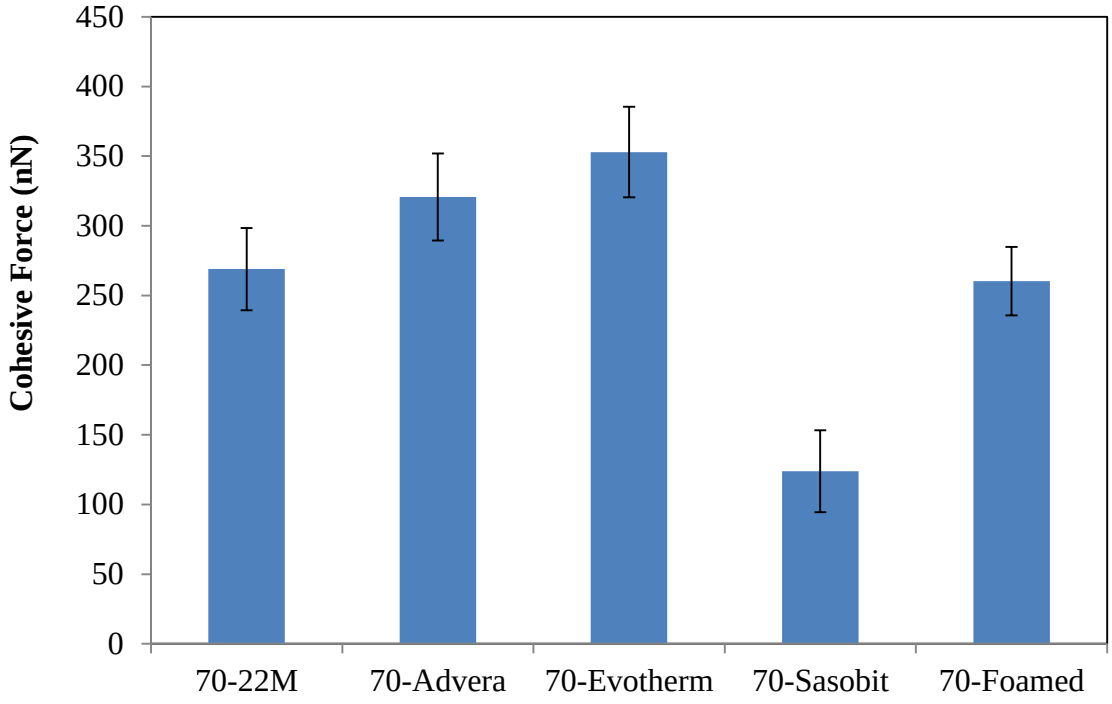

Figure 5.23: Cohesive forces for unconditioned dry 70-22M samples using –OH tip.

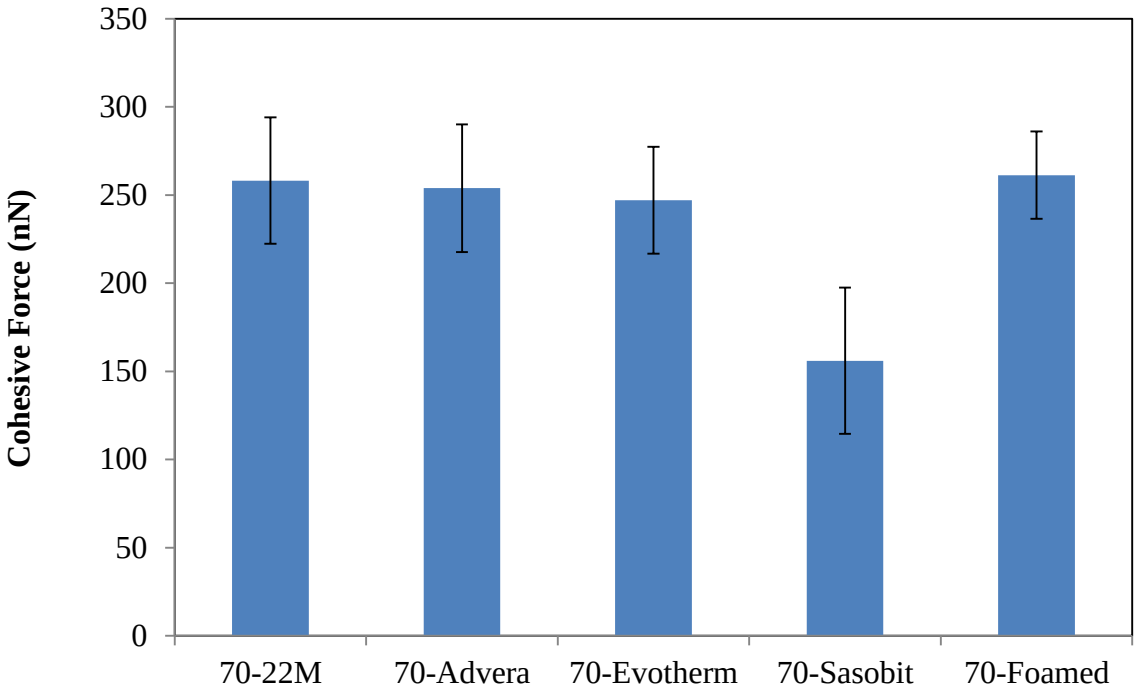

Figure 5.24: Cohesion forces for unconditioned dry 70-22M samples using –COOH tip.

between asphalt binder and -OH tip. The Sasobit and foamed WMA resulted in a decrease in those forces; however, that decrease was much more pronounced in the 70-Sasobit binder. On the other hand, while the inclusion of the Evotherm resulted in a slight decrease in the interaction forces with the –COOH group, the Advera and foamed WMA had similar values as the control 70-22M binder. Furthermore, as with –OH group, the tests with the –COOH functionalized tips showed a significant reduction in the cohesive forces within the asphalt binder due to the addition of the Sasobit. This reduction is attributed to the increase in the hydrophobicity of the asphalt binder caused by the Sasobit (Sasol Wax Co., 2008), which reduced the interaction forces between the hydrophilic –OH and –COOH chemical groups and the asphalt binder.

In an effort to provide additional insight for the force spectroscopy experiments on dry samples, ANOVA and post ANOVA LSM analyses were conducted using SAS software to statistically evaluate the results in Figures 5.22 through 5.24. Table 5.6 presents the results of this analysis. At 95% confidence level (p-value < 0.05), the effect of binder type was significant. This suggests that the WMA additives had significant effect on the binder adhesive and cohesive forces. Table 5.7 presents the results of the grouping of the asphalt binders that was determined using the post ANOVA LSM analyses conducted on the results of force spectroscopy

experiments using the different types of tips. It is noted that all WMA binders had significantly higher adhesive forces. The foamed WMA had the highest value among all other asphalt binders. This may have contributed to the high ITS value of the dry foamed 70-22M mixture obtained in the AASHTO T283 test. While the Evotherm and Advera WMA had significantly higher interaction forces with –OH tip, the inclusion of Sasobit additive significantly reduced those forces. The foamed WMA had statistically similar cohesive force values to that of the control 70-22M binder. Finally, the results of the post ANOVA-LSM analyses showed that the interaction between the asphalt binder and –COOH chemical group is not significantly affected by the Advera, Evotherm, or foamed WMA. However, the inclusion of the Sasobit had an adverse effect on this interaction.

5.5.2 Results of Conditioned 70-22M samples

Force spectroscopy experiments using different functionalized tips were also conducted on the conditioned samples of control and WMA asphalt binders. Figure 5.25 compares the average maximum pull-off force and standard error obtained in those experiments. The average adhesive force for conditioned samples of the control polymer modified asphalt binder was higher than that of the unconditioned dry samples. Tarefder and Zaman (2010) reported similar results. They suggested that the action of water has induced polarization by a repulsion of negatively charged electron clouds in nonpolar polymer modified asphalt molecules creating temporary dipoles in those asphalt samples, which has resulted in a larger Van der Waals attraction force in the asphalt binder system, and hence higher forces for the conditioned control and WMA samples. The results in Figure 5.25 also indicate that the conditioned samples Evotherm and Advera had average adhesive force values similar to that of the control. On the other hand, the Sasobit had a lower value. Figures 5.26 and 5.27 present the average cohesive forces for 70-22M asphalt binders that are obtained from force spectroscopy experiments conducted using –OH and –COOH functionalized tips, respectively. The cohesive forces of the control conditioned samples had higher values than the dry unconditioned ones. The Advera and Sasobit WMA exhibited lower cohesive forces than the control asphalt binder. However, the Evotherm had a slightly higher interaction forces with –OH group, but lower value with –COOH group.

Table 5.6: ANOVA results for adhesive & cohesive forces of unconditioned 70-22M samples.

Effect	F-value	p-value
WMA Technology -Silicon Nitride Tip	46.20	<.0001
WMA Technology - -OH Tip	22.49	<.0001
WMA Technology - -COOH Tip	62.90	<.0001

Table 5.7: Post ANOVA results for adhesive & cohesive forces of unconditioned 70-22M samples.

Grouping of Binders for Silicon Nitride Tip		
WMA Technology	Force Estimate (nN)	Letter Group
70-Foamed	200.36	A
70-Evotherm	173.71	B
70-Advera	149.66	C
70-Sasobit	126.29	D
70-22M (control)	91.65	E
Grouping of Binders for -OH Tip		
WMA Technology	Force Estimate (nN)	Letter Group
70-Evotherm	352.93	A
70-Advera	320.63	B
70-22M (control)	268.90	C
70-Foamed	260.28	C
70-Sasobit	123.53	D
Grouping of Binders for -COOH Tip		
WMA Technology	Force Estimate (nN)	Letter Group
70-Foamed	261.26	A
70-22M (control)	254.99	A
70-Advera	253.89	A
70-Evotherm	247.00	A
70-Sasobit	160.94	B

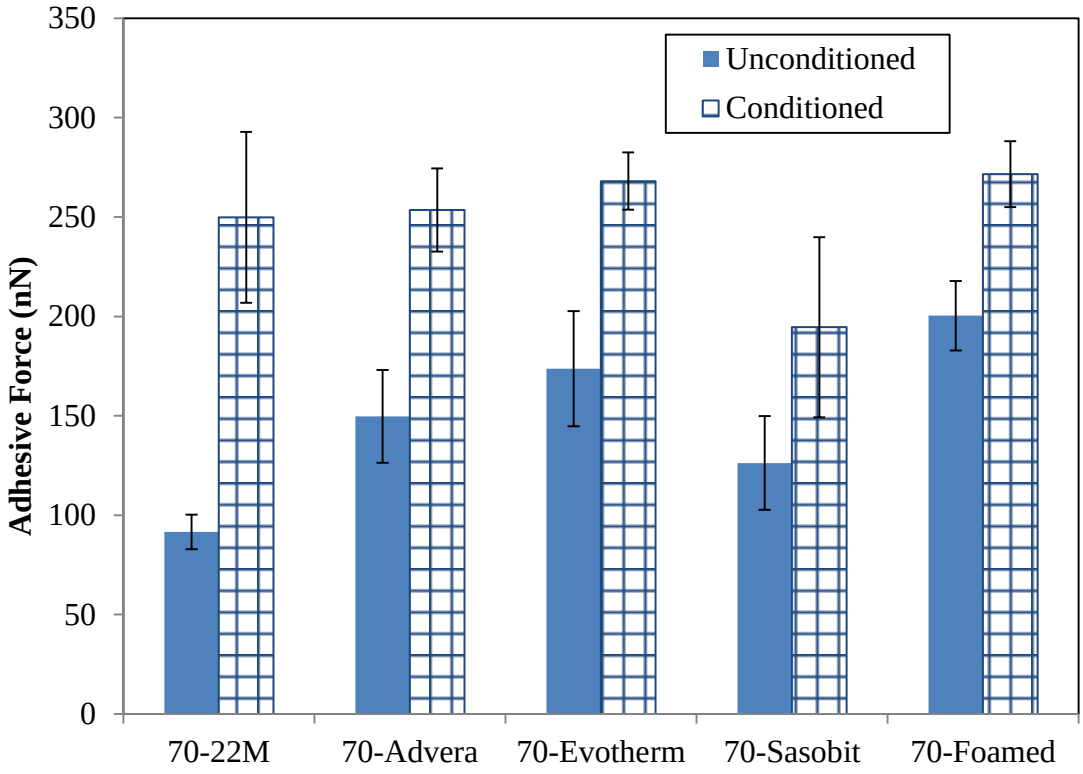

Figure 5.25: Adhesive force for conditioned 70-22M binders.

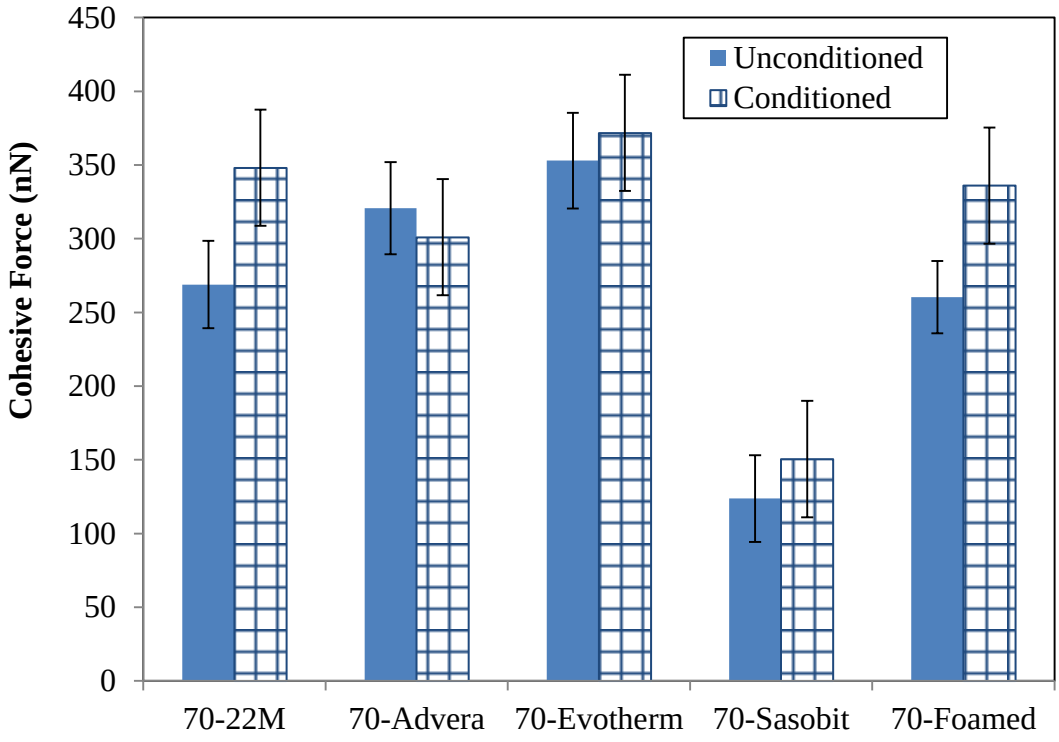

Figure 5.26: Cohesive force for conditioned 70-22M binders using –OH tips.

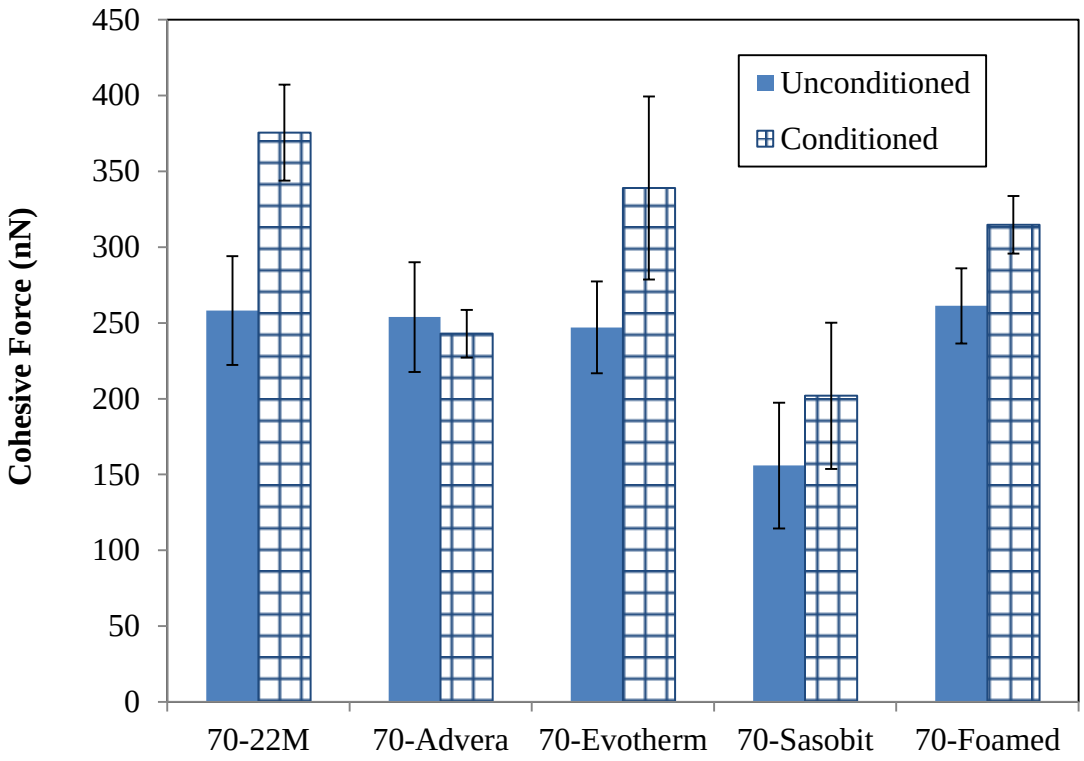

Figure 5.27: Cohesive force for conditioned 70-22M binders using –COOH tips.

Single factor ANOVA and post ANOVA-LSM analyses were conducted to statistically examine the results presented in Figures 5.25 through 5.27. Table 5.8 presents the results of these ANOVA analyses. At 95% confidence level (p-value < 0.05), the WMA technology had a significant effect on the conditioned samples adhesive and cohesive forces. Table 5.9 presents the results of the grouping of the conditioned asphalt binders. While the conditioned Advera, Evotherm, and foamed WMA had statistically indistinguishable adhesive force values from that of the conditioned control 70-22M binder, the Sasobit had significantly lower value. In addition, the conditioned Evotherm and foamed WMA had statistically similar –COOH and –OH interaction forces to that of the conditioned control 70-22M binder. On the contrary, the conditioned Advera and Sasobit had statistically lower cohesive force values than the conditioned control binder. Thus, the results are suggesting that the Evotherm WMA will have the best resistance to moisture induced damage among all WMA technologies evaluated in this study, which is similar to that of the control binder. This may be attributed to the anti-strip additive that Evotherm contains. This result is consistent with that of the macro-scale test (i.e. AASHTO T283) that was performed in this study.

Table 5.8: ANOVA results for adhesive & cohesive forces of conditioned 70-22M samples.

Effect	F-value	p-value
WMA Technology -Silicon Nitride Tip	27.55	<.0001
WMA Technology - -OH Tip	231.14	<.0001
WMA Technology - -COOH Tip	62.90	<.0001

Table 5.9: Post ANOVA results for adhesive & cohesive forces of conditioned 70-22M samples.

Grouping of Binders for Silicon Nitride Tips		
WMA Technology	Force Estimate (nN)	Letter Group
70-Foamed	271.58	A
70-Evotherm	267.19	A
70-Advera	254.20	A
70-22M (control)	249.84	A
70-Sasobit	194.57	B
Grouping of Binders for -OH Tip		
WMA Technology	Force Estimate (nN)	Letter Group
70-Evotherm	371.74	A
70-22M (control)	348.12	AB
70-Foamed	336.00	B
70-Advera	301.01	C
70-Sasobit	151.69	D
Grouping of Binders for -COOH Tip		
WMA Technology	Force Estimate (nN)	Letter Group
70-22M (control)	375.50	A
70-Evotherm	338.96	AB
70-Foamed	314.68	B
70-Advera	240.17	C
70-Sasobit	201.07	D

5.5.3 Results of Unconditioned 64-22 Samples

Figure 5.28 presents the average values and standard deviation values of the adhesive force of the WMA and control 64-22 binders. As with the 70-22M binders, the different WMA technologies enhanced the adhesive force of the asphalt binder. The foamed WMA technology resulted in the greatest improvement; while the Sasobit WMA had the least improvement. Figures 5.29 and 5.30 show the average value of the cohesive forces for the different binders that were measured using –OH, –COOH tips, respectively. While the Evotherm and foamed WMA had higher cohesive forces than the 64-22 binder, the Sasobit had lower average value. For the –COOH tip, all WMA technologies reduced the interaction forces. However, the Advera and Sasobit had the largest reduction in these forces. As previously stated, the reduction in the Sasobit is attributed to its tendency to increase the hydrophobicity of the asphalt binder. It is worth noting that the reduction of the cohesive forces due to the inclusion of the Sasobit is less pronounced in the 64-22 binder as compared to 70-22M binder.

ANOVA and post ANOVA LSM analyses were conducted to statistically evaluate the results of force spectroscopy test conducted on the unconditioned control and WMA 64-22 samples. Table 5.11 presents the results of the ANOVA analysis. It is noted that at 95% confidence level (p-value < 0.05) the effect of the WMA technologies was significant. This suggests that the WMA technologies had significant influence on the adhesive and cohesive forces of the 64-22 binder. Table 5.11 provides the grouping of the asphalt binders that was determined using the post ANOVA LSM analyses. It is noted that only the Advera and foamed WMA had significantly higher adhesive forces than the control 64-22 binder. While the Advera and Sasobit had significantly lower interaction forces with –OH tip, the foamed WMA had statistically similar value. On the contrary, the Evotherm resulted in significant increase in the interaction force with –OH. Finally, only the Evotherm and foamed WMA had statistically similar –COOH interaction forces as that of the control 64-22 binder, while the other WMA technologies resulted in significant decrease in these forces.

5.5.4 Results of Conditioned 64-22 Samples

Figures 5.31 through 5.33 present the results of the force spectroscopy experiments conducted using the silicon nitride tip and the -COOH and –OH functionalized tips, respectively,

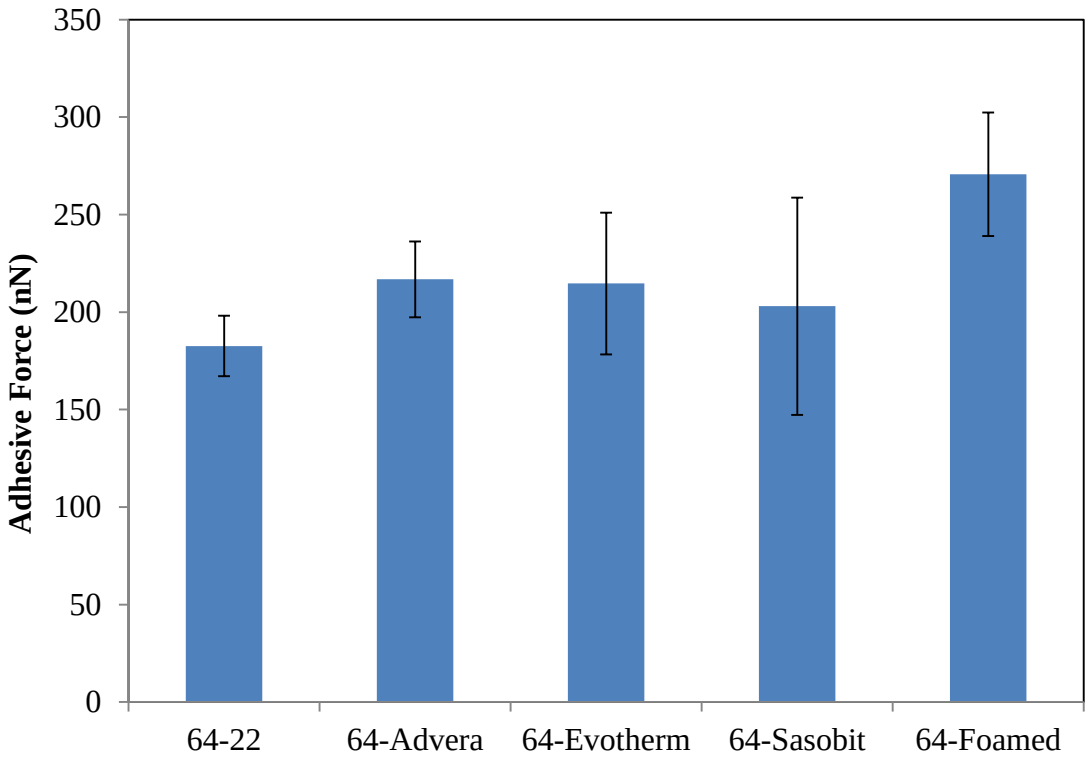

Figure 5.28: Adhesive force for unconditioned dry 64-22 samples.

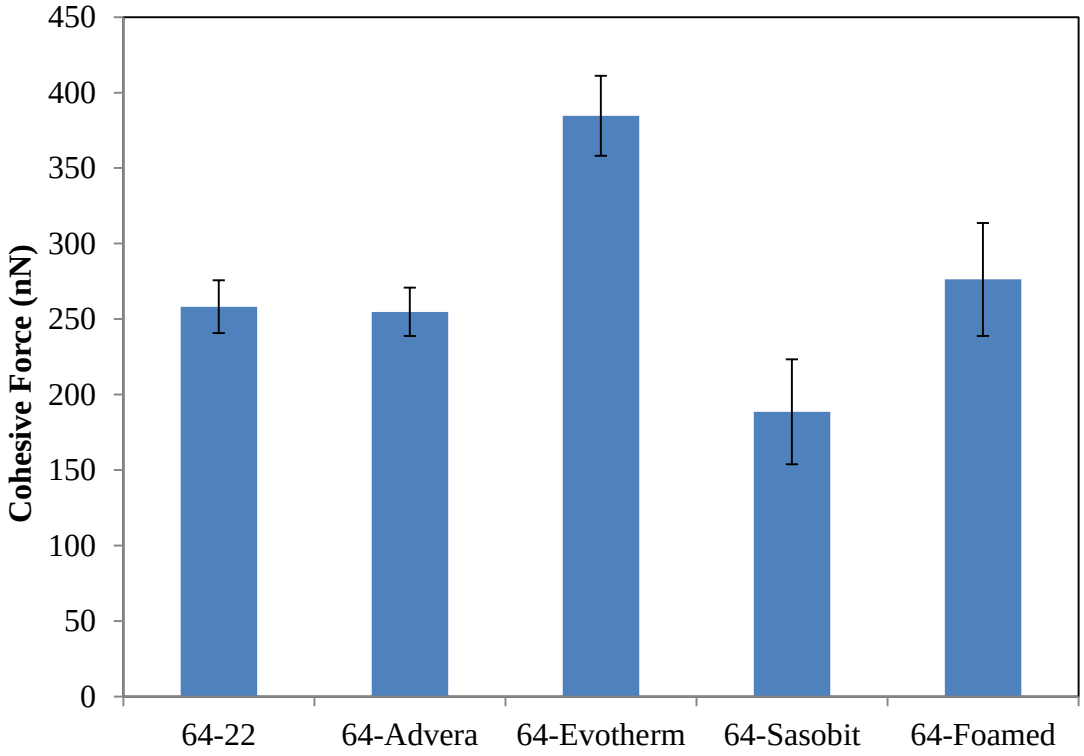

Figure 5.29: Cohesive forces for unconditioned dry 64-22 samples using –OH tip.

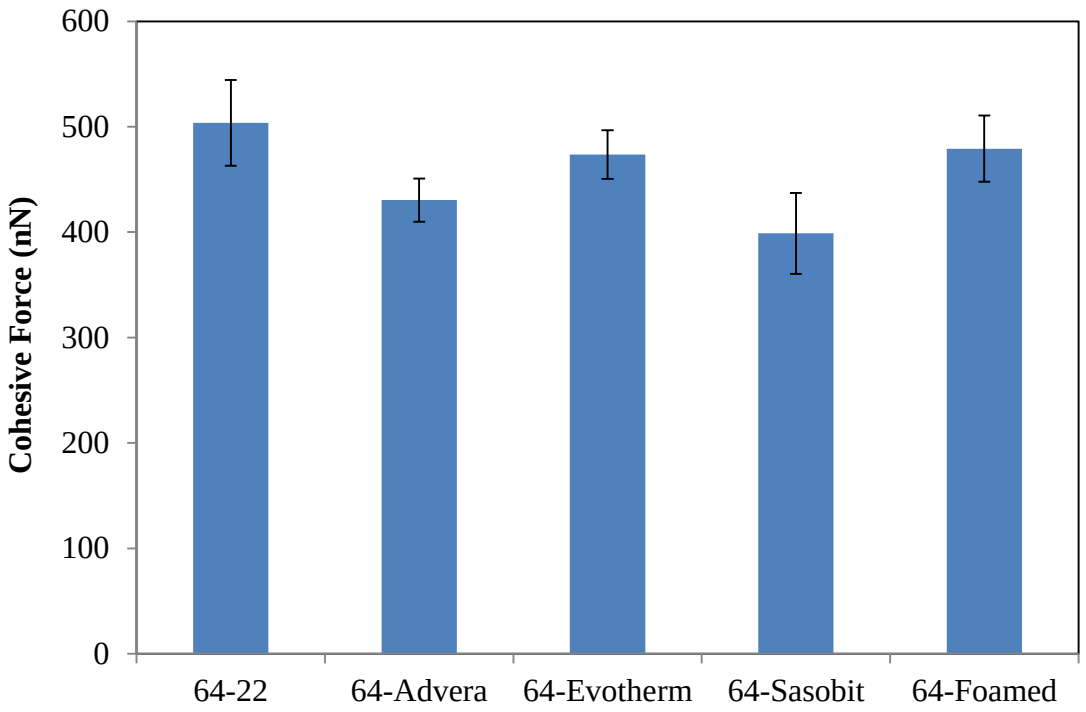

Figure 5.30: Cohesive forces for unconditioned dry 64-22 samples using –COOH tip.

on the conditioned control and WMA 64-22 samples. It is clear that the adhesive forces were significantly decreased due to conditioning. This behavior was different than that observed for the polymer modified 70-22M binder, which indicates that the neat 64-22 binder is more susceptible to moisture damage. This is consistent with the AASHTO T283 test results, where the WMA and HMA 70-22M mixtures showed higher TSR values as compared to their corresponding 64-22 mixtures. Figure 5.31 is also showing that while the control and Evotherm 64-22 binders exhibited the least reduction in the adhesive forces, the Advera binder had the highest decrease after conditioning. It is worth noting that the Advera 64-22 mixture had the lowest TSR values among all other WMA and HMA mixtures.

The results in Figure 5.32 indicate that there was a reduction in the interaction forces with –OH upon conditioning, but it was less pronounced than that observed for the adhesive forces. Furthermore, the Sasobit had the largest decrease. Finally, all conditioned HMA and WMA 64-22 samples except the Evotherm had lower interaction cohesive forces with –COOH chemical group as compared to the unconditioned dry ones, Figure 5.33. The Advera and Sasobit showed the highest reduction and least interaction force values.

Table 5.10: ANOVA results for adhesive & cohesive forces of unconditioned 64-22 samples.

Effect	F-value	p-value
WMA Technology -Silicon Nitride Tip	39.70	<.0001
WMA Technology - -OH Tip	231.14	<.0001
WMA Technology - -COOH Tip	62.90	<.0001

Table 5.11: Post ANOVA results for adhesive & cohesive forces of unconditioned 64-22 samples.

Grouping of Binders for Silicon Nitride Tips		
WMA Technology	Force Estimate (nN)	Letter Group
64-Foamed	254.76	A
64-Advera	216.77	B
64-Evotherm	207.56	BC
64-Sasobit	191.84	CD
64-22 (control)	183.24	D
Grouping of Binders for -OH Tip		
WMA Technology	Force Estimate (nN)	Letter Group
64-Evotherm	384.60	A
64-Foamed	276.28	B
64-22 (control)	258.22	BC
64-Advera	254.79	C
64-Sasobit	188.63	D
Grouping of Binders for -COOH Tip		
WMA Technology	Force Estimate (nN)	Letter Group
64-22 (control)	503.60	A
64-Foamed	479.17	AB
64-Evotherm	473.56	AB
64-Advera	430.36	BC
64-Sasobit	398.79	C

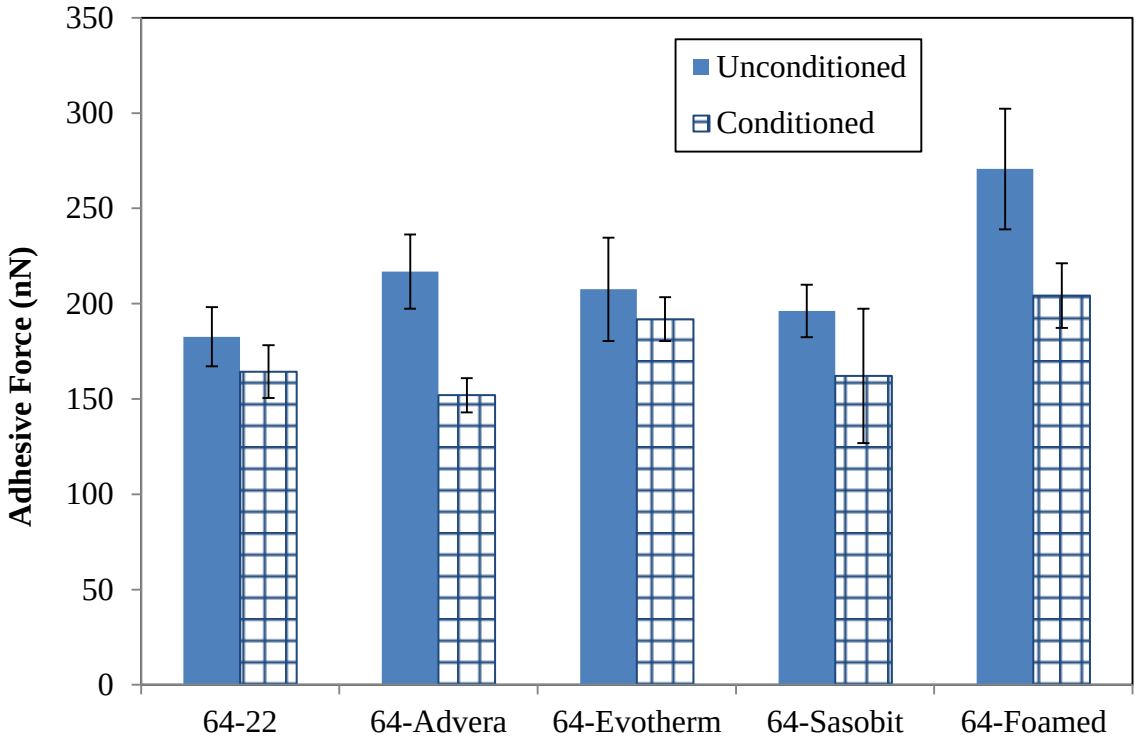

Figure 5.31: Adhesive forces for conditioned 64-22 samples.

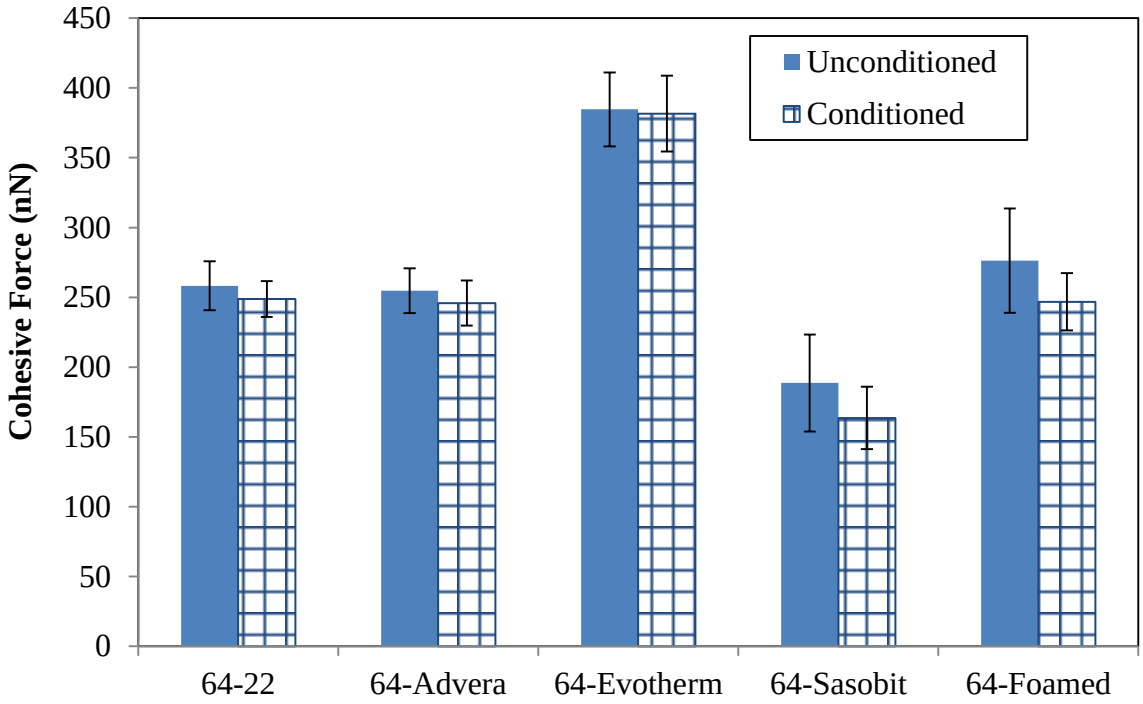

Figure 5.32: Cohesive forces for conditioned 64-22 samples using –OH tip.

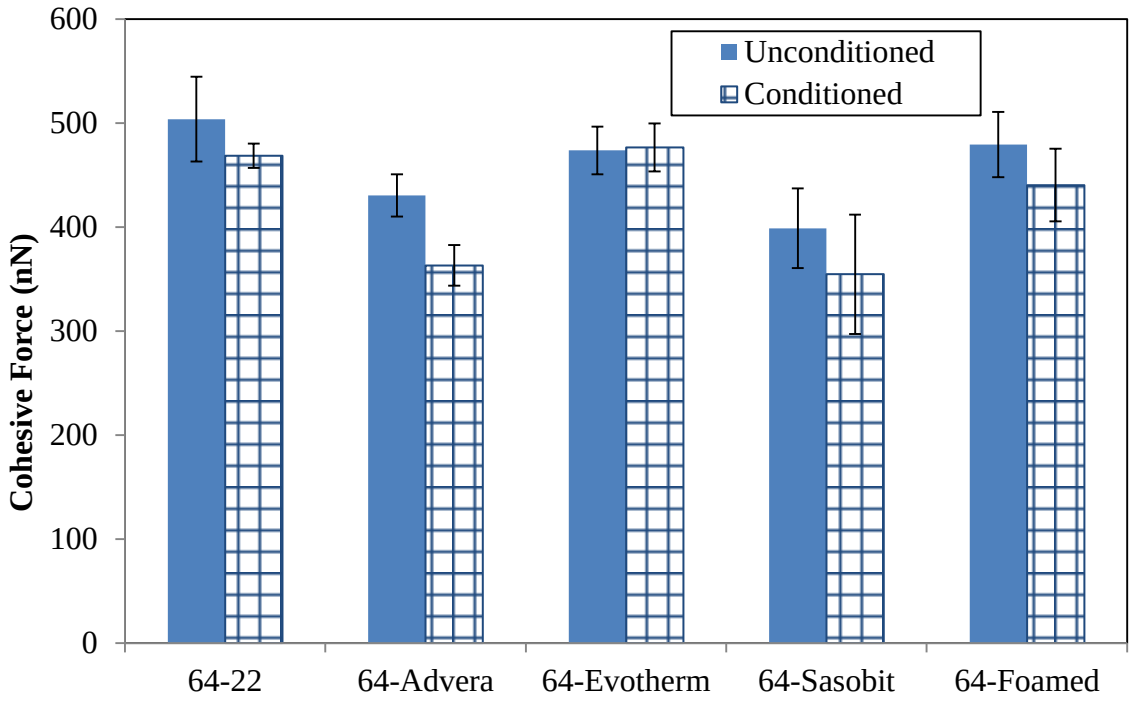

Figure 5.33: Cohesive forces for conditioned 64-22 samples using –COOH tip.

Single factor ANOVA and post ANOVA LSM analyses were conducted on the data obtained from force spectroscopy experiments performed on the conditioned WMA and HMA 64-22 samples. Table 5.12 presents the results of the ANOVA analysis. The WMA technologies have a significant effect on the conditioned samples adhesive and cohesive forces at 95% confidence level (p-value < 0.05). The F-value for adhesive forces of the conditioned samples was higher than that of the unconditioned samples (Table 5.10), which suggests that the WMA technologies effect was more pronounced upon conditioning. However, similar to the unconditioned samples, the greatest effect of WMA technologies was on the –OH interaction cohesive forces, as indicated by the F-values.

Table 5.13 presents the results of the grouping of the conditioned 64-22 asphalt samples. The conditioned foamed WMA and Evotherm had significantly higher adhesive forces than the conditioned 64-22; however, the conditioned Sasobit and Advera had statistically similar values to it. The results in Table 5.13 are indicating that based on the tests done using –OH tip, only the conditioned Evotherm and Sasobit had statistically higher and lower cohesive forces than the conditioned 64-22 samples, respectively. Finally, the conditioned Evotherm and foamed binders had statistically similar interaction forces with the –COOH group to that of the conditioned

control PG 64-22 binder. Furthermore, the conditioned Advera and Sasobit had similar cohesive force values, which were statistically lower than that of the conditioned PG 64-22 binder.

Table 5.12: ANOVA results for adhesive & cohesive forces of conditioned 64-22 samples.

Effect	F Value	p-value
WMA Technology -Silicon Nitride Tip	54.17	<.0001
WMA Technology - –OH Tip	231.14	<.0001
WMA Technology - –COOH Tip	62.90	<.0001

Table 5.13: Post ANOVA results for adhesive & cohesive forces of conditioned 64-22 samples.

Grouping of Binders for Silicon Nitride Tips		
WMA Technology	Force Estimate (nN)	Letter Group
64-Foamed	204.21	A
64-Evotherm	191.86	A
64-22 (control)	164.31	B
64-Sasobit	162.07	B
64-Advera	151.94	B
Grouping of Binders for –OH Tip		
WMA Technology	Force Estimate (nN)	Letter Group
64-Evotherm	362.93	A
64-22 (control)	248.73	B
64-Foamed	246.79	B
64-Advera	245.87	B
64-Sasobit	163.62	C
Grouping of Binders for –COOH Tip		
WMA Technology	Force Estimate (nN)	Letter Group
64-Evotherm	476.36	A
64-22 (control)	468.44	AB
64-Foamed	440.25	B
64-Advera	363.07	C
64-Sasobit	354.62	C

The results of the AFM force spectroscopy tests on 64-22 binders are indicating that the Evotherm and foamed WMA have the best resistance to moisture induced damage among all WMA technologies evaluated in this study and they did not show any adverse effects on cohesive or adhesive bonds upon moisture conditioning. This result is consistent with AASHTO T283 results, which indicated that the Evotherm and foamed WMA mixtures had TSR values similar to that of the control PG 64-22 mixture. In addition, the Advera and Sasobit had greater reduction in the adhesive and cohesive forces and exhibited the lowest values upon conditioning. This is may explain the lower TSR values that their mixtures possessed. It is worth noting that although the Advera and foamed WMA technologies results in foaming of the asphalt binder, they have different effects on its adhesive and cohesive properties upon conditioning. This may be attributed to the fact that the Advera is a hydrophilic material (attracts water) and may results in an increase in the hydrophilicity of the asphalt binder.

5.5.5 Influence of Different Factors on Adhesive And Cohesive Forces

Multi-factor ANOVA analyses were also performed on all force spectroscopy test results for the 64-22 and 70-22M binders to examine the effect of binder type, WMA technology, conditioning and their interactions on the adhesive as well as the –OH and –COOH cohesive forces. A linear CRD model similar to that presented Equation 5.1 was used in this analysis; however, the dependent variables used in the analysis were adhesive and the –OH and –COOH cohesive forces. Table 5.14 presents the results of the multi-factor ANOVA analysis that was performed on adhesive forces measured in the force spectroscopy tests using silicon nitride tips. It is noted that the effects of binder type, WMA technology and conditioning and their interactions were significant at a 95% confidence level. The conditioning effect and its interaction with the binder type were the most significant factors affecting the adhesive force values, as indicated by the F-value. The significance of the interaction between the binder type, WMA technology, and conditioning interaction suggests that the effect of WMA depends on the binder type and conditioning.

Tables 5.15 and 5.16 present the summary of the results of the multi-factor ANOVA analyses that was conducted on the –OH and –COOH cohesive forces, respectively. At a confidence level of 95%, all three factors and their interactions have affected significantly both types of cohesive forces. However, as indicated by the F-factor values, the factors significance

on the cohesive forces varied. While WMA technologies had the most significant effect on –OH cohesive forces, the binder type was the most influential factor for the –COOH cohesive force. This suggests that factors affecting the different cohesive forces within asphalt are not the same. Therefore, the evaluation of any modification performed on an asphalt binder requires examining the interaction forces with the different asphalt chemical groups.

Table 5.14: Multi-Factor ANOVA results for adhesive forces.

Effect	F-value	p-value
Binder type	5.88	0.0158
WMA Technology	74.49	<.0001
Binder type * WMA Technology	8.36	<.0001
Conditioning	154.64	<.0001
Binder type * Conditioning	675.92	<.0001
WMA Technology * Conditioning	15.46	<.0001
Binder type * WMA Technology * Conditioning	11.74	<.0001

Table 5.15: Multi-Factor ANOVA results for –OH cohesive forces.

Effect	F-value	p-value
Binder type	41.34	<.0001
WMA Technology	348.28	<.0001
Binder type * WMA Technology	32.25	<.0001
Conditioning	11.34	0.0008
Binder type * Conditioning	75.66	<.0001
WMA Technology * Conditioning	9.11	<.0001
Binder type * WMA Technology * Conditioning	12.05	<.0001

5.6 Comparison Between The Results Of Nano And Macro-Scale Tests

The results of the different AFM force spectroscopy test were compared to those obtained from the AASHTO T283 macro-scale test. Figures 5.34 a,b present the relationship between the adhesive forces and ITS values for the unconditioned and conditioned WMA 70-22M samples, respectively. It is worth noting that only the results of WMA mixtures were used since they were

all prepared at the same temperature, which was lower than the HMA. As indicated by the R^2 value, a relatively good correlation exists between the adhesive forces and the ITS values particularly for the dry unconditioned samples. The relationship between the cohesive forces measured in AFM experiments and ITS samples for unconditioned and conditioned samples was also evaluated, as shown in Figure 5.35 and Figure 5.36. In general, poor correlations exist between cohesive forces and ITS values especially those related to the –COOH chemical group.

Table 5.16: Multi-Factor ANOVA results for –COOH cohesive forces.

Effect	F Value	p-value
Binder type	1510.28	<.0001
WMA Technology	122.33	<.0001
Binder type * WMA Technology	15.96	<.0001
Conditioning	16.61	<.0001
Binder type * Conditioning	157.77	<.0001
WMA Technology * Conditioning	14.02	<.0001
Binder type * WMA Technology * Conditioning	4.34	0.0019

Figure 5.37a,b compare the adhesive forces and the ITS values for the unconditioned and conditioned WMA 64-22 samples. The adhesive forces have an excellent correlation with the ITS values. On the contrary, as shown in Figure 5.38 and Figure 5.39 poor correlations exist between the cohesive forces and the ITS. This result is similar to that obtained with 70-22M samples, which suggests that ITS values are more affected by the adhesive forces than the cohesive forces. This is consistent by previous experimental and numerical studies on indirect tensile strength test, which suggested that sample's cracking in the indirect tensile strength test has more tendency to occur at the interface between the aggregate and the binder (i.e., adhesive failure) due to the high stress concentration (Abbas et al., 2008; Lytton et al., 2004).

5.7 Results of Healing Experiments

The results of AFM experiments were analyzed to evaluate the two mechanisms of healing in the different binders considered in this study: wetting and intrinsic healing. The proceeding sections present the results of the conducted analyses.

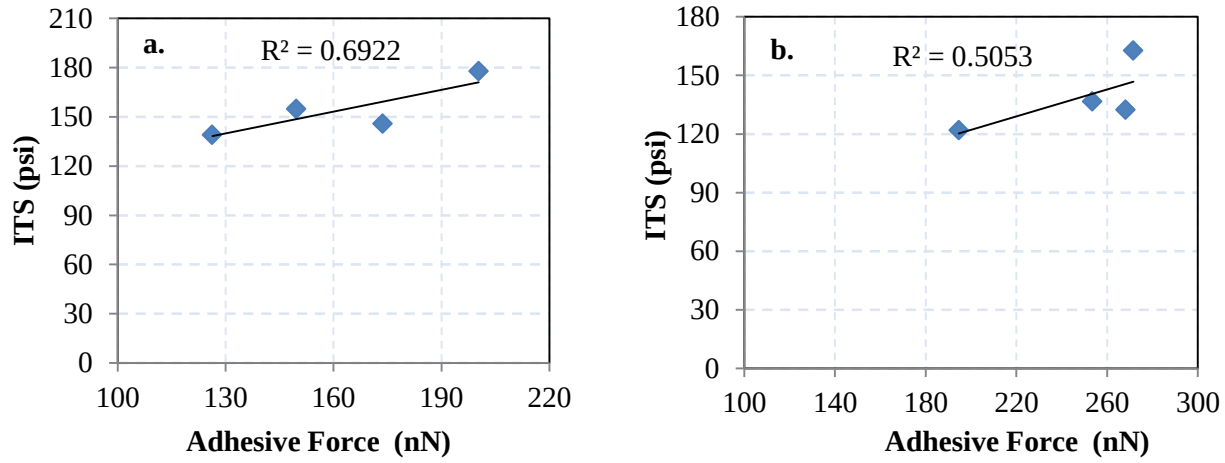

Figure 5.34: Relationship between Adhesive forces ITS for 70-22M materials: a) unconditioned samples; b) conditioned samples.

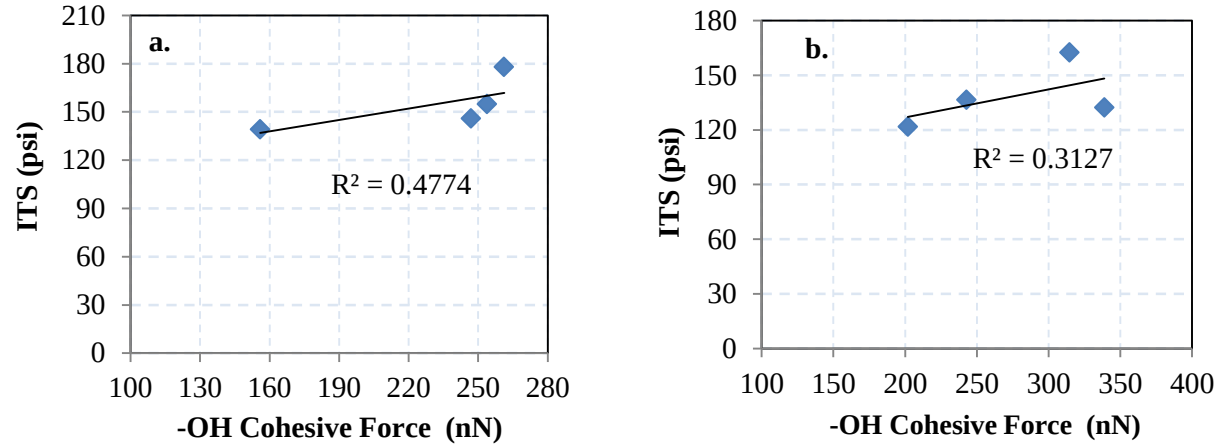

Figure 5.35: Relationship between –OH Cohesive forces ITS for 70-22M materials: a) unconditioned samples; b) conditioned samples.

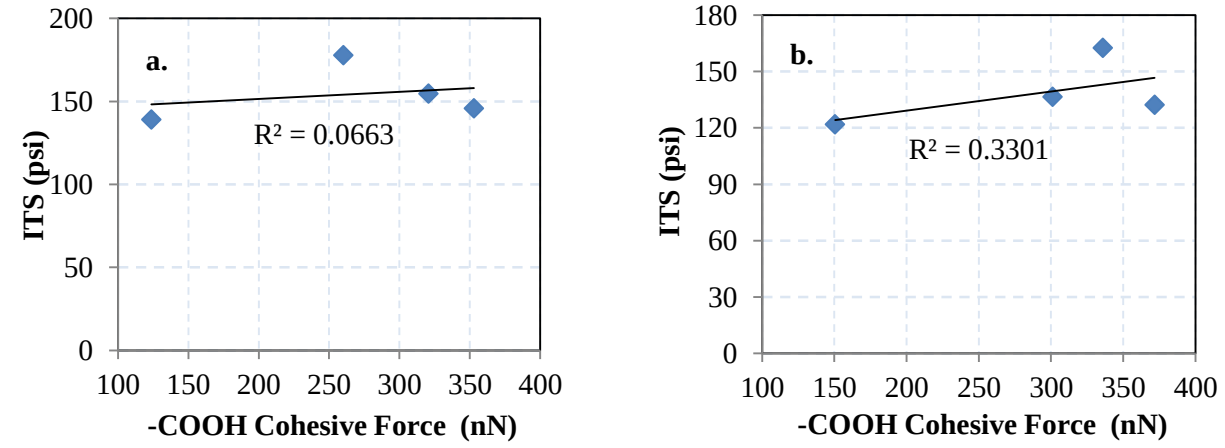

Figure 5.36: Relationship between –COOH Cohesive forces ITS for 70-22M materials: a) unconditioned samples; b) conditioned samples.

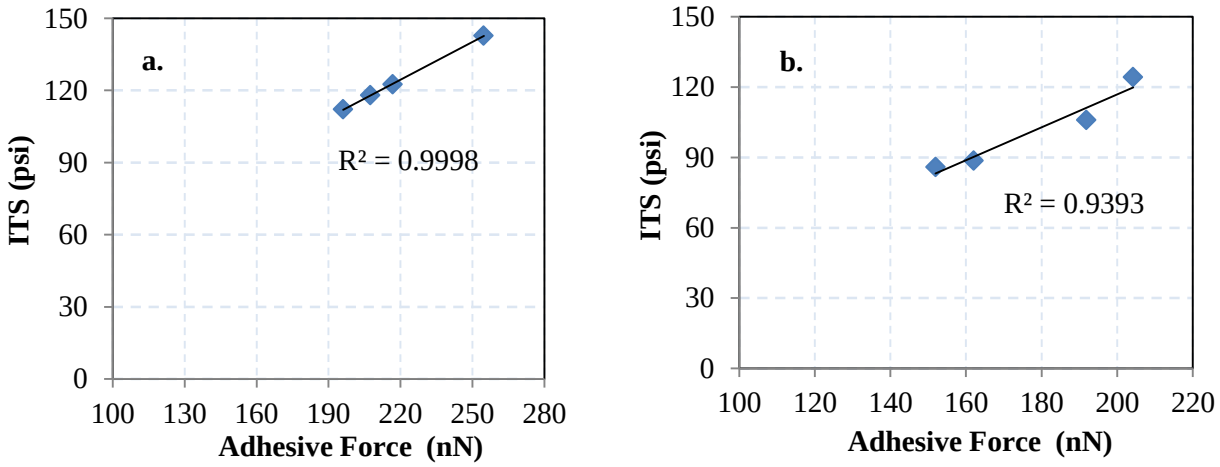

Figure 5.37: Relationship between Adhesive forces ITS for 64-22 materials: a) unconditioned samples; b) conditioned samples.

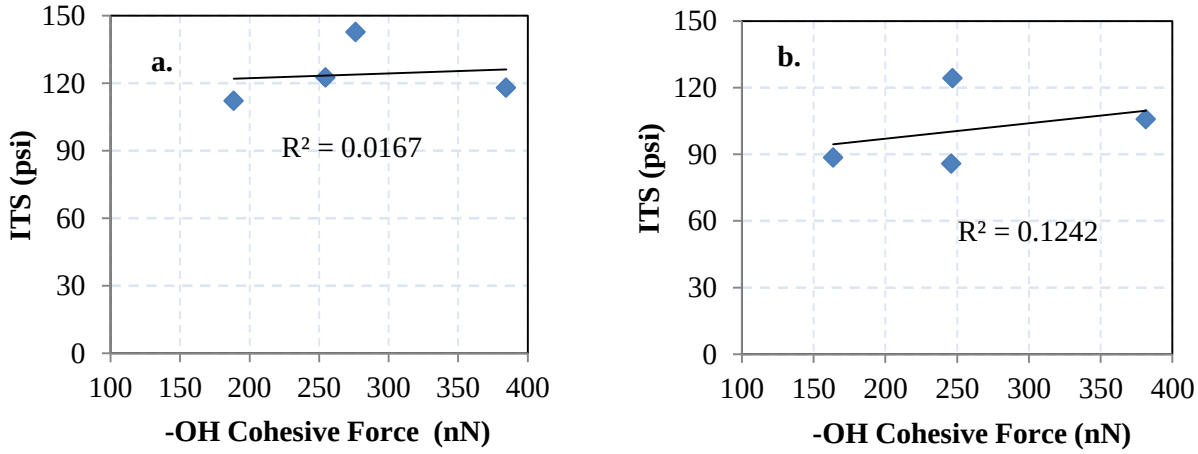

Figure 5.38: Relationship between –OH Cohesive forces ITS for 64-22 materials: a) unconditioned samples; b) conditioned samples.

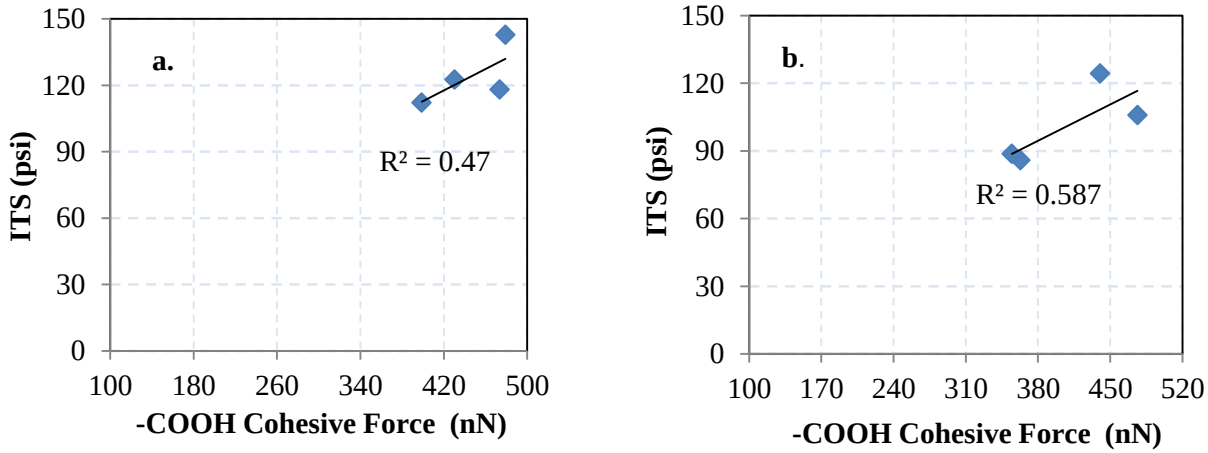

Figure 5.39: Relationship between –COOH Cohesive forces ITS for 64-22 materials: a) unconditioned samples; b) conditioned samples.

5.7.1 Evaluation of Wetting Mechanism

To evaluate the wetting mechanism, a crack was initiated in the asphalt binder and the closure of the crack with time was monitored by continuously taking AFM images. Figure 5.40 presents the topographical images that were taken before and after the 70-22M asphalt sample was probed. As it can be noted, a relatively flat spot was identified and indented; this resulted in a nano-crack as shown in Figure 5.40b, which mitigated with time, Figure 5.40c,d. To evaluate the closure rate (wetting), the images were post-processed and analyzed to determine how the crack volume changed with time for the different tested points for each sample.

5.7.1.1 Wetting of 70-22M Binders

Figure 5.41 present a typical plot of the crack volume as a function of time for the control and WMA 70-22M samples. It is noted that the volume decreases with time nonlinearly for all asphalt binders evaluated. However, the rate of decrease for each binder is different. To examine that, a power function was fitted through the obtained data as shown in Figure 5.41. Figure 5.42 presents the power coefficients of the fitted functions for the control and WMA 70-22M binders. It is noted that all the Evotherm, Advera, and foamed WMA technologies had resulted in increasing the magnitude of the power function coefficient and hence in improving the rate of micro-crack closure. On the contrary, Sasobit caused a decrease in the power function coefficient value. By comparing the results in Figure 5.42 with those in Figure 5.22 through Figure 5.24 it can be noticed that the power function coefficient trend was very similar to that for the –OH cohesive interaction forces, such that the Evotherm and Sasobit had the highest and lowest values in both figures. This suggests that the interaction in –OH chemical is related to the micro-crack closure rate and to the wetting mechanisms in asphalt binders. Figure 5.43 evaluate the relationship between these two parameters for all 70-22M binders. It is noted that a fair correlation exists. This result is consistent with the model proposed by Bhasin et al. (2008).

5.7.1.2 Wetting of 64-22 Binders

Figure 5.44 shows an example of the change of the crack volume with time for the control and WMA 64-22 samples. The results in Figure 5.44 were analyzed to determine the coefficient of power function that can fit each of the rate of crack volume change with time curves. Figure 5.45 presents the coefficients of the fitted power function for the HMA and WMA

64-22 samples. It is noted that all 64-22 binders had higher power function coefficient values and better closure rate than the 70-22M. However, as with 70-22M binders, only the Sasobit had reduced the power function coefficient and decreased the rate of micro-crack closure, while the other WMA technologies had improved it. Figure 5.46 shows the relationship between the obtained power function coefficients and –OH cohesive forces for control and WMA 64-22 binders. It is noted a good correlation exists between those two parameters.

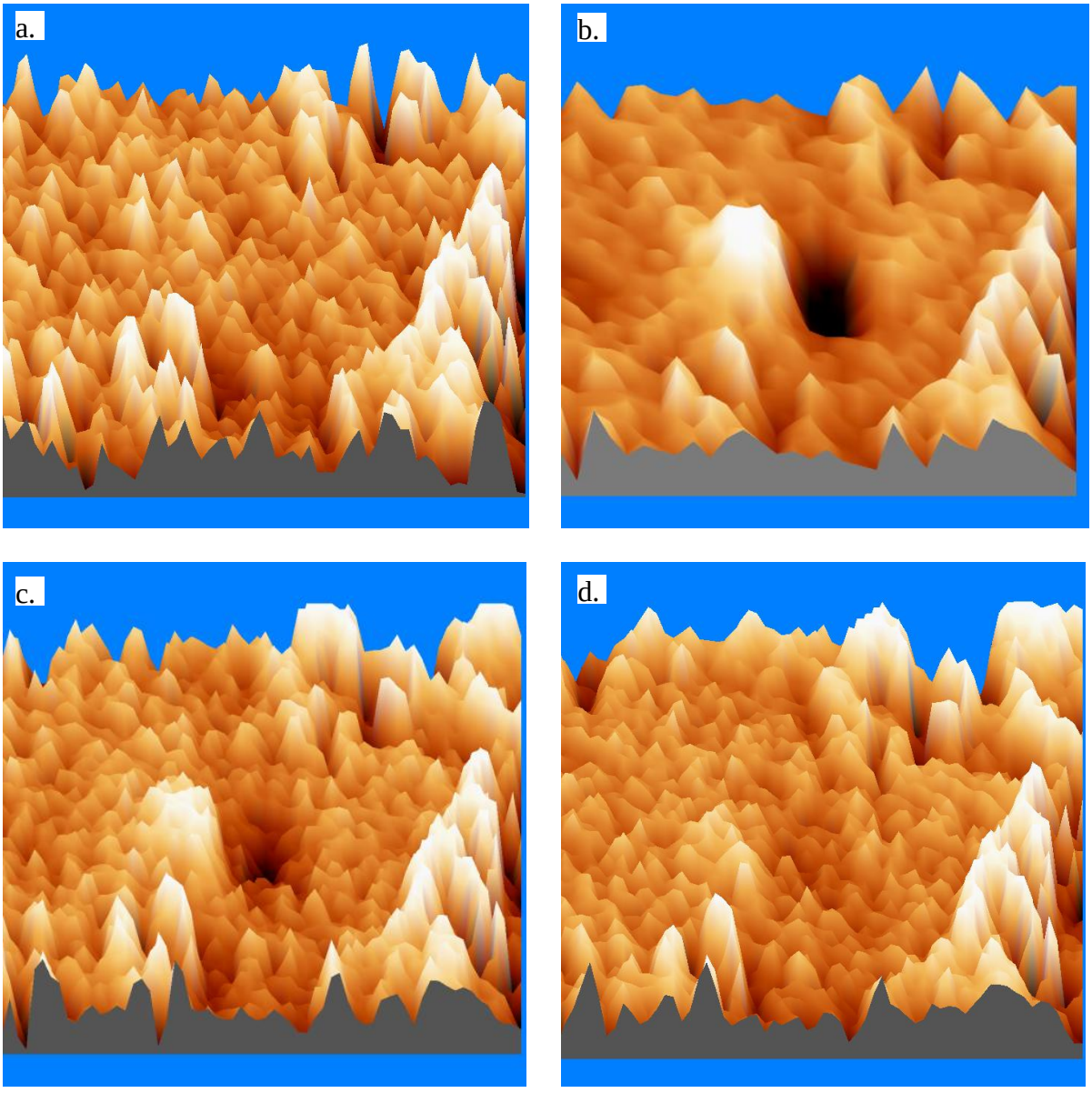

Figure 5.40: AFM topographical images: a) Directly before probing b) 163 sec after probing c) 350 sec after probing d) 800 sec after probing.

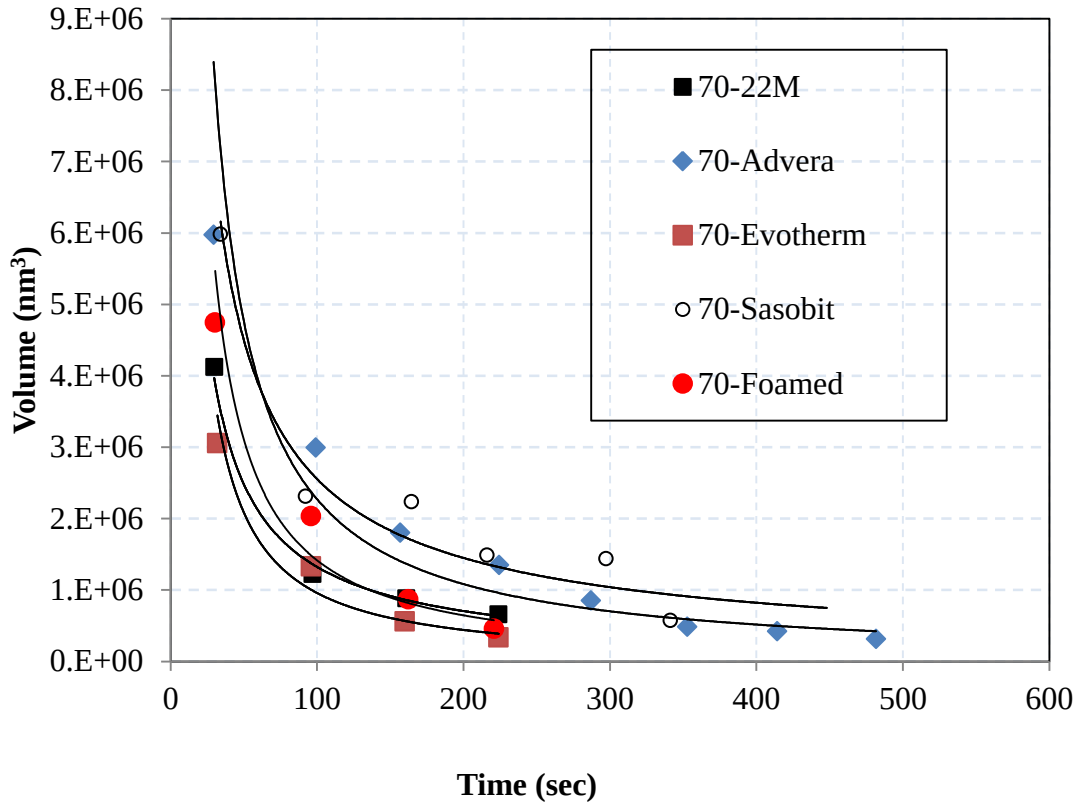

Figure 5.41: Crack Volume Decrease with time for 70-22M samples.

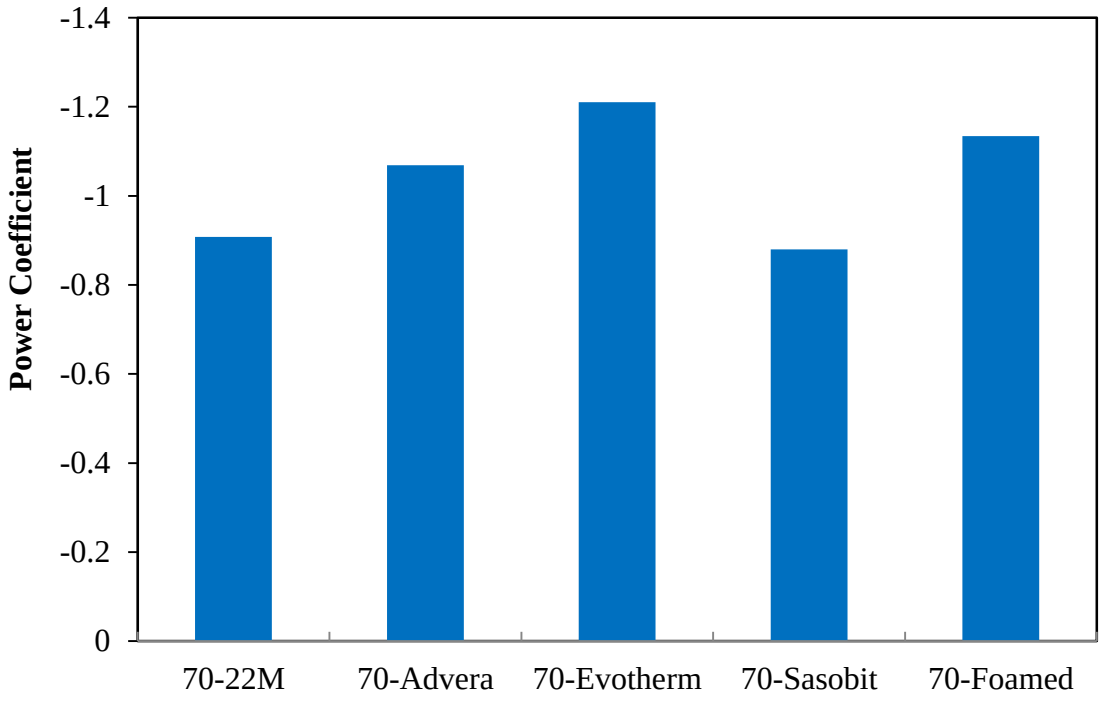

Figure 5.42: Crack closure rate for 70-22M samples.

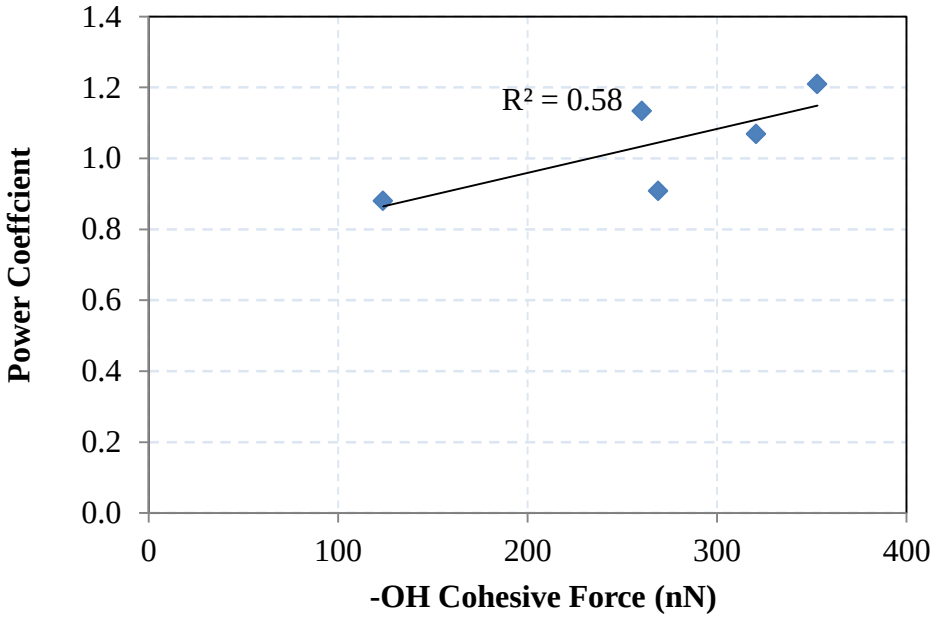

Figure 5.43: Crack closure rate vs. –OH Cohesive Force for 70-22M samples.

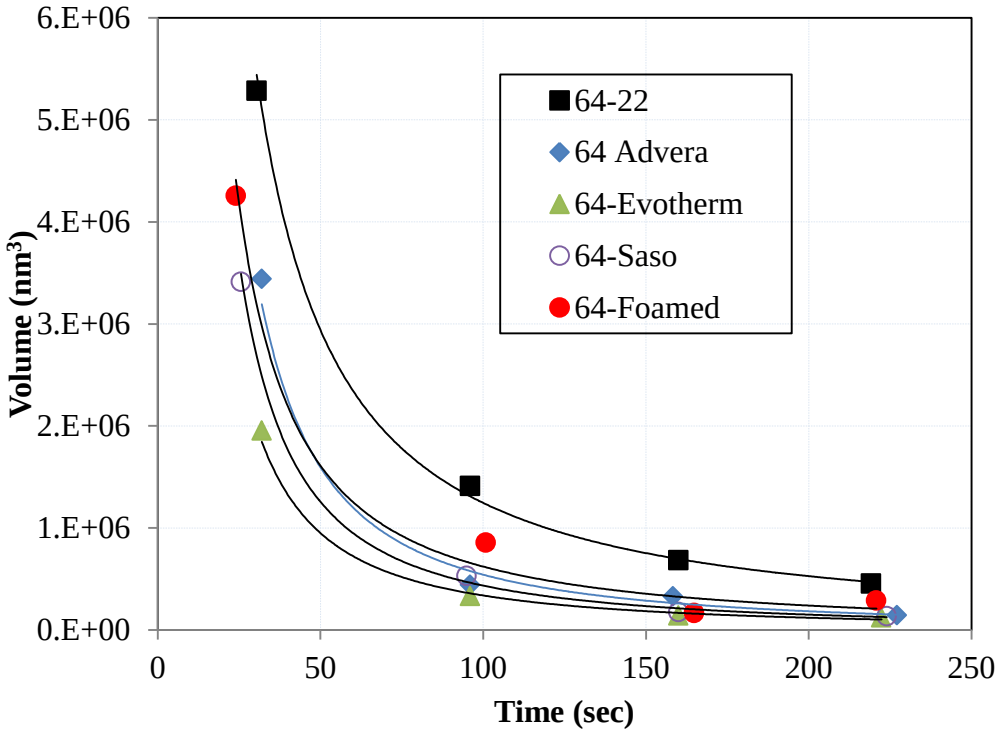

Figure 5.44: Crack Volume Decrease with time for 64-22 samples.

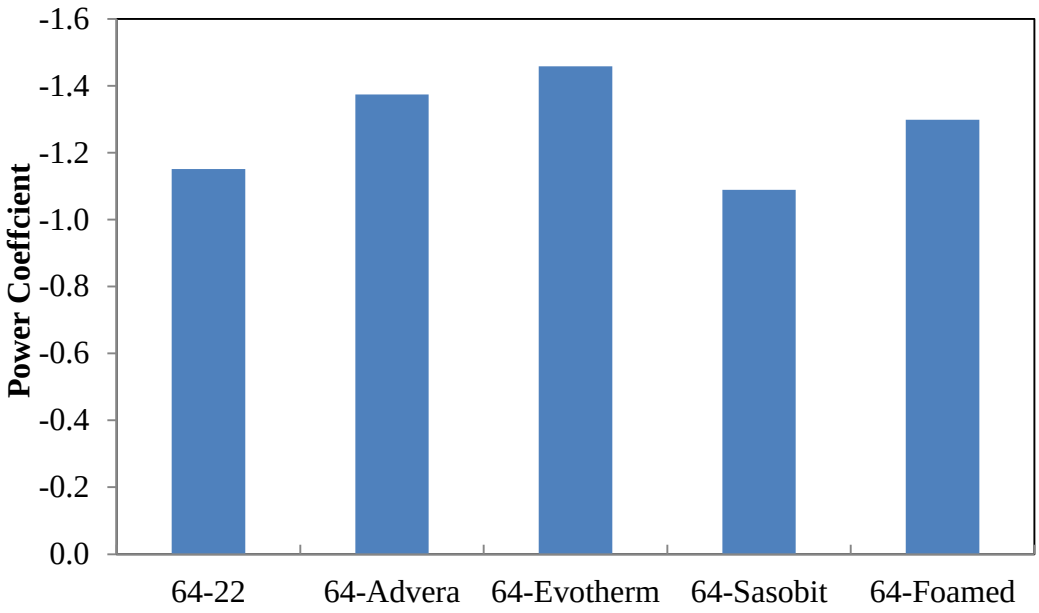

Figure 5.45: Crack closure rate for 64-22 samples.

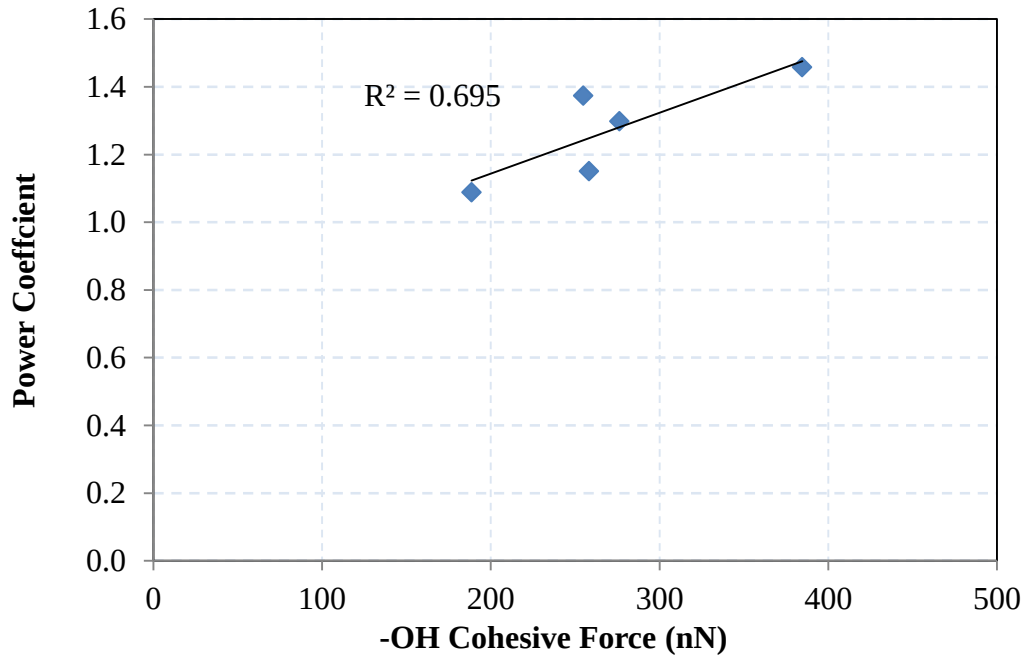

Figure 5.46: Crack closure rate vs. –OH Cohesive Force for 64-22 samples.

5.8.2 Intrinsic Healing

The strength gained by the wetted crack interface, referred to as the intrinsic healing, is another important mechanism in the healing phenomena in asphalt binders. This depends on the

cohesive bonds within the asphalt binder. In this cohesive bonding energy of the asphalt binder was used to evaluate intrinsic healing of asphalt binders, which is the energy required to overcome cohesion bonds within a material. To obtain this parameter, the shaded area under the retraction curve of the force spectroscopy experiment performed using tips functionalized with –OH and –COOH was computed as shown in Figure 5.47.

Figures 5.48 and 5.49 compare the average bonding energy values of the different WMA and HMA 70-22M binders obtained from experiments conducted using –OH and –COOH functionalized tips, respectively. It is noted that for the –OH chemical group, only the Sasobit resulted in a significant decrease in the cohesive bonding energy with 70-22M binder. The Sasobit also had the least bonding energy when –COOH functionalized tips were used. However, the other WMA technologies resulted in a reduction in the bonding energy, but this reduction was much less pronounced. Thus, the results suggests that the Sasobit might have an adverse effect on the intrinsic healing of the 70-22M binder, while the other WMA technologies improve or won't influence this property.

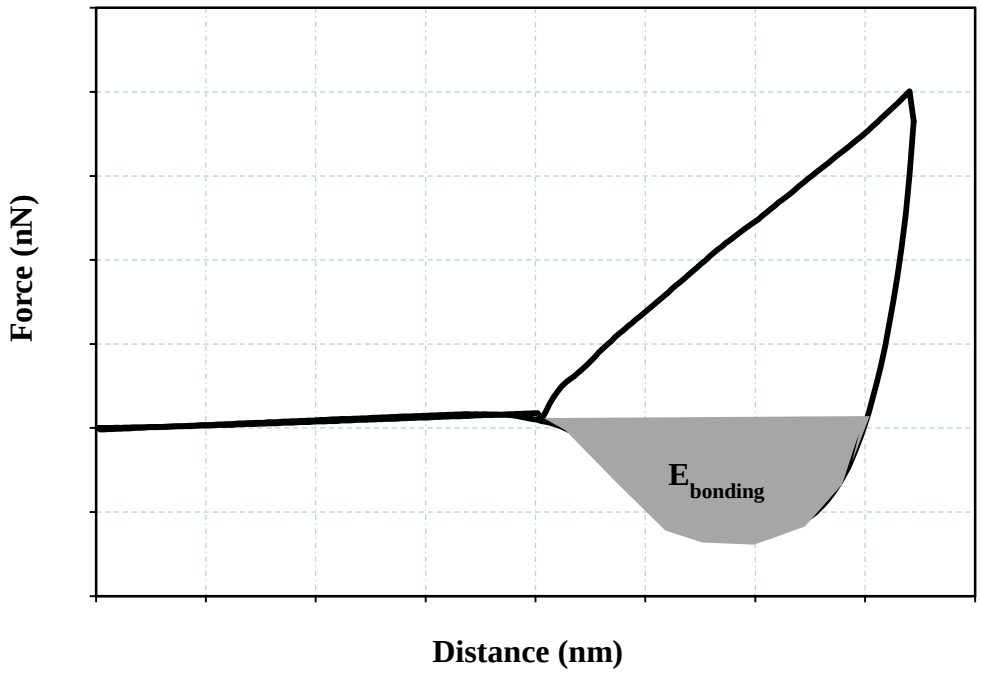

Figure 5.47: Determining Cohesive Bonding Energy.

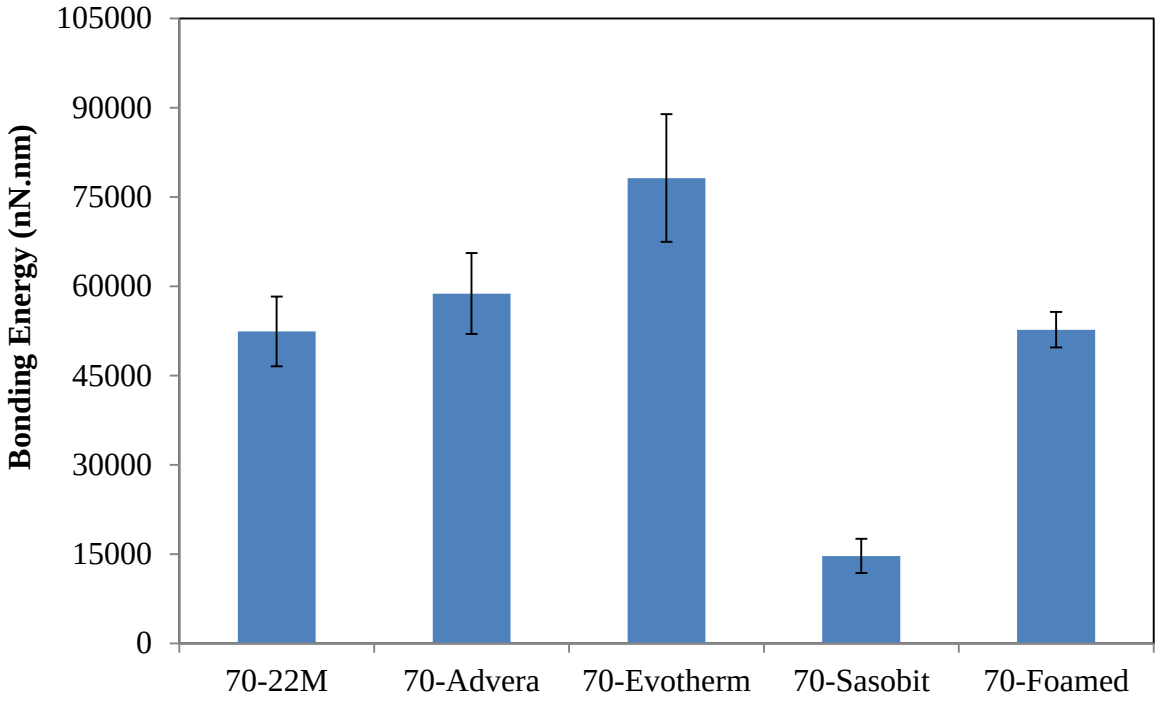

Figure 5.48: Cohesive Bonding Energy using –OH tips for 70-22M samples.

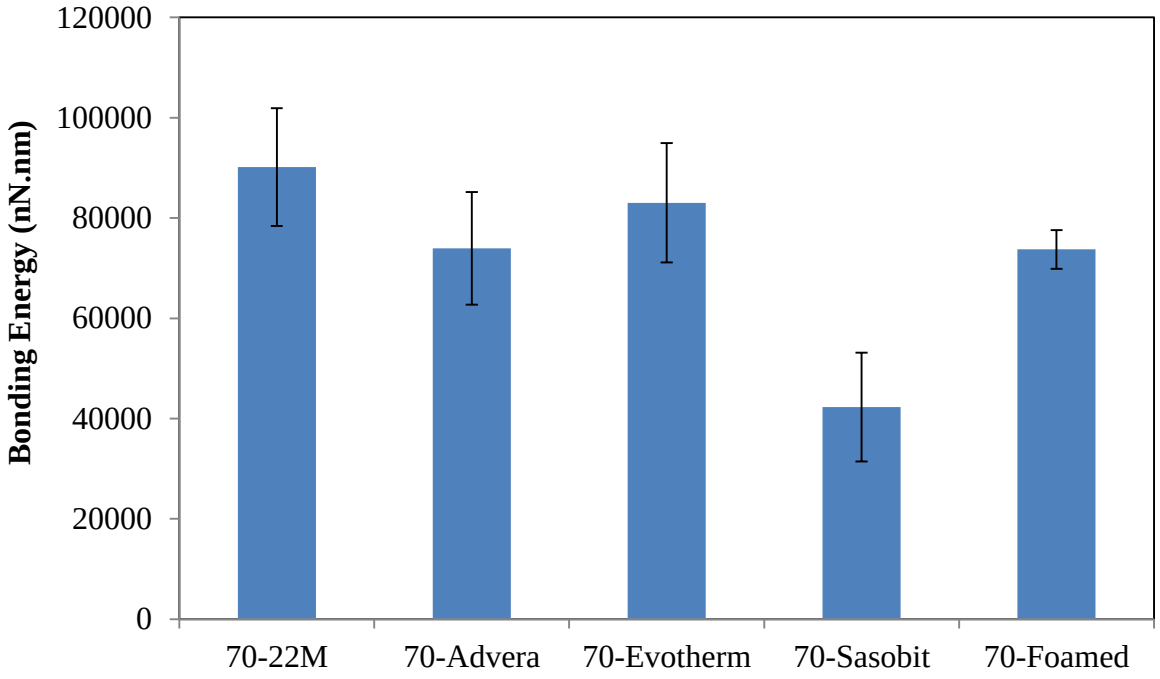

Figure 5.49: Cohesive Bonding Energy using –COOH tips for 70-22M samples.

Figures 5.50 and 5.51 present the bonding energy values for the control and WMA 64-22 samples that were obtained from force spectroscopy experiments performed using –OH and –COOH functionalized tips, respectively. All WMA technologies except the Sasobit improved the –OH cohesive bonding energy of the 64-22 binder. This improvement was much more pronounced in the case of the Evotherm. The results in Figure 5.51 are indicating that all WMA technologies had similar –COOH cohesive bonding energy to that of the control 64-22. These results suggest that the Evotherm have an improvement in the intrinsic healing of the 64-22 binder, while the addition of the Sasobit additive might adversely influence this property. Advera and foamed WMA technologies does not have a significant effect on the intrinsic healing of the 64-22M binder.

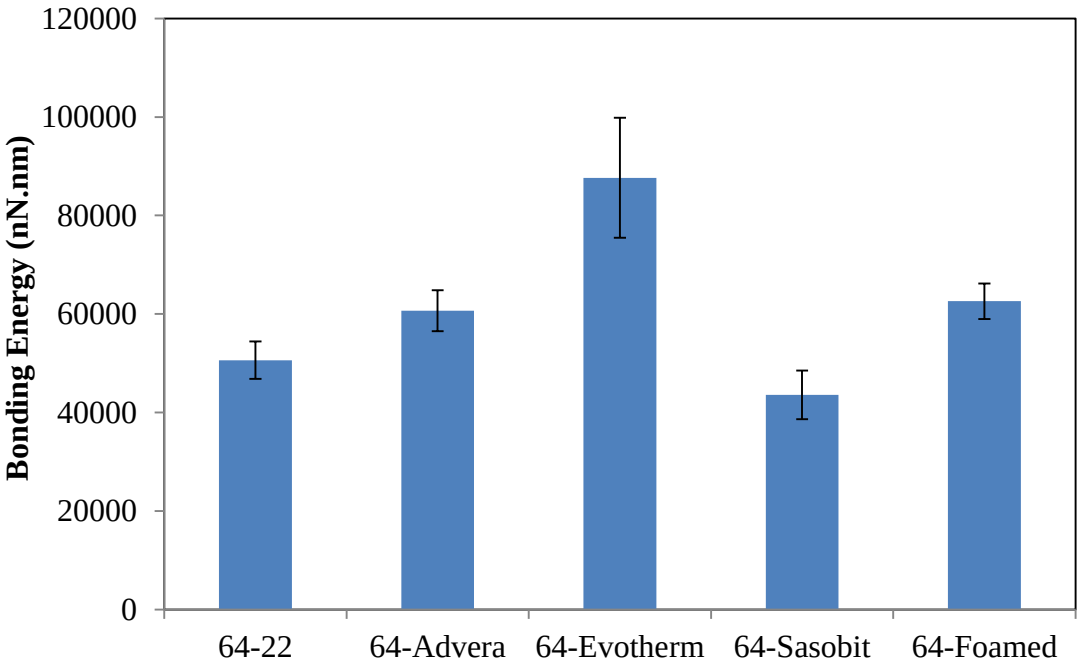

Figure 5.50: Cohesive Bonding Energy using –OH tips for 64-22 samples.

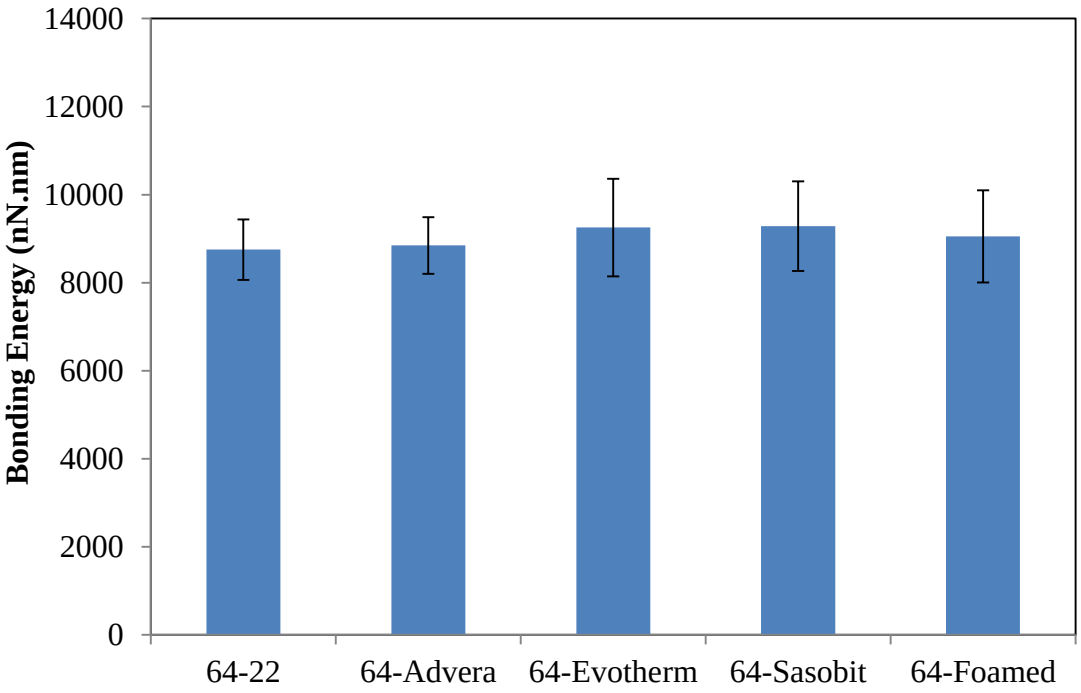

Figure 5.51: Cohesive Bonding Energy using –COOH tips for 64-22 samples.

Chapter 6 CONCLUSIONS AND RECOMMENDATIONS

6.1 Summary and Conclusions

In this study, macro and nano-scale tests were conducted to evaluate the influence of different WMA technologies on the moisture susceptibility and healing characteristics of two types of asphalt binders commonly used in Ohio. Four types of WMA technologies were considered, including: Advera, Evotherm, Sasobit, and foamed WMA. The macro-scale experiments included conducting AASHTO T283 and dynamic shear rheometer tests. In addition, different AFM based experiments were performed, including: AFM imaging, force spectroscopy, and healing experiments. The following sections provide the main conclusions that were made based on the results of the experimental tests and the findings of subsequent statistical analyses.

6.1.1 AASHTO T283 Test

- The addition of the Sasobit to the PG 70-22M and PG 64-22 binders had resulted in significant reduction in the ITS values of the unconditioned mixtures.
- In general, the Advera mixtures had the lowest TSR value among all WMA and HMA mixtures, while the Evotherm had the highest value.
- The Sasobit and Advera WMA 70-22M mixtures had slightly higher reduction in the ITS values upon conditioning and lower TSR as compared to the other WMA and HMA 70-22M mixtures. However, all mixtures had TSR higher than the minimum value of 0.8 specified in ODOT C&MS for heavy traffic surface mixtures.
- The Advera and Sasobit 64-22 mixtures had much more pronounced reduction in the ITS values upon conditioning as compared to the other WMA and HMA 64-22 mixtures. Such that for conditioned 64-22 mixtures, the Advera and Sasobit WMA mixture exhibited statistically lower ITS values than that of the HMA control mixture. The Evotherm and foamed WMA had statistically similar values to that of the control HMA.

6.1.2 DSR Test

- Sasobit stiffened the PG 64-22 and PG 70-22M asphalt binders and resulted in higher G* modulus values.
- The Evotherm resulted in a slight increase in the G* values of the PG 70-22M, but had no significant effect on the G* values PG 64-22 binder.
- The foaming of PG 70-22M binder resulted in a slight decrease in the G* values but did not have any effect on these values for PG 64-22.
- The Advera did not influence the G* values of the PG 70-22M, but decreased the stiffness of PG 64-22 binder.

6.1.3 **AFM Experiments**

6.1.3.1 General Comments

- The AFM was found to be a viable device to examine the moisture damage mechanisms by conducting force spectroscopy experiments using chemically functionalized tips that resembles the aggregates particles and asphalt molecules and measuring the adhesive and cohesive forces using the procedure described in this report.
- The AFM is an effective tool to examine the two main healing mechanisms in asphalt materials, namely, wetting and intrinsic healing, using the method described in this report.
- Method-I described in this report is recommended to be used for preparing AFM samples, since it was found to produce asphalt films with uniform and consistent thicknesses required for all AFM characterization techniques.

6.1.3.2 AFM Imaging

- The inclusion of the Sasobit WMA additive reduced the dimensions of the so called ‘bee-like’ structures within the neat and polymer modified asphalt binders. However, the other WMA technologies did not have any significant effects on the dimensions of these structures.
- The Sasobit additive resulted in increasing the relative stiffness of dispersed domains containing the ‘bee-like’ structure in comparison with the flat asphalt matrix for both

types of binders. The stiffer domains resulted in enhancing of the stiffness properties of the Sasobit modified asphalt binder as compared to the control asphalt binder, which explains the higher G* value obtained in the DSR test for this binder.

- The phase image showed that the inclusion of Evotherm did not have a significant effect on the domains viscoelastic properties of the PG 70-22M and PG 64-22 binders. This is consistent with DSR test results.
- According to the AFM phase image, the foaming of the polymer modified asphalt binders through adding Advera additive or by water injection resulted in reducing the relative stiffness between the dispersed domains and the flat asphalt matrix.
- The phase contrast between the flat matrix and dispersed domains remained unchanged due to the foaming of the PG 64-22 binder.

6.1.3.3 Force Spectroscopy Experiments

- Based on the results of the AFM force spectroscopy results, the indirect tensile strength measured in the AASHTO T283 test was found to depend more on the adhesive bonds (forces) between the aggregate and binder as compared to the cohesive bonds (forces) within the binder itself.
- For the unconditioned samples, all WMA technologies had resulted in increasing the adhesive forces for both types of asphalt binders. Advera and foamed WMA had the highest improvement to these forces, while the Sasobit had the least. This result may explain the lower ITS values obtained due to the addition of the Sasobit.
- For the unconditioned 70-22M samples, the inclusion of the Evotherm and Advera WMA additives resulted in significantly increasing the interaction forces with –OH tip, but the Sasobit additive significantly reduced these forces.
- For the unconditioned samples, only the Sasobit has resulted in significant reduction in the –COOH cohesive forces for both types of binders. However, the other WMA technologies did not have any significant effect on these forces.
- The adhesive forces were significantly decreased due to conditioning of the control and WMA 64-22 binders. This behavior was different than that observed for the polymer

modified PG 70-22M binder, which indicates that the PG 64-22 binder is more susceptible to moisture damage.

- Upon conditioning of the PG 64-22 binder, the control and Evotherm WMA binders exhibited the least reduction in the adhesive forces. Furthermore, the Advera binder had the highest decrease after moisture conditioning. This is may explain the lower TSR values that Advera 64-22 mixture exhibited.
- The Sasobit and Advera led to a reduction in the cohesive forces within both types of asphalt binders after moisture conditioning, indicating that it might adversely affect cohesive bonds within the asphalt binder.
- According to AFM tests, the Evotherm WMA will have the best resistance to moisture-induced damage among all WMA technologies evaluated in this study, which is similar to that of the control asphalt binder. This may be attributed to the anti-strip additive that Evotherm contains.

6.1.3.4 Healing Experiments

- The Evotherm, Advera, and foamed WMA technologies had resulted in improving the rate of micro-crack closure rate in both types of binders considered in this study. On the contrary, Sasobit had an adverse effect on this rate.
- The micro-crack closure rate, and hence the wetting mechanisms is related to the interaction forces with –OH chemical group in an asphalt binder.
- Only the Sasobit resulted in significant decrease in the cohesive bonding energy; indicating that it might adversely affect the intrinsic healing of the considered asphalt binders.
- All WMA technologies except the Sasobit improved the –OH cohesive bonding energy of the both types of binders. This improvement was much more pronounced in the case of the Evotherm.
- All WMA technologies except the Sasobit had similar –COOH cohesive bonding energy to that of the control asphalt binders.
- The Evotherm might improve the intrinsic healing of the both asphalt binder, while the addition of the Sasobit additive might adversely influence this property.

- Advera and foamed WMA technologies do not have a significant effect on the intrinsic healing of the considered asphalt binders.

6.2 Study Limitations

This study had a number of limitations, which include:

- The use of only two types of asphalt binders and one type of aggregates.
- The use of fully dried aggregates in preparing the asphalt mixtures.
- Only one type of macro-scale test was used in this study to evaluate moisture susceptibility of asphalt mixtures.
- The foaming parameters, which include: foaming water content, air pressure, water pressure, and foaming temperature, were not varied and thus their influence on moisture susceptibility was not investigated.

6.3 Recommendations for Further Study

It is recommended that future work expands the current study to include other types of aggregates and asphalt binders used in Ohio. In addition, future studies are needed to evaluate the use of other macro-scale tests that has the capability to examine adhesive as well as cohesive failures within an asphalt system. This will allow having a more fundamental and better evaluation of the moisture susceptibility of asphalt materials. It is also recommended to conduct a comprehensive evaluation of the effects of the foaming parameters on the moisture susceptibility of WMA binders and mixtures.

The AFM was found to be a viable device in studying the moisture susceptibility and healing characteristics of asphalt materials. However, there are other useful applications for this device. Future research should explore the other AFM techniques such as the nano-indentation to study other problems related to asphalt binders and mixtures.

6.4 Recommendations for Implementation

During the last few years, the amount of asphalt mixture produced using the foamed WMA technology in Ohio has increased from 10,430 tons in 2008 to 2,800,000 tons in 2011,

which represents about 56% of the total amount of asphalt mixtures produced in the state. As part of this study the influence of foamed WMA technology on the moisture susceptibility and healing characteristics of asphalt binders was evaluated. The results showed that the foamed WMA technology does not have any significant effect on the moisture susceptibility of the considered asphalt binders. Furthermore, the foamed WMA technology was found to improve the micro-crack closure rate of asphalt binders, but it did not influence their intrinsic healing properties.

This study showed that the AASHTO T283 used by ODOT to evaluate moisture susceptibility of asphalt mixtures depends on the adhesive bonds between the asphalt binder and aggregate and may not predict moisture-induced damage problems in the mixture associated with failures in the cohesive bonds within the asphalt binder itself. Thus, it is recommended to use an additional test to supplement the AASHTO T283 and examine the cohesive failures within an asphalt mixture.

REFERENCES

- AASHTO T283. *Standard Method of Test for Resistance of Compacted Hot Mix Asphalt (HMA) to Moisture-Induced Damage*. American Association of State Highway and Transportation Officials (AASHTO), 2007.
- Abbas, A. (2008), "Simulating the Deformation Behavior of Hot Mix Asphalt as Tested in the Indirect Tension Test." ASCE Geotechnical Special Publication No. 182, Geo-Institute, Reston, VA, pp. 16-23
- Abu Al-Ru, R., Masad, E., and Graham, M. (2010). Physically Based Model for Predicting the Susceptibility of Asphalt Pavements to Moisture-Induced Damage, Final Report, Southwest University Transportation Center, Report # SWUTC/10/476660-0012-1.
- Agilent Technologies, Inc. (2008). *Agilent 5500 LS AFM/SPM User Manual.* Agilent Technologies, Palo Alto, California.
- Ali, A., Abbas, A., and Nazzal, M. (2012) "Laboratory Evaluation of Foamed Warm Mix Asphalt." *International Journal of Pavement Research and Technology*.
- Astec, Inc. Webpage (http://www.astecinc.com/).
- Barthel, W. and M. von Devivere (2003). "Warm Asphalt Mixes by Adding Aspha-Min. A Synthetic Zeolite." *Proceedings of the 48th Annual Convention of the National Asphalt Pavement Association (NAPA)*, San Diego, CA, January 11-17.
- Bhasin, A., Masad, E., Little, D., Lytton, R.: Limits on adhesive bond energy for improved resistance of hot mix asphalt to moisture damage. Transportation Research Record 1970, 3-13 (2006).
- Bhasin, A.: Development of methods to quantify bitumen-aggregate adhesion and loss of adhesion due to water. PhD dissertation, Texas A&M University, College Station, Texas (2006).
- Bhushan, B. and Qi, J., 2003. Phase contrast imaging of nanocomposites and molecularly thick lubricant films in magnetic media. Nanotechnology, 14: 886-895.
- Bonaquist, R. (2011). *NCHRP Project 9-43: Mix Design Practices for Warm Mix Asphalt.* Final Report Pending, Transportation Research Board, National Highway Research Council, NCHRP, Washington, D.C.

- Buss, A., Williams, C., Schram, S., Kvasnak, A (2011). "Investigation of warm-mix asphalt using Iowa aggregates." Proceedings of the 90th Transportation Research Board Annual Meeting, Washington, D.C.
- Carbognani, L., DeLima, L., OreaM.&Ehrmann, U. , 2000. Studies of large crude oil alkanes. II. Isolation and characterization of aromatic waxes and waxy asphaltenes. Petroleum Science Technology, 18, 607–634.
- Caro, S., Masad, E., Bhasin, A., Little, D. (2008) Moisture susceptibility of asphalt mixtures, Part 1: Mechanisms. International Journal of Pavement Engineering, 9, 81–98.
- Corrigan, M. (2010). "What's New with WMA?" *Presented at the North Central Asphalt User/Producer Group (NCAUP) Hot Mix Asphalt Technical Conference*, Overland Park, KS, February 2-4.
- Csanyi, L. H. (1957). "Foamed Asphalt in Bituminous Pavements." *Highway Research Board Bulletin*, Vol. 10, No. 160, pp. 108-122.
- D'Angelo, J., Harm, E., Bartoszek, J., Baumgardner, G., Corrigan, M., Cowsert, J., Harman, T., Jamshidi, M., Jones, W., Newcomb, D., Prowell, B., Sines, R., and B. Yeaton (2008). *Warm-Mix Asphalt: European Practice*. Federal Highway Administration (FHWA), Report No. FHWA-PL-08-007. Federal Highway Administration (FHWA) Warm Mix Asphalt Webpage (http://www.fhwa.dot.gov/pavement/asphalt/wma.cfmb).
- Davidson, J. K. (2007). "Warm Asphalt Mix Technology-The Canadian Perspective." Australian Asphalt Pavement Association.
- Ferry, J. D. 1980. Viscoelastic properties of polymers. John Wiley & Sons, New York.
- Fischer-Cripps AC, 2006. Critical review of analysis and interpretation of nanoindentation test data. Surf. Coat Technol, 200:4153.
- Hodo, W., Kvasnak, A., and Brown, R. (2009). "Field and Laboratory Investigation of Foamed Asphalt (Warm-Mix Asphalt) with High Recycled Asphalt Pavement Content for Sustainment and Rehabilitation of Asphalt Pavement." *Proceedings of the 88th Transportation Research Board Annual Meeting*, Washington, D.C.
- Horcas, I., Fernandez, R., Gomez-Rodriguez, J.M. Colchero, J. Gomez-Herrero, J. and Baro, A. M. Rev. Sci. Instrum. 78, 013705 (2007).

- Hurley, G. C. and B. D. Prowell (2005a). *Evaluation of Aspha-Min Zeolite for Use in Warm Mix Asphalt*. National Center for Asphalt Technology (NCAT) Report 05-04.
- Hurley, G. C. and B. D. Prowell (2005). *Evaluation of Sasobit for Use in Warm Mix Asphalt*. National Center for Asphalt Technology (NCAT) Report 05-06.
- Hurley, G. C. and B. D. Prowell (2006a). *Evaluation of Evotherm for Use in Warm Mix Asphalt*. National Center for Asphalt Technology (NCAT) Report 06-02.
- Hurley, G. C. and B. D. Prowell (2006b). "Evaluation of Potential Processes for Use in Warm Mix Asphalt." *Journal of the Association of Asphalt Paving Technologists*, Vol. 75, pp. 41-90.
- Hurley, G. C., and B.D. Prowel. (2005). "Evaluation of Aspha-min Zeolite for Use in Warm Asphalt Mixes." NCAT Report 05-04, National Center of Asphalt Technologiest, Auburn University, Auburn, AL, June 2005.
- Hurley, G.C., and B.D. Prowell (2006). "Evaluation of Potential Processes for Use in Warm Mix Asphalt," Journal of the Association of Asphalt Paving Technologists, Volume 75, Savannah, Georgia, 2006, pp. 41 - 90.
- Jenkins, K. J. and M. F. C. van de Ven (1999). "Mix Design Considerations for Foamed Bitumen Mixtures." *Proceedings of the 7th Conference on Asphalt Pavements for Southern Africa*, Victoria Falls, Zimbabwe.
- Jenkins, K. J., J. L. A. de Groot, A. A. A. Molenaar, and van de Ven (1999). "Half-Warm Foamed Bitumen Treatement, a new process." *Proceedings of the 7th Conference on Asphalt Pavements for Southern Africa*, Victoria Falls, Zimbabwe.
- Kanitpong, K., S. Sonthong, K. Nam, W. Martono, and H. Bahia (2007). "Laboratory Study on Warm Mix Asphalt Additives," *Proceedings of 86th Annual Meeting of the Transportation Research Board*, National Academy of Sciences, Washington, D.C.
- Kiggundu B. M. and Roberts, F. L. (1988) "Stripping in HMA Mixtures: Stateof-The Art And Critical Review of Test Methods." NCAT, Auburn University, Auburn, Alabama, Report No. 88-2.
- Kim, Y., Lee, H., and M. Heitzman (2007). "Experience of Developing and Validating a New Mix Design Procedure for Cold In-Place Recycling Using Foamed Asphalt." *Proceedings of the 2007 Mid-Continent Transportation Research Symposium*, Amex, Iowa.

- Koenders, B. G., Stoker, D. A., Bowen, C., de Groot, P., Larsen, O., Hardy, D., and K. P. Wilms (2000). "Innovative Process in Asphalt Production and Application to Obtain Lower Operating Temperatures." *2nd Eurasphalt & Eurobitume Congress*, Barcelona, Spain.
- Kringos, N., Pauli, T., Schmets, A. & Scarpas, T. (2012). Demonstration of a New Computational Model to Simulate Healing in Bitumen. Journal of the Association of Asphalt Paving Technologists.
- Kristjansdottir, O. (2006). *Warm Mix Asphalt for Cold Weather Paving*, Master Thesis, Report No. WA-RD 650.1, University of Washington, Seattle, Washington.
- Kristjansdottir, O., Muench, S. T., Michael, L., and G. Burke (2007). "Assessing Potential for Warm-Mix Asphalt Technology Adoption." Journal of the Transportation Research Board, Transportation Research Record 2040, pp. 91-99.LEA-CO Webpage (http://www.lea-co.com/).
- Kvasnak, A., Taylor, A., Signore, J., and Bukhari, S. (2010). *Evaluation of Gencor Green Machine Ultrafoam GX*. National Center for Asphalt Technology, NCAT Report 10-03.
- Kvasnak, A., West, R., Moore, J., Nelson, J., Turner, P., and Tran, N. (2009). "Case Study of Warm Mix Asphalt Moisture Susceptibility in Birmingham." *Proceedings of the 88th Transportation Research Board Annual Meeting*, Washington, D.C.
- Loeber, L., Muller, G., Morel, J. & Sutton, O. Bitumen in colloidal science: a chemical, structural and rheological approach. Fuel, 77, 1443–1450, 1998.
- Lu, X.H., Langton,M., Olofsson, P.&Redelius,P., 2005.Waxmorphology in bitumen. J. Mater. Sci., 40: 1893–1900.
- Maccarrone, S., Holleran, G. and A. Ky (1994). "Cold Asphalt Systems as an Alternative to Hot Mix." *Proceedings of the 9th International Australian Asphalt Pavement Association (AAPA) Conference*, Queenland, Australia.
- Masson, J-F., Leblond, V. And Margeson, J. (2008). "Bitumen morphologies by phase detection atomic force microscopy." *Journal of Microscopy*, Vol. 221, pp. 17–29, 2006.
- MeadWestvaco. (2012). Evotherm M1 Product Data Bulletin. Retrieved July 7, 2012, from Evotherm® Warm Mix Asphalt: http://www.meadwestvaco.com/SpecialtyChemicals/AsphaltAdditives/MWV002106
- Middleton, B. and Forfylow, R.W. (2009). "Evaluation of Warm Mix Asphalt Produced With the Double Barrel Green Process." *Journal of the Transportation Research Board*,

- Moulthrop, J., McDaniel, R., McGennis, R., Mohammad, L. and Kluttz, R.(2007). "Asphalt Mixture Innovations: State of the Practice and Vision for 2020 and Beyond," TR News No. 253 Highway Design and Construction A 2020 Vision, pp.20-23.
- Muthen, K. M. (1998). *Foamed Asphalt Mixes-Mix Design Procedure*. Sabita Ltd. and CSIR Transportek, Report CR-98/077, South Africa.
- Nazzal , M., Kaya, S., Abu-Qtaish, L. (2012) "Evaluation of the Healing Properties Of Asphalt Binders Using Atomic Force Microscopy" The RILEM Book series, Vol. 4.
- Nazzal , M., Sargand, S. , and Al-Rawashdeh, A., (2010). Evaluation Of Warm Mix Asphalt Mixtures Containing RAP Using Accelerated Loading Tests. *ASTM Journal of Testing and Evaluation,* Vol. 39, No. 3.
- Nguyen, T., Gu, X., Fasolka, M., Briggman, K., Hwang, J., Karim, A., and Martin, J., 2005. Mapping chemical heterogeneity of polymeric materials with chemical force microscopy. Polym. Mater. Sci. Eng., 90: 141–143.
- ODOT CMS (2010), *Construction and Material Specifications,* Ohio Department of Transportation, Columbus, Ohio.
- Pellinen, T. K. and Witczak, M. W. (2002). "Stress Dependent Master Curve Construction for Dynamic (Complex) Modulus." *Journal of Association of Asphalt Paving Technologists*, Volume 71, pp. 281-309.
- Petersen, J. C., 1984. Chemical composition of asphalt as related to asphalt durability: state of the art, Transportation Research Board , 999: 13-30.
- Prowell, B. D., Hurley, G. C., and Crews, E. (2007). "Field Performance of Warm-Mix Asphalt at National Center for Asphalt Technology Test Track." *Journal of the Transportation Research Board*, Transportation Research Record 1998, pp. 96-102.
- Prowell, B.D., G.C. Hurley, and E. Crews (2007) " Field Performance of Warm-Mix Asphalt at the NCAT Test Track." 86th Transportation Research Board Annual Meeting, Washington, D.C..
- Romier, A., Audeon, M., Jac, D., Martineau, Y., and F. Olard (2006). "Low-Energy Asphalt with Performance of Hot-Mix Asphalt." *Journal of the Transportation Research Board,* Transportation Research Record 1962, pp. 101-112.
- Ruckel, P. J., Acott, S. M., and R. H. Bowering (1983). "Foamed-Asphalt Paving Mixtures: Preparation of Design Mixes and Treatment of Test Specimens." *Journal of the*

Transportation Research Board, Transportation Research Record 991, pp. 88-95.

- SAS Institute Inc. (2004). SAS OnlineDoc® 9.1.2**.** Cary, NC, SAS Institute Inc.
- Sasol Wax Webpage: (http://www.sasolwax.com/).
- Tarefder, R. & Zaman, A.(2010). "Nanoscale Evaluation of Moisture Damage in Elastomeric Polymer Modified Asphalts", ASCE *Journal of Materials in Civil Engineering*, 2010.
- Vavrik, W. R., Pine, W. J., and S. H. Carpenter (2002). "Aggregate Blending for Asphalt Mix Design: Bailey Method." *Journal of the Transportation Research Board*, Transportation Research Record 1789, pp. 146-153.
- Warm Mix Asphalt Technical Working Group Webpage (http://www.warmmixasphalt.com/).
- Wasiuddin, N. M., Selvamohan, S., Zaman, M. M., and M. L. T. A. Guegan (2008). "Comparative Laboratory Study of Sasobit and Aspha-Min Additives in Warm-Mix Asphalt." *Journal of the Transportation Research Board*, Transportation Research Record 1998, pp. 82-88.
- Wielinski, J., Hand, A., and Rausch, D. (2009). "Laboratory and Field Evaluations of Foamed Warm-Mix Asphalt Projects." *Journal of the Transportation Research Board*, Volume 2126, pp. 125-131.
- Wu, S. P., Pang, L., Mo, L. T., Chen, Y. C., and Zhu, G. J. (2010). "Influence of Aging on the Evolution of Structure, Morphology and Rheology of Base and SBS Modified Bitumen." *Constr Build Mater*, Vol. 23, pp. 1005–1010.
- Xiao, F., Amirkhanian, S., and Putman, B. (2009). "Evaluation of Rutting Resistance in Warm Mix Asphalts Containing Moist Aggregate." *Journal of the Transportation Research Board*, Volume 2126, pp. 115-124.
- Zhang, H., Wang, H., Yu, J. (2011). "Effect of Aging on Morphology of Organo-Montmorillonite Modified Bitumen by Atomic Force Microscopy." *Journal of Microscopy*, Vol. 242, pp. 37–45.